

SENSITIVITY OF CHANNEL-SIZE ESTIMATIONS ON FLOOD INUNDATION

by

Leo Leummens

In partial fulfilment of the requirements for the degree of Master of Science in Water Engineering and Management at the University of Twente

December 2021

Enschede

Contact:

lleummens@gmail.com

Graduation Committee:

Dr. J.J. Warmink

(University of Twente)

Dr.ir. A. Bomers

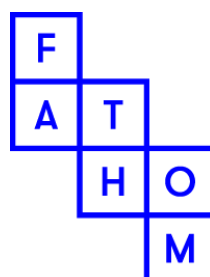
(University of Twente)

Dr. O. Wing

(Fathom, Bristol)

Dr. N. Quinn

(Fathom, Bristol)



**UNIVERSITY
OF TWENTE.**

Preface

This report is the result of the master thesis project that was carried out in cooperation with Fathom, Bristol over a period of nine months, and it is also the final part of my study at the University of Twente. First of all, I would like to thank Anouk Bomers, who was my UT supervisor for almost a year, for her truly boundless patience which made it possible for me to finish my research and for her ideas during our many meetings. Also I would like to thank Oliver Wing and Jord Warmink for the valuable feedback during all stages of the project and for their support even when I was facing difficulties with my study. Finally, I would like to thank my fellow students from UTwente who helped me a lot during my time at University. And though I was far away for a long time now, I still feel as part of this wonderful society.

I hope that you will enjoy reading this report

Sincerely,
Leo Leummens

Moscow, December 2021

Summary

Currently, almost 30% of total world population live in close proximity to the locations which are exposed to floods of 100 years return period (Rentschler and Salhab, 2020). The ongoing coast habitation combined with the climate change effect leads to the increased potential flooding damage both to human health and infrastructure. However, much of the damage caused by flooding could be alleviated using various safety measures which often include inundation modelling.

More accurate, dense and widespread data of ground elevation and flood extents have enabled the rapid development of hydrodynamic modelling across the globe (Teng et al., 2017). Unfortunately, due to inability of modern remote sensing instruments to penetrate water, channel size measurement techniques have not benefited from these advances, therefore channel size approximations are widely used in hydraulic modelling in data-scarce regions.

It is a common assumption that the river channel size or rather channel conveyance corresponds to the dominant discharge value (Wolman and Miller, 1960). Most commonly, for modelling purposes, the dominant flow rate is adopted as an annual maximum flow of 1-in-2 years frequency (Woodyer, 1968; Williams, 1978; Wilkerson, 2008). However, this is in spite of understanding that some rivers may flow out of bank seasonally (e.g. the River Niger) or much more infrequently due to human modifications (e.g. the River Thames in central London).

In accordance with the defined problem and present knowledge and technology gap, the main research objective of this master thesis project is to increase the understanding and to quantify how different channel size estimates influence the performance of flood inundation modelling.

In order to reach the objective of this research, the commonly used channel size estimation should be tested first. Thus, the LISFLOOD-FP model has been set up, calibrated and validated on 2 independent hydrology data series for December 1993 – January 1994 and January 1995 flood events. The value for 1-in-2 years annual peak flow was found to be equal to 6160 m³/s. After the 1-in-2 years annual maximum discharge was transited into bankfull depth approximation for river channel, the built model was used to perform a simulation run for the assessment of the adopted assumption. Good alignment of the model built on proposed bankfull discharge estimate with the measurement data was observed. The maximum deviation of the water depth data was limited by 5%, while the also only 5% error was made in prediction of the inundation area.

Then, other channel size estimates were tested in a similar way to find which of them shows the best-fitted prediction for water level series over the Lower Rhine basin. Those assumptions for bankfull discharge value considered annual maximum and mean discharges of various frequency, regionally defined value, effective and half-yield discharge estimates. It was found that the best-fitted simulation results were obtained for the initial guess of 1-in-2 years annual maximum discharge as well as for the regionally defined discharge value obtained from the hydraulic geometry relationships. The latter was estimated to be equal to 6100 m³/s. Additionally, annual mean discharges of 10 and 50 years recurrence period were found to perfectly balance each other in terms of the river sections where their simulation run results have shown sufficiently good alignment with measurements. Thus, the symbiosis of those two assumptions could have also been judged as one of the best fitted estimates.

As the result of this study, the means for channel approximation in modelling cases of rivers with relatively flat and densely populated large watershed areas with Western and Central hydrometeorological conditions were provided. The 1-in-2 years annual maximum flow and hydraulic geometry assumptions were considered best for such situations. Moreover, the sediment-related assumptions have shown really poor performance throughout this research, which could be related to the uncertainties introduced in sediment regional curves calculation by urbanization, climate change or other sources. This implies caution while using such type of channel size estimations in hydrodynamic modelling for areas similar to Lower Rhine basin. Finally, it was found that the annual mean discharge assumption performance is highly dependent on the average channel width and its variability along the specified river reach. Thus, it could be concluded that $Q_{k,mean}$ assumptions are too unstable to be used on large urbanised areas, where various aspects influence the river channel up to high extent, without any supporting parameters. The solution would be representing the large basin as a set of the smaller catchments with distinctive channel approximation techniques.

Table of Contents

Preface	2
Summary	3
List of figures	6
List of tables	8
1. Introduction	9
1.1. Problem definition	9
1.2. Objective and research questions	10
1.3. Research outline	11
2. Research background	12
2.1. Study area	12
2.2. Flooding in Lower Rhine	13
2.2.1. December, 1993 – January, 1994	14
2.2.2. January, 1995 – February, 1995	15
2.3. Model framework	17
2.3.1. Flood inundation modelling	17
2.3.2. LISFLOOD-FP model	17
2.4. Channel size approximations	20
3. Data & Methodology	22
3.1. Modelling approach	22
3.2. Model input parameters	24
3.2.1. Raster datasets	24
3.2.2. River network	27
3.2.3. Boundary conditions	29
3.3. Calibration & Validation	30
3.4. Statistical analysis	31
4. Channel size estimates	32
4.1. Flood frequency assumptions	33
4.1.1. Annual maximum discharge	34
4.1.2. Annual mean discharge	35
4.2. Hydraulic geometry	36
4.3. Dominant discharge	37
5. Results of reference case scenario	41
5.1. Calibration	41
5.1.1. Flood extent	41
5.1.2. Water level at gauge location	44
5.2. Validation	47
5.2.1. Water level at gauge location	47
5.2.2. Flood extent	48
6. Channel size estimates assessment	51
6.1. Annual maximum discharge	51

6.2.	Annual mean discharge	55
6.3.	Hydraulic geometry	60
6.4.	Dominant discharge	61
6.5.	Goodness-of-fit analysis.....	63
7.	Discussion.....	65
8.	Conclusions & Recommendations	67
8.1.	Conclusions.....	67
8.2.	Recommendations	69
	References	70

List of figures

Figure 1 – Map of the Rhine basin (by Daniel Ullrich)	12
Figure 2 – Variation of mean monthly discharges at selected gauges on the River Rhine (Engel, 1997)	13
Figure 3 – High-water discharges series for the 1891-1995 period at the Cologne gauging station on the Rhine (Engel, 1997)	14
Figure 4 – Lower Rhine tributary discharge series with applied Lag	15
Figure 5 – Stereographic representation of the flood waves of December 1993/January 1994 and January 1995 floods on the River Rhine (Engel, 1997)	16
Figure 6 – Concept of (A) LISFLOOD-FP base model, (B) sub-grid channels model and (C) sub-grid section (Neal et al., 2012)	19
Figure 7 - Modelling domain, Lower Rhine	24
Figure 8 – DEM of the Lower Rhine for: (a) $\Delta x = 10$ m; (b) $\Delta x = 100$ m with abrupt Dikes; (C) $\Delta x = 10$ m with manually restored dikes.....	25
Figure 9 – Roughness classes in Lower Rhine basin with (A): 10x10m or (B): 100x100m resolution .	26
Figure 10 – Digital Elevation Model of Lower Rhine basin with (A) and without (B) a river channel....	27
Figure 11 - Variability in the river channel width (A) and bankfull depth (B) for the Lower Rhine basin	28
Figure 12 - Discharge series at Andernach, Bonn and Cologne hydrological stations during 1993 flood	29
Figure 13 – Discharge series measured at Andernach (Applied for Bonn) during January, 1995 flood event.....	30
Figure 14 – Flood frequency distribution for annual maximum flow of the Rhine river in Cologne, Dusseldorf and Lobith	34
Figure 15 – Flood frequency distribution for annual mean flow of the Rhine river in Cologne, Dusseldorf and Lobith	35
Figure 16 – QH-curve for Lobith hydrological station with trend lines	36
Figure 17 – Frequency of discharge values occurrence for Lobith hydrological station.....	38
Figure 18 – Sediment rating curve For Rees Hydrological station	39
Figure 19 – Sediment yield density interpolated to Lobith hydrological station	39
Figure 20 – Cumulative sediment yield curve for Lobith hydrological station.....	40
Figure 21 – Simulated flood extent on January 31 st , 1995 in the downstream part of the Lower Rhine basin.....	41
Figure 22 – Simulated flood extent on January 31 st , 1995 in the middle part of the Lower Rhine basin	42
Figure 23 – Simulated flood extent on January 31 st , 1995 in the upstream part of the Lower Rhine basin.....	42
Figure 24 – Model calibration by comparing predicted and measured water level series in lower rhine during the January, 1995 flood	43
Figure 25 – Calibration between detrended water level predictions and measurement regardless of their location.....	46
Figure 26 – Comparison of predicted and observed Water level series of December, 1993 flood in Lower Rhine	47
Figure 27 – Simulated flood extent on December 25 th , 1993 in the downstream part of the Lower Rhine basin	48
Figure 28 – Simulated flood extent on December 25 th , 1993 in the middle part of the Lower Rhine basin.....	49
Figure 29 – Simulated flood extent on December 25 th , 1993 in the upstream part of the Lower Rhine basin.....	50
Figure 30 – Comparison between measurement data, reference scenario and prediction for water level in Lower Rhine using annual maximum discharge with 2 years return period as bankfull flow approximation.....	51
Figure 31 – Comparison between measurement data, reference scenario and prediction for water level in Lower Rhine using annual maximum discharge with 1.5, 2.0 and 5.0 years return period as bankfull flow approximation.....	52

Figure 32 – Correlation plot for predicted and reference water levels in Lower Rhine using annual maximum discharge with 1.5, 2.0 and 5.0 years return period as bankfull flow approximation (Part 1)	53
Figure 33 – Correlation plot for predicted and reference water levels in Lower Rhine using annual maximum discharge with 1.5, 2.0 and 5.0 years return period as bankfull flow approximation (Part 2)	54
Figure 34 – Comparison between measurement data, reference scenario and prediction for water level in Lower Rhine using annual mean discharge with 2 years return period as bankfull flow approximation	55
Figure 35 – Comparison between measurement data, reference scenario and prediction for water level in Lower Rhine using annual mean discharge with 10 years return period as bankfull flow approximation	56
Figure 36 – Comparison between measurement data, reference scenario and prediction for water level in Lower Rhine using annual mean discharge with 50 years return period as bankfull flow approximation	57
Figure 37 – Comparison between measured and predicted inundated area in Lower Rhine using annual mean and maximum discharges approximation	58
Figure 38 – Comparison between modelled flood extents in middle part of the Lower Rhine for reference scenario (left) and 1-in-2 years Annual maximum discharge assumption	59
Figure 39 – Comparison between modelled flood extents in upper part of the Lower Rhine for reference scenario (left) and 1-in-2 years Annual maximum discharge assumption	59
Figure 40 – Comparison between measurement data, reference scenario and prediction for water level in Lower Rhine using hydraulic geometry relationships to determine bankfull flow approximation	60
Figure 41 – Comparison between measurement data, reference scenario and prediction for water level in Lower Rhine using effective discharge as bankfull flow approximation	61
Figure 42 – Comparison between measurement data, reference scenario and prediction for water level in Lower Rhine using half-yield discharge as bankfull flow approximation	62
Figure 43 – Comparison between measurement data, reference scenario and prediction for water level in Lower Rhine using infinite dikes assumption	66

List of tables

Table 1. Tributary effect on the Lower Rhine flow	15
Table 2. Numerical schemes implemented in LISFLOOD-FP model (Bates et al., 2013).....	18
Table 3. Parameter values used for different types of simulations	23
Table 4. Roughness classes	26
Table 5. Flood frequency distribution quality assesment for annual maximum flow of the Rhine river in Cologne, Dusseldorf and Lobith.....	34
Table 6. Calculation of average bankfull depth for annual maximum discharge approximations.....	34
Table 7. Flood frequency distribution quality assesment for annual mean flow of the Rhine river in Cologne, Dusseldorf and Lobith.....	35
Table 8. Calculation of average bankfull depth for annual mean discharge approximations	35
Table 9. The assesment of $W_{bf} = Q_{k,mean}$ assumption	35
Table 10. Volume of the dike overflow happened due to uncertainties in The model input files in simulation of January, 1995 flood	43
Table 11. Assesment of calibration parameters efficiency for Lower Rhine	44
Table 12 – Integrated overview of calibration run performance with Manning’s $n = 0.028 \text{ s/m}^{1/3}$ for January, 1995 flood.....	46
Table 13. Integrated overview of validation run performance for December, 1993 flood	48
Table 14. Volume of the dike overflow happened due to uncertainties in The model input files in simulation of December, 1993 flood	50
Table 15. Integrated goodness-of-fit metrics (part 1).....	63
Table 16. Integrated goodness-of-fit metrics (part 2).....	64
Table 17. Maximum observed deviation of the water level prediction from the reference case scenario for infinite dike assumption.....	66

1. Introduction

1.1. Problem definition

Floods are one of the most common natural disaster on Earth. Over the last century, floods have led to more than 540,000 deaths and 360,000 injuries, excluding the estimated 40,000 – 2.7 million injuries that went unrecorded (Doocy et al., 2013). The modern trend for intensification of extreme weather conditions due to Climate Change, as well as, deforestation, population growth and its increasing proximity to the coastal areas allows to suggest the rise of these numbers. Currently, almost 30% of total population around the world (2.2 billion people) of the Earth live in close proximity to the locations which are exposed to floods of 100 years return period (Rentschler and Salhab, 2020). In recent years, even more people have settled in close vicinity of the coast or overflowing river banks, which certainly leads to the increase in potential flooding damage both to human health and infrastructure.

However, much of the damage caused by flooding could be alleviated using various safety measures. Many of such include the flood inundation modelling in its implementation. The modelling is necessary part of the flood defences construction, as well flood hazard maps are most often used during the planning process for land use. In summary, flood inundation models help to estimate the damage from the possible flood event and transfer this knowledge into decision making during urban development planning.

The results of such models' simulations are commonly used by a wide range of end users starting from farmers and ending with governmental services. However, high data availability demands and computational requirements of relevant hydraulic or hydrological models make the flood prediction in many of the developing countries nearly impossible to implement. The recent advances in the field of global flood inundation modelling were achieved mainly through the increased availability of remote sensing data. More accurate, dense and widespread data of ground elevation and real flood event extents have enabled various empirical, conceptual and hydrodynamic models to be developed, calibrated and validated across the globe (Teng et al., 2017).

Unfortunately, due to inability of modern remote sensing instruments to penetrate water, our understanding of the shape and size of river channels at any meaningful spatial scale has not benefited from these advances. This creates some major challenges which had to be faced in further progress of flood inundation models. Sampson et al. (2015) has defined six key elements of a good global flood inundation model:

1. Global terrain data quality;
2. Extreme flow simulation;
3. *Global river network and geometry representation;*
4. Flood defences implementation;
5. Computational hydraulic engine;
6. Automated framework creation.

Each element is of a great importance to the performance of the model. Currently, several main constraints could be identified in the field of global flood simulation including (1): difficulties with distinction of the urban and vegetated landscapes from the surface layer during remote elevation measurements; (2): scarce precipitation data, land use interference into the runoff process; (3): the problem of this research, it is discussed more closely in the next paragraph; (4): the problems with the small scale defences implementation into the model; (5): the representation of dynamic nature of the river system and (6): input parameters.

Another feature required in any good flood inundation model concerns the representation of river network in general and channel dimensions particularly (3). However, inability of remote sensing measurements to account for the channel size in rivers makes the flood prediction in data scarce regions nearly impossible. According to the topic of this research, the main focus will be concentrated on estimation of various channel size approximations effect on the performance of flood inundation models. For rivers where explicit field measurements of channel bathymetry are unavailable, various channel size estimates are adopted to account for bed morphology in flood inundation models.

It is a common assumption that the river channel size corresponds to the dominant discharge value (Wolman and Miller, 1960). In other words, the channel conveyance, or bankfull discharge, in rivers of unknown bathymetry is often assumed to be equal to the water discharge rate which induces

the most bed sediment transport over a long period, thus causing the most significant river channel evolution. Most commonly, for modelling purposes the dominant flow rate is adopted as a flow of 1-in-2 years frequency (Woodyer, 1968; Williams, 1978; Wilkerson, 2008). This is in spite of understanding that some rivers may flow out of bank seasonally (e.g. the River Niger) or much more infrequently due to human modifications (e.g. the River Thames in central London).

Generally, dominant discharge and, thus, the value of bankfull discharge differs significantly depending on hydrological regime and local river basin conditions. However, referring to global modelling objectives, this local influence could not be studied explicitly for most of the rivers. Therefore, the simplifications of channel size, as for now, are an essential part of global flood inundation modelling and should be addressed with the great accuracy.

1.2. Objective and research questions

One of the aims of flood inundation modelling is to predict flood events and implement measures accordingly. In highly populated areas this becomes even more important as the larger amount of people and infrastructure is exposed to the influence of the river and its dangers. Additionally, urbanised areas in the close proximity of the flooding rivers enhance water run-off from the watershed to the river channel increasing the danger posed by inundation. The Lower Rhine basin, that has been studied specifically in this research, will serve as a representative case of a flooding river with the high influence of anthropogenic factors.

In accordance with the topic of this study and present knowledge gap, the main research objective is *to quantify how different channel size estimates influence the performance of flood inundation modelling*. Both qualitative and quantitative impact of such assumptions are considered. The qualitative assessment will consider the overall analysis of the studied estimates effect on the simulation outcome based on the visual compliance of produced characteristics series, while the quantitative analysis will include the calculation of statistical significance for the noted differences between simulated runs for various channel size assumptions. To fulfil the suggested goal, two research questions will be studied separately throughout the research.

1. How does 1-in-2 years bankfull discharge assumption influence the outcome of flood inundation modelling?

As it was mentioned previously, although the assumption of a river going out of its banks once in 2 years (1-in-2 years bankfull discharge) being most commonly applied, it does not hold for the most of the rivers. While some flood seasonally, others could not exceed their banks in a long time due to a number of reasons. This could be caused by human induced flood management or by the features of the climate in the region. However, such an assumption proved to be sufficient for the flood modelling purposes (Wolman and Miller, 1960; Sampson et al., 2015).

This research intends to optimise the performance of the global flood inundation model based on its channel size assumption. Therefore, it is required to perform a comparative analysis of the different approximation techniques. For this purpose, the exact impact of each method should be determined.

2. How do flood inundation models perform considering other methods to estimate the river channel size are applied compared to 1-in-2 years bankfull discharge assumption?

In order to improve the model performance, the best way to represent the river channel should be found. Such methods should not depend on bathymetry measurement data availability, as well as they should be physically or statistically based on some theoretical background. In this research, 4 methods to account for the channel bathymetry are studied. These are:

- Maximum annual flow characteristic value (for 1.5, 2.0 and 5.0 years return periods);
- Mean annual flow characteristic value (for 2, 10 and 50 years return periods);
- Hydraulic geometry relationship;
- Dominant discharge characteristic value.

The procedure for determining each of the channel size assumptions is presented in Chapter 4. The provided assumptions will be tested using statistical metrics for the compliance with the reference scenario with known bathymetry.

1.3. Research outline

This master thesis report contains six chapters. In the Chapter 2 the theoretical background as well as geographical reference are specified. It includes the information about the simulated flood events, which is provided in high detail, along with the description of the model regarding both its background and history of development as well as technical details on the program used during the study. Additionally, theoretical information about the concept of channel size assumptions, common approaches to its determination and worldwide experience is stated in that section. Chapter 3, in its turn, is devoted to the practices which were applied during the research for preparation of the model input data, as well as description of the data required for the model to work properly. Also, the approach to performing model runs were detailed in there including the attitude towards calibration and validation of the model and assessment of their results. Chapter 4 explains the approaches for dealing with channel size assumptions, how they are created and what information is required to do it. Also some first-hand theory behind these assumptions is specified where needed. Chapter 5 presents the results of the model set up including calibration and validation results. Since the validation run serves as a reference to other simulation output, the results of validation model are thoroughly studied in this section using various statistical metrics and comparison graphs. Chapter 6 consists of the model outputs for different channel size assumption scenarios containing the resulting graphics and goodness-of-fit for all tried methods.

As the first research question has considered the sole channel size assumption, the single Section 6.1 of the results modelling results chapter was dedicated to answering it thoroughly. In order to answer the first research question, first of all, the LISFLOOD-FP model has been set up, calibrated and validated on 2 independent hydrology. Then, the flood frequency distribution was found based on historical river flow series in order to determine 1-in-2 years annual peak discharge value which is commonly used as a bankfull flow estimation. After the annual maximum discharge was transited into bankfull depth approximation for river channel, the built model was used to perform a simulation run for the assessment of the derived 1-in-2 years assumption. The performance of the biennial bankfull flow scenario run was evaluated by comparison with the measurement data using several skill tests including visual compliance, statistical metrics, correlation graphs and signal detection theory (SDT) based on 2 flood characteristics: water level series and flood extent. Finally, the conclusions were drawn based on the finding made during the analysis.

The second research question was then being addressed throughout the whole Chapter 6. To answer this research question, the model framework used in previous question was also used. 3 different channel size approximation approaches were considered, namely: hydrologically-driven (based on flood frequency distribution); process-driven (based on sediment transport relationships); and based on regionalised parameter relationships. All of the channel size assumptions were considering some bankfull discharge estimation from which the channel size was derived based on Chézy formula and, consequently, used within the LISFLOOD-FP model framework. After the completion of all simulation runs, the goodness-of-fit analysis was conducted comparing the modelling output to measurement data, referential scenario output with known channel dimensions and to the outcome of the 1-in-2 years annual maximum discharge assumption, as the generally used assumption for channel size in river without elaborate bathymetry data. The main drawbacks and advantages of each of the selected channel assumption were distinguished to answer the second research question.

The discussions, conclusions and recommendations drawn from the analysis made during this research are generalised in Chapters 7 and 8. The results of the conducted evaluation of the various channel size assumptions performance were used to draw final conclusions, as well as, provide practical recommendations on the applicability of proposed methods and further research prospects. The discussions section considered the effect which urbanization and heavy anthropogenic load in the basin has on the procedure of flood inundation modelling, its outcome and the applicability of the channel size assumptions, as well as, it elaborated on the major uncertainty sources which were incorporated in the research and their influences.

2. Research background

2.1. Study area

The study area of this research covers the section of the Rhine river basin between Bonn, Germany and Lobith, Netherlands also known as Lower Rhine (Niederrhein; Figure 1). The Rhine is the second-longest river in Central and Western Europe, with its length of about 1230 km it runs through 6 countries until it eventually flow into the North Sea. Due to its geographical location, Rhine river serves as a vital navigation waterway carrying trade and goods starting from ancient times. Moreover, the population which is highly exposed to the influence of the Rhine in the studied region reaches almost up to 10 million people (Cologne and Dusseldorf regions populations combined according to State Office for Information and Technology..., 2020).



FIGURE 1 – MAP OF THE RHINE BASIN (BY DANIEL ULLRICH)

Although Lower Rhine flows through highly urbanised territory of North Rhine-Westphalia, the levees are located at some distance from the river so that during high water Lower Rhine waters has some space for widening unlike in upstream reaches of the Rhine where it is mostly locked within its banks. The most populated and industrialised areas within the study area are the agglomerations of Cologne, Dusseldorf and Ruhr area.

The downstream boundary of the domain was chosen so that it will be located before the Rhine partitioning into Waal and Nederrijn rivers. This will allow to set easier downstream boundary conditions and achieve greater stability of the model. The upper boundary of the study domain, on the other hand, coincides with Bonn hydrological station which allows to inflict the measurement data as the boundary condition there. The domain also includes the largest tributaries of the Lower Rhine, which are Sieg, Ruhr and Lippe rivers. Their inflow represents a substantial part of the overall Rhine runoff at the studied reach, therefore it was important to include them as the part of study area during this research.

The flow regime of the Rhine River is dominated by snowmelt and precipitation runoff from the Alps in summer months, and by precipitation runoff from the uplands in winter. Further downstream, the influence of the uplands grows more significant, and over the year the discharge becomes very even. The annual hydrographs of some gauges along the Rhine (Figure 2) illustrate the changes in the flow regime along the river course and show that the discharge components from the

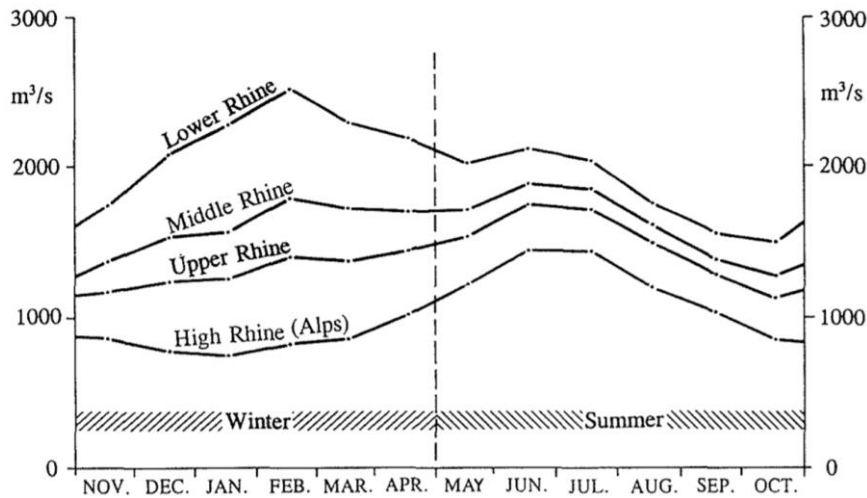


FIGURE 2 – VARIATION OF MEAN MONTHLY DISCHARGES AT SELECTED GAUGES ON THE RIVER RHINE (ENGEL, 1997)

The hydrological regime of the Lower Rhine river is characterised by the winter maximum, typically the peak discharges are observed from January to February. However, the maximum discharge values on average do not significantly exceed the annual discharges of late Spring and Summer periods. The low-water period on the Rhine basin could be observed in middle to late Autumn.

The Rhine River basin consists of a number of sub-basins which respond to very different meteorological conditions. Rhine floods have always become catastrophic when extreme runoff was discharged from several of these sub-basins at the same time. However, the long series of hydrological records (since 1000 AD) does not list a single flood event that has occurred simultaneously in all sub-basins with comparable magnitude (Engel, 1997).

2.2. Flooding in Lower Rhine

Although, the Rhine basin has always been a subject to extreme flood events, the current level of urbanization in this territory does not sufficiently influence, and certainly not create, the severity or even frequency of such events (Engel, 1997). Locally, effects of urbanization, such as paved surfaces, can significantly intensify the formation of floods. On a large-scale, however, the proportion of anthropogenically sealed land surfaces, for instance, on German territory is only around 12%. Meanwhile runoff coefficients of more than 50%, which are necessary to generate major floods, can be produced only by natural processes.

The series of annual peak discharges of some Rhine gauging stations since 1891 show an increasing tendency for extreme flood events. For instance, such series has been designed for the Cologne gauge (Figure 3). This applies to all the stretches of the Rhine, but it is more profound in the Lower Rhine (Engel, 1993). The trend is alternating interannually being occasionally interrupted by several years of recession, but showing a positive growth over the past century. The similar conclusions were made on the annual low-flow mean discharges (Engel, 1997). All of this implies the growth of the flooding threat to the population and assets located on the Rhine river floodplains.

The research of the channel size estimates applicability would be done based upon two separate extreme flood events occurred in Lower Rhine almost 20 years ago. One of the flood events will be used for calibration of the model with elaborate channel dimensions while the other will participate in assessment of the channel conveyance estimate assumptions.

The description of 1993 and 1995 floods was based on the work of Disse and Engel (2001) and is presented in Sections 2.2.1 – 2.2.2.

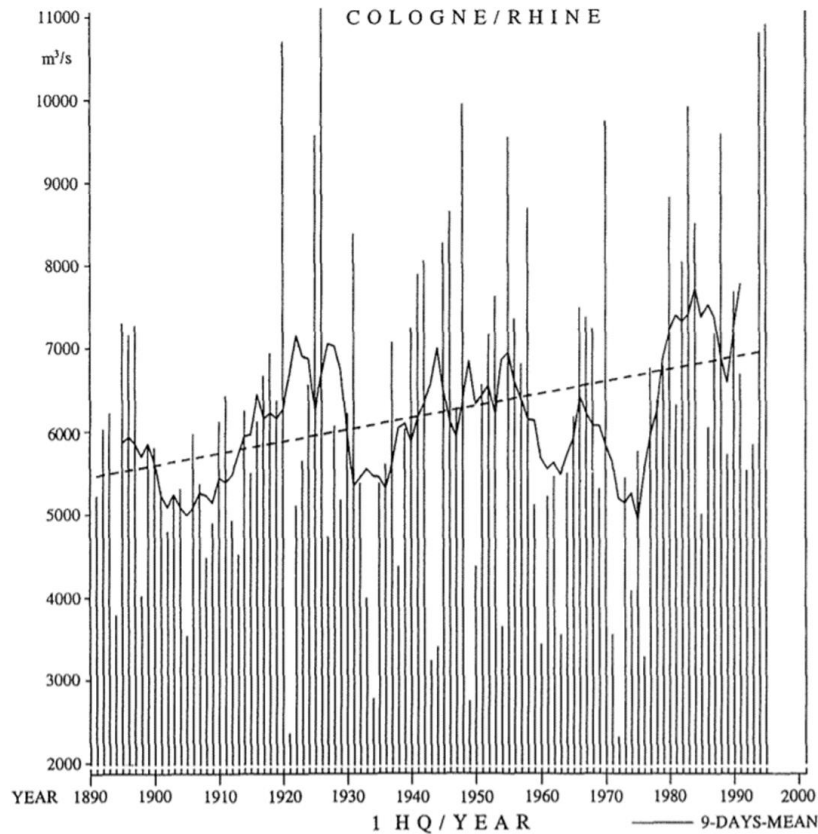


FIGURE 3 – HIGH-WATER DISCHARGES SERIES FOR THE 1891-1995 PERIOD AT THE COLOGNE GAUGING STATION ON THE RHINE (ENGEL, 1997)

2.2.1. December, 1993 – January, 1994

In 1993 (Engel et al., 1994), after a period of heavy rainfall from 7th to 18th December, an extreme hydrological situation was created simultaneously on several Rhine tributaries in the upper reaches of the basin. The rain has brought almost average monthly precipitation value in a week time. Subsequently, soil in the basin was saturated quickly leading to extreme catchment runoff.

Then the inflows from the Neckar, Main and Nahe rivers came in and increased the recurrence probability of the peak flow in River Rhine to about 35 years. At Koblenz, the discharge peaks of the Rhine and Moselle rivers met with some time lag. The flow in the lower Moselle, with nearly 4200 m³/s, the highest since the beginning of regular observations in 1817, generated a wave in the Lower Rhine with a peak that had been exceeded in this century only once.

At Cologne it has reached such high surface elevation and stayed there over such long period of time that the temporary flood protection wall, that had been constructed there to protect the old city, was overflowed for almost 70 hours. The substantial dikes, that begin just a few kilometres north of Cologne, largely prevented flooding and damage further downstream.

The 1993 flood hydrographs of the tributaries included into the research show significant differences not only in absolute values of the discharge but also in its form (Figure 5). The major distinction occurs in ranges of river discharge variability which mainly is affected by local landscape and the size of the basin. The Ruhr hydrograph for 1993 December – January flood event is characterised by the most intense variations in discharge during the 3rd peak (30.12.1993 – 12.01.1994) when the flow rate increases from 200 to 900 m³/s and back over the span of 2 weeks. Despite the smaller average discharge in Sieg river, the absolute values of the 1st (13.12 – 18.12.1993) and 2nd (19.12 – 29.12.1993) peaks are comparable to those in Ruhr river with maximum discharge rates of around 350 and 550 m³/s, respectively. The 1993 flood event observed at the Schermbeck (Lippe) hydrological station could be characterised as prolonged period of smooth discharge raise from 50 to 300 m³/s over the period of 1.5 month.

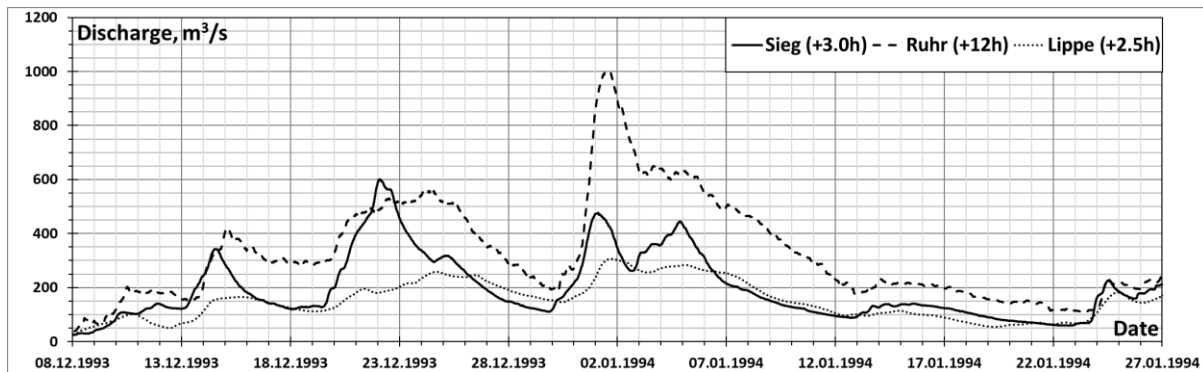


FIGURE 4 – LOWER RHINE TRIBUTARY DISCHARGE SERIES WITH APPLIED LAG

All 3 implemented tributaries vary by effect they enact on the overall Rhine flood hydrograph (Table 1). The most significant influence on the flow of the Rhine during the studied period in 1993 was exerted by the Ruhr river. At the largest discharges it has reached almost 10% of the overall flow coming into the domain. However, the significance of the Ruhr inflow is more limited during low flow periods. Both other tributaries' effect was found to be limited by less or equal than 5% depending on situation. However, as was mentioned earlier, the precision of the input discharge values in the LISFLOOD-FP should be up to $\pm 10\%$ in order to accurately represent the hydrodynamics using the model. Therefore, including those tributaries' inflow is extremely important to obtain the best representation of the studied flood events as their combined impact exceeds this criterion.

TABLE 1. TRIBUTARY EFFECT ON THE LOWER RHINE FLOW

	Sieg	Ruhr	Lippe	Rhine (Bonn)
$Q_{\text{average}}, \text{m}^3/\text{s}$	169	270	140	4381
%	4%	6%	3%	100%
$Q_{\text{max}}, \text{m}^3/\text{s}$	561	901	306	10500
%	5%	9%	3%	100%

The temporal discrepancy between the flow peaks occurrence on the Rhine river and its tributaries also deserves the attention. From the hydrographs comparison (Figure 12 and Figure 4) the lag between maximal discharge values arrival on different river in Lower Rhine basin varies from 1 to 7 days due to complex nature of the flood genesis which considers many spatially and temporally volatile parameters. The Sieg river is characterised by the most similar to the Rhine's flow variability at Bonn, which is explained mainly by their relative spatial proximity resulting in homogeneity of meteorological, hydrological and local conditions. The high influence, which the Ruhr inflow imposes on the overall Rhine discharge at their confluence location (Table 1), induces the high importance of the lag on the simulation outcome. The most significant impact could be observed on January 1st of 1994 when 900 m^3/s is discharged into the Rhine river from the Ruhr's channel while the Rhine's discharge before confluence is around 5000 m^3/s .

2.2.2. January, 1995 – February, 1995

The flash flood effect in 1995 originated from severe snow melting and frozen soil other than from soil saturation, thus leading to rapid runoff of the extreme rainfall from the watershed into the river channel. Such heavy precipitation resulted in catastrophic runoff events. The amount of rain falling during these periods was equivalent to 200% of the 30-year means of December and January, respectively.

In 1995 (Engel, 1995) the peak discharge at the border of the Alps corresponded to a recurrence period of about 20 years, but the flood situation there lasted even less than 24 hours. In the course of one day, discharges returned to the long-term mean high water. Because the inflows along the Upper Rhine were rather insignificant, the recurrence interval of the peak in the River Rhine downstream to the mouth of the River Main fell below 10 years. However, with extreme flood flow in River Main, the maximum discharge in the Middle Rhine exceeded that of Christmas 1993. The situation was different

at Koblenz, where the peak discharge of the River Moselle was more than 600 m³/s less than in 1993, so that the water level remained 31 cm below that of 1993.

Widespread extreme precipitation in the headwater region of a small tributary north of the mouth of the River Moselle increased the flood towards Cologne so much that – despite these favourable conditions upstream – the gauge there climbed 6 cm higher than in 1993, to reach the same level as the maximum water stage at Cologne in this century (in January 1926). Finally, the last gauging station before the German – Dutch border recorded 12 000 m³/s and a stage 1 cm above the 1926 mark.

The two flood events described in this section were characterized by a very steep rise at the beginning. For instance, the 5 m increase in water level of lower Moselle over 24 hours has set historical record. Additionally, both flood was characterised by significantly high water discharged at the time of the inundation. shows stereographic representations of the flood waves in the River Rhine of December 1993/January 1994 and of January 1995 (Engel, 1997).

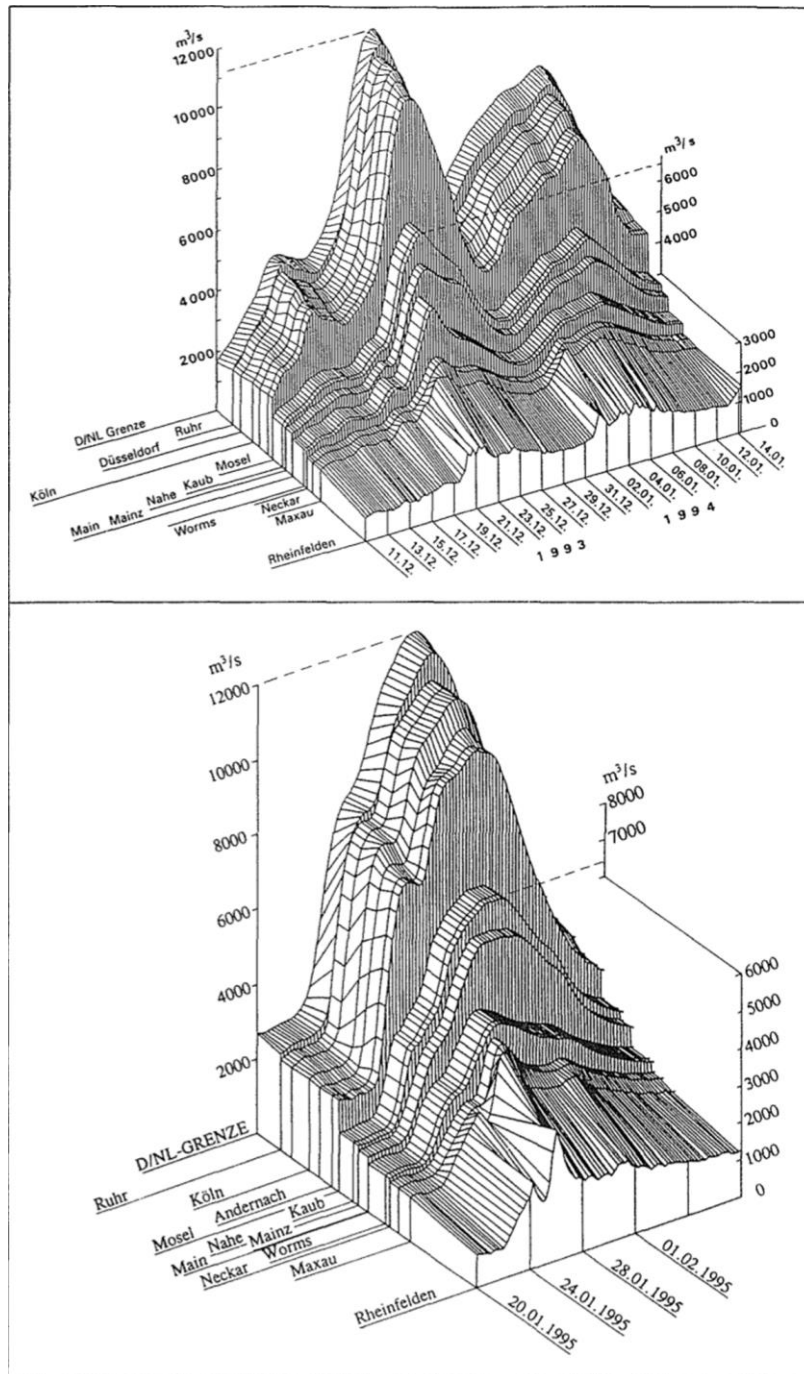


FIGURE 5 – STEREOGRAPHIC REPRESENTATION OF THE FLOOD WAVES OF DECEMBER 1993/JANUARY 1994 AND JANUARY 1995 FLOODS ON THE RIVER RHINE (ENGEL, 1997)

It could be seen from the picture above that the two studied floods are represented by different shape of the flood wave. Due to duality of its genesis, the December 1993 flood is characterised with two separate peaks values corresponding to the lag observed between maximum flood in the Rhine upstream of Koblenz and in the Moselle. The January 1995 flood, on the other hand represents a simple single-peak flood event, though with slightly higher maximum water levels.

2.3. Model framework

2.3.1. Flood inundation modelling

Rapid development of global flood inundation modelling techniques started less than 20 years ago. One of the first models to simulate this process were often based on linking regional or global climate models with flow routing through the river catchment. The hydrological scheme could include several components depending on the response rate of the layer. Commonly, modern models make distinction between surface and subsurface flow. The simulated flow in climate-routing model could depend on such parameters as meteorological condition, orography, soil properties, land type and other regional characteristics.

Another type of global flood inundation models utilizes a link between water storage, water level and flooded area based on a digital elevation model (DEM) data in order to realistically represent the floodplain inundation dynamics during the flood. Such models use a diffusive wave equation to determine flow rates in a physically justified way. However, although they showed good correlation with the extent of real flooding events, hydrodynamic models are largely dependent on availability and quality of the input parameters. Also a number of uncertainties are always included into the formulation of the model as the simulation requires many assumptions to be made in parametrization of the natural processes.

Lastly, throughout recent years several global models were created based on volume spreading algorithms of various kind. This type of models is based on so-called “bathtub” approach, meaning that flood extent is derived from link between water level (volume) and altitudinal horizontal planes of DEM. Such models often use climatic data sets of precipitation, temperature and potential evaporation to drive global hydraulic flow routing models (Winsemius et al, 2013). However, such modelling approach generally does not consider anthropogenic impact on flooding probability and is limited to low protection standards due to short climatic input data series.

The software used in this research, LISFLOOD-FP, was produced by the employees of School of Geographical Sciences of University of Bristol and Fathom back in 2015. It is a global flood inundation model based on shallow water equations, which could work with a spatial resolution of approximately 90 m and was designed to be used in the areas of limited local observation data (Sampson, 2015).

2.3.2. LISFLOOD-FP model

In this work the shareware implementation of the LISFLOOD-FP raster flood inundation model version 5.9.5 was used. It provides the user with a general tool for simulating fluvial or coastal flood spreading. As the output, the model gives a set of raster maps of values for a number of flood water parameters such as water depth, water surface elevation, velocity, etc. for each grid cell in selected time intervals. The values for water stage and discharge could also be obtained in initially determined gauge locations.

The LISFLOOD-FP model operates with a set of shallow water equations (SWE) differing slightly depending on a choice of numerical scheme used to represent the hydrodynamics of the flow (De Almeida and Bates, 2013). The momentum and continuity equations for the 1D full shallow water equations are given below:

$$\frac{\partial Q_x}{\partial t} + \frac{\partial}{\partial x} \left(\frac{Q_x^2}{A} \right) + gA \frac{\partial(h+z)}{\partial x} + \frac{gn^2 Q_x^2}{R^{4/3} A} = 0,$$

$$\frac{\partial A}{\partial x} + \frac{\partial Q_x}{\partial x} = 0,$$

where Q_x is volumetric flow rate in the x Cartesian direction (m^3/s), A – the cross sectional area of flow (m^2), h – the water depth (m), z – the bed elevation (m), g – gravity (m/s^2), n – the Manning’s coefficient of friction (-), R – the hydraulic radius (m), t – time (s) and x – the distance in the x Cartesian direction (m).

Once the bankfull height of particular part of the channel reach is exceeded, water moves from channel to the adjacent floodplains where two-dimensional lateral flood spreading is simulated using a storage cell concept applied over a raster grid. This concept could be realised within the model using three distinctive options varying in their physical complexity.

The numerical schemes (or solvers) used in the model differ for floodplain and channel flow simulations and give opportunities to adjust the simulation to the needs of the research and available computation resources. Generally, solvers vary from each other on account of shallow water term included or excluded in the simulation (Table 2).

TABLE 2. NUMERICAL SCHEMES IMPLEMENTED IN LISFLOOD-FP MODEL (BATES ET AL., 2013)

Solver	Dimen- sions	SWE terms included	SWE terms assumed negligible	Time step	Further details
Solvers for floodplain flow simulation					
Routing	1D on 2D grid	User specified velocity and bed slope direction	All	Adaptive	Sampson et al., 2012
Flow-limited	1D on 2D grid	Friction and water slopes	Local and convective acceleration	Fixed	Bates and De Roo, 2000
Adaptive	1D on 2D grid	As above	As above	Adaptive	Hunter et al., 2005
Acceleration	1D on 2D grid	Friction and water slopes, local acceleration	Convective acceleration	Adaptive	De Almeida and Bates, 2013
Roe	2D	All	None	Adaptive	Neal et al., 2012b
Solvers for channel flow simulation					
Kinematic	1D	Friction slope and water slope including bed gradient (dz/dx)	Local and convective acceleration, free surface gradient (dh/dx)	Linked to floodplain solver or fixed	Bates and De Roo, 2000
Diffusive	1D	Friction slope and water slope including bed and free surface gradients ($d[z+h]/dx$)	Local and convective acceleration	As above	Trigg et al., 2009
Sub-grid channel	1D	Friction and water slopes, local acceleration	Convective acceleration	Adaptive	Neal et al. 2012a

Most of the model solvers exclude the local acceleration term from the SWE formulation. However, this term is crucial during modelling scenarios with dynamic water surface gradient, and therefore is needed for this research. From the channel flow solver only sub-grid version does not exclude local acceleration term from the Shallow Water Equations. Additionally, sub-grid model provides the user with easy tool for implementing channel size assumption via its special river channel definition method. Therefore, in order to reduce the amount of uncertainty sources the sub-grid channel solver which is mandatory coupled with acceleration model will be used in this research to perform a flood inundation modelling using LISFLOOD-FP. As an example of possible uncertainties to which the model could be exposed in case of local acceleration exclusion, few comes to mind. For instance, flood wave propagation speed could be underestimated in case of extremely low Manning's friction coefficient values or relatively high Froude number (De Almeida and Bates, 2013).

Sub-grid solver is the most recently developed method for representing rivers channels in LISFLOOD-FP embedded with the 2D domain. Flow between channel segments is calculated based on the friction and water slopes, and local water acceleration (i.e. using the 'acceleration' model equations). Only convective acceleration is assumed negligible. For any cell containing a sub-grid channel segment, the solver calculates the combined flow of water within the cell, contained both within the channel located in that cell and across the adjacent floodplain. The model is designed to operate over large data sparse areas where limited channel section data are available. Regarding the most accurate channel flow solver, only the convective acceleration has been assumed negligible in the sub-grid solver. However, due to the nature of channel flow during flood event, this will not pose any significant inaccuracies in the modelling outcome (Abebe et al., 2016). Additionally, the sub-grid numerical scheme adds the ability to simulate channel flow for rivers of width smaller than the grid resolution as an extension to LISFLOOD-FP (Neal et al., 2012a).

The LISFLOOD-FP model requires several datasets to serve as an input data. The most basic are: the surface elevation in the studied region; boundary condition (typically defined at the borders of the domain); channel geometry in the river network including channel slope, channel width and bankfull depth and friction parameters in both channel and surrounding floodplains.

Additionally, the LISFLOOD-FP demands user to determine the model time step. However, in most of the solvers, as well as in sub-grid/acceleration model, the adaptive time step function is enabled. That means that the optimum value for time step to maintain stability is calculated according to the Courant-Friedrichs-Lewy (CFL) condition for shallow water models which is related to the values of the cell size and water depth. The value of the time step changes after each iteration until the user-defined maximum CFL value is met. By default, the CFL value is set equal to $C_{max} = 0.7$.

The base two-dimensional LISFLOOD-FP model uses an explicit forward difference scheme on a staggered grid. Though arranged in two dimensions, the momentum equation implemented across each face of each grid cell is in fact a one-dimensional calculation such that the fluxes through each cell face are decoupled from each other (Bates et al., 2013).

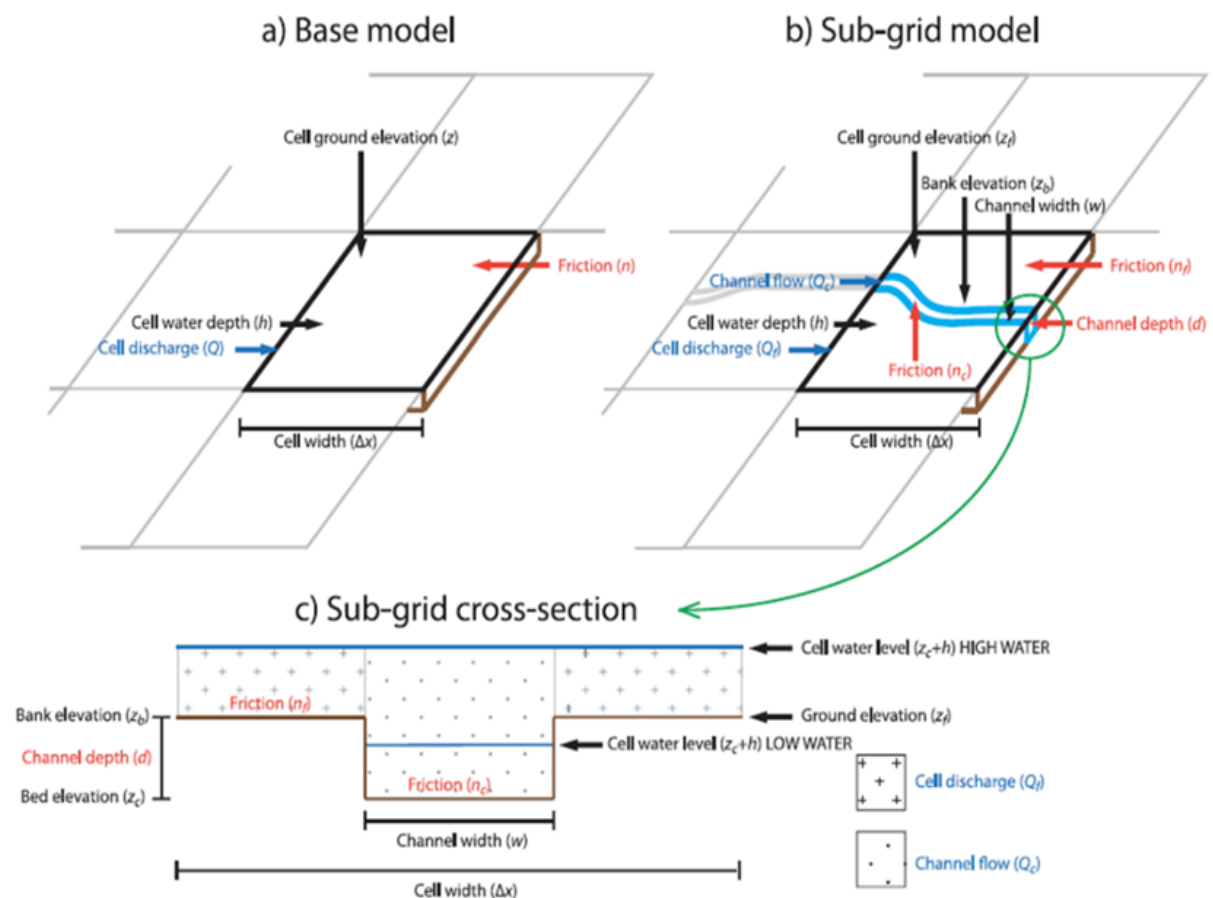


FIGURE 6 – CONCEPT OF (A) LISFLOOD-FP BASE MODEL, (B) SUB-GRID CHANNELS MODEL AND (C) SUB-GRID SECTION (NEAL ET AL., 2012)

To extend the base model for sub-grid implementation at large scale application two major changes are made in the model (Figure 6):

1. A sub-grid scale channel network was introduced allowing any size of river channel to be represented in the model;
2. An estimation of unknown channel depth using hydraulic geometry theory and data on channel width and bank elevation values was incorporated.

One of the main inaccuracies in hydraulic modelling lies within parameterization of a global channel. This is especially true for the LISFLOOD-FP and sub-grid model solver specifically. That implies that, at low flow, the lack of knowledge about local hydrology properties and assumption of rectangular channel geometry may play a major role in creating deviation from the observed picture. Therefore, additional focus should be put on improvement of channel representation methods in the future.

There are some key model assumptions and related limitations which should be addressed before the model could be implemented (Bates et al., 2013):

- The model is limited to situations of substantial data availability on boundary conditions and channel geometry in fluvial flows;
- The model assumes flow to be gradually varied, however the Roe solver could also handle rapidly varying in time flows;
- The river channel is approximated as a rectangle with sufficiently large width (so that lateral friction is neglected and wetted perimeter could be simplified as the channel width);
- Floodplain flow is treated as a series of storage cells which are represented with a raster grid where the flow goes in Cartesian coordinate directions only;
- There is no exchange of momentum between the channel and floodplain flows, only mass exchange is present;
- Lateral friction is assumed negligible during floodplain flow.

By the direct benchmark trial against high-quality process-based model simulations it was determined that the LISFLOOD-FP model is typically able to capture between 65 – 85% of actual flooded area (for non-tidal rivers) which is extremely close to the effectiveness of the local scale models. However, it was found that the model performance reduces along smaller channels while overestimating their discharges due to higher uncertainty in surface elevation data (Sampson, 2015).

The model according to the performance test has indicated a great potential to be used for flood hazard estimation in areas where there is no detailed measurement data available. However, at smaller scales, knowledge of the catchment, channel and floodplain topography becomes a restricting factor for such model. Therefore, further investment into higher resolution terrain sets and into better estimation of river channels is required in sake of the global flood inundation modelling development.

2.4. Channel size approximations

In order to determine the extreme flow rates in river channels during the flood, it is drastically important to correctly estimate the river channel conveyance, characterised by both the channel's width and depth (Fewtrell et al., 2011). The river width could currently be estimated using remote sensing methods, namely with the help of satellite imagery. It is still impossible, however, to measure channel depth remotely on regional or global scale (Sampson et al., 2015). So, the only option to perform the flood inundation modelling for areas where no measurement data is present is using an appropriate channel size assumption.

Generally, there are several methods to define river channels in data sparse flood inundation models could be distinguished (Neal et al., 2020). Namely, these are:

1. No channel method (simplest, bankfull flow estimate removed from design flood);
2. Empirical/Hydraulic geometry method (geographical analogy, rough estimation);
3. Uniform flow theory (water depth calculated from Manning's equation);
4. Non-uniform flow (numerical iterations from control point with known uniform flow).

The first approach has been omitted from the scope of this research due to many uncertainties related to it. In this research, the methods 2 and 3 will be viewed closely as they are much less data-dependent compared to the method 4.

As it was stated previously, often river channel is approximated by the value of bankfull discharge equal to 1-in-2 years flow rate for the studied location (Andreadis et al., 2013; Leopold, 1994). The discharge value of required return period is usually found from flood frequency distribution based on the historical measurement series. Further, the Manning's equation is used to evaluate the channel depth with the help of bankfull discharge value, channel width and surface slope estimated from DEM.

Moreover, application of this simple channel approximation to rivers with measured bathymetry has shown a good level of compliance (>70%) with the flood inundation extent related to more complex model results (Sampson et al. 2015).

Nevertheless, it has been found that significant amount of uncertainties in flood inundation modelling come from the channel size estimation (Bradbrook et al., 2004, Sampson et al., 2015). And while considering the ongoing development in global river width databases and future research on possibility of remote channel depth observation these uncertainties should be alleviated in modern

modelling approaches. This could be done through introduction of a better way to account for river channel bathymetry

Regarding the river network representation, the recent researches have suggested the possibility of global estimation of river widths using either commonly known geomorphological relationships of Wolman and Miller (1960) at large scales (Andreadis et al., 2013) or satellite images processing techniques (Pavelsky and Smith, 2008; Yamazaki et al., 2011 and other). These could also be enhanced by linking data on river networks to web-based imagery services such as Google maps. It would lead to more accurate river width estimations in the area of interest or regions with enlarged complexity of the banks morphology (Sampson et al., 2015).

The uncertainty is larger in case the channel is imposed to the human interventions to some extent. Similarly, it has been concluded that the value of the bankfull flow estimate depends on other aspects of river channel capacity as well (e.g. type and density of vegetation, sediment transport) receiving another source of uncertainty (Gomez, 2007; Johnson, 1996). Furthermore, the ambiguities in global regionalized frequency analysis impose some uncertainty on values of bankfull discharge estimates and, thus, on values of channel depth

Obviously, the assumption of 1 in 2 years bankfull flow does not hold uniformly for all regions of the world. The effectiveness of this approximation depends heavily of local conditions including variability in the dominant discharge values. For example, according to the value obtained for Svitava River in the urban area of Brno by probabilistic assessment of the river channel capacity, the return period of the bankfull flow discharge equals to about 15 years (Riha and Golik, 2005). The similar analyses have been conducted in other river basin around the world (Endreny, 2007; Castro, 2001 and other). Similarly, channel size estimates will differ for various hydraulic parameters, channel geometry types and design discharges all over the world.

Some researchers also use co-called hydraulic geometry (HG) method, which consists of analysing geomorphic features of the river in order to determine regional HG relationships in gauged river basins and transfer them to the data scarce areas (Wolman and Miller, 1960). HG curves, obtained through such analysis, show relation between drainage area and bankfull river characteristics (e.g. discharge, width, mean depth, mean velocity, cross-sectional area). The advantage of HG curves is that they remain quite accurate even for the river basins with different local conditions. Bankfull properties of the river are closely tied to the concept of hydraulic geometry according to many studies (Harman, 2008). As an example of HG analysis result it was found that estimated bankfull discharges for Han River basin exceed the observed mean daily discharges by 7 – 10 times (Lee and Choi, 2018). Other applications of hydraulic geometry could be found in many works (Parker, 2007; Castro, 2001 and other)

Another opportunity to obtain bankfull discharge estimation is through remote sensing techniques, as was shown by Bjerklie (2007). In his paper, an equation was developed in which the channel slope and the length of rivers bends were used to estimate the velocity at the bankfull discharge. The related channel depth in its turn were suggested to be determined from relation with observed values of width and slope. It was concluded that the bankfull flow could be estimated remotely with mean uncertainty of less than 24% (mainly coming from depth estimation). This would be a particularly valuable tool for regions where observations could prove to be difficult and costly, however the issue of observation frequency remains an important problem with respect to monitoring the dynamics of river flow (Bjerklie, 2007). Another one example of remote sensing used in determining bankfull channel characteristic is presented in Mersel (2013).

3. Data & Methodology

All the data used in this research except for the data on roughness classes and DEM has been obtained from open sources. Considering the wide spread of free DEM sources and availability of the land use data in services similar to OpenStreetMaps, all of the carried out simulations could be done for any river with available data on surface elevation and discharge.

3.1. Modelling approach

To answer the research question of this study, the modelling of the flood waves of 1993 and 1995 events in the Lower Rhine basin was implemented. The approach used in both cases was the same to ensure representability of the modelling output and to enable possibility of model calibration and further validation on two separate flooding events.

The LISFLOOD-FP model allows to differ which of the SWE terms could be assumed negligible depending on the situation and the choice of the user by means of various channel and floodplain flow solvers described in Section 2.3. Most of these solvers exclude local acceleration term from the set of the ruling equation, however for the flood wave hydrodynamic modelling over the large areas this term is crucial to account for the moving flood wave which changes the surface gradient over the domain as the flood wave passes. Since the modelling case considers a huge reach of the Rhine during the prolonged flood events, the sub-grid channel solver is used for calculating the flow in the channel. The sub-grid version of LISFLOOD-FP work only in combination with the acceleration floodplain solver and adaptive time step. Thus, framework of the LISFLOOD-FP model has been chosen.

The general data requirements for the model are addressed separately in the following sections:

- Raster DEM (Section 3.2.1);
- Boundary conditions (Section 3.2.3);
- Channel geometry (Section 3.2.2);
- Channel and floodplain friction (Section 3.2.1);
- Model time step (the adaptive time step to maintain stability).

It is worth noting that the implementation of the sub-grid model requires a special set of data regarding the channel representation compared to other channel flow solvers. Those requirements implied the raster based channel dimension datasets. The technique used in order to create these special datasets is described in Section 3.2.2.

The modelling runs have been divided according to their purpose into 3 different types. Those types have pursued various goals and thus different sets of the model parameters were used for their implementation. The types are:

1. Calibration runs;
2. Validation run / Reference run;
3. Channel size assumption runs.

Type 1 or Calibration runs were performed to estimate the calibration parameters in order to receive the best possible simulation results using the given scenario. The calibration was performed based on the 1995 flood event and was aimed at achieving the best goodness-of-fit for the water level values along the studied domain. More details on how calibration was performed and assessed could be found further in Section 3.3.

Type 2 or Validation run or Reference scenario was performed to assess the calibration outcome on the independent set of hydrological data. The discharge series at Bonn hydrological station for 1993 flood event has been used as boundary condition in this scenario. The precision of validation outcome has been assessed similarly to the calibration outcome assessment. More details on how validation was performed and assessed could be found further in Section 3.3.

Type 3 or Channel size assumption runs consider various substitutions for the elaborate measured channel geometry which was used as an input to other two main types of modelling runs. To avoid the creation of additional uncertainty sources, other model parameters were usually left intact compared to the Reference case. As those runs play the key role in answering the research questions, the separate Chapter was devoted to describe the methods which were used to create channel size estimates. The description of the theoretical background behind each of the channel size assumptions as well as nuances of how they were calculated and implemented into the model could be found in Chapter 4.

The following table (Table 3) lists the parameters that were specified in the model runs depending on the purpose (type) of simulation. It allows to view more closely on the modelling approach for each of the case scenarios.

Table 3. Parameter values used for different types of simulations

Parameter	Value in runs of various Type		
	1. Calibration	2. Validation	3. Assumptions
Simulation parameters			
Total length of the simulation in seconds	2242800 = 26 days	5353200 = 62 days	
Input files parameters			
Digital Elevation Model (DEM)	100x100m DEM with erased channel		
Floodplain roughness values	100x100m Manning's n raster		
Downstream boundary condition	Basin slope I = 0.000182		
Upstream boundary condition (including tributary inflow)	Hydrological data of 1995 flood event	Hydrological data of 1993 flood event	
Initial conditions	Output water depth file from one of previous simulations		
Model solver parameters			
File containing a raster of sub-grid channel widths. Initiates sub-grid and acceleration model versions	Raster of channel width measured from DEM. Initiates sub-grid and acceleration model versions		
River channel parameters			
Sub-grid channel bank heights	Raster of channel floodplain surface elevation measured from DEM		
Sub-grid channel bankfull depth or bed elevation	Raster of channel bed elevation obtained from DEM	Various global multiplier r and power p values for calculating the sub-grid channel bankfull depth	
Global channel friction coefficient n value for the sub-grid channel	Set of different n values from 0.025 to 0.035 s/m ^{1/3}	Manning's n value adopted as a result of calibration (n = 0.028 s/m ^{1/3})	
Global sub-grid channel shape type	Parabolic	Rectangular	
Output files parameters			
Model gauge locations	Gauge locations in Bonn, Cologne, Dusseldorf, Ruhrort/Duisburg, Wesel, Rees, Emmerich and Lobith		
Other parameters			
Courant-Friedrichs-Lewy (CFL) stability coefficient	0.7		

3.2. Model input parameters

All of the model's input files were prepared for the territory slightly bigger than the area enclosed within the first embankment line where all of the flooding was observed. It was done to allow detection of the unrealistic dike overflow events happening according to the model output. In such way any unexpected model behaviours could be found and then prevented. The area which has been used for simulation in the model could be seen on Figure 7.

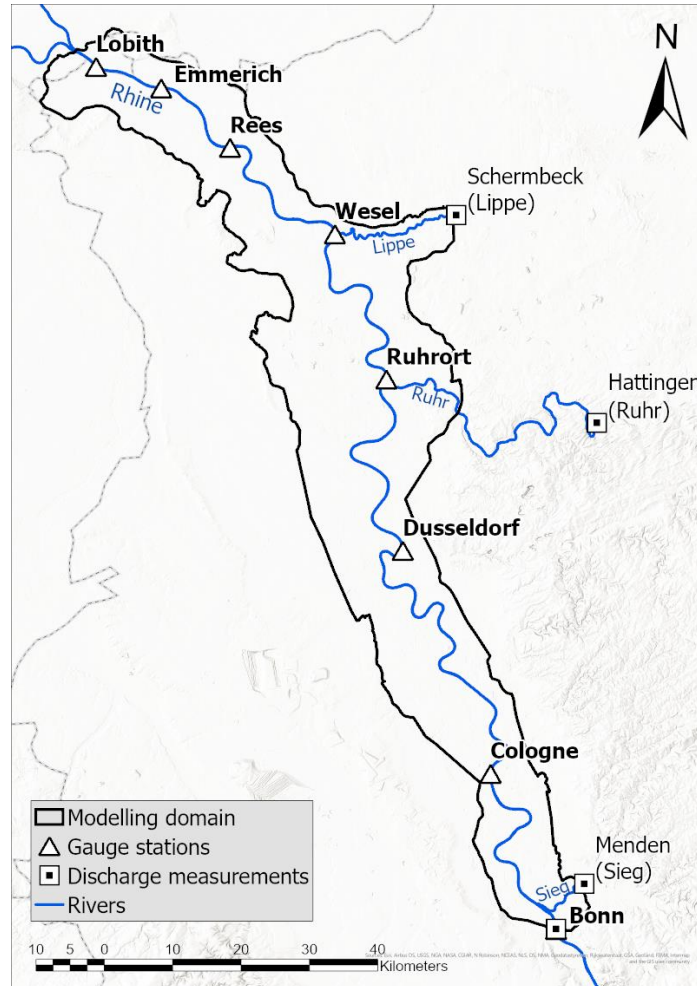


FIGURE 7 - MODELLING DOMAIN, LOWER RHINE

In order to set the model running a set of general input data is required, which contains of:

- Surface elevation data over the model domain (raster Digital Elevation Model);
- Channel geometry information (if not incorporated into DEM) consisting of:
 - Channel slope;
 - Channel width;
 - Bankfull depth.
- Channel and floodplain friction;
- Boundary conditions (inflow discharge hydrograph, flow across domain edge or point source within the domain).

The format of the input data depends heavily on the type of solvers used for floodplain and channel flow simulation (listed in Section 2.3), which should be chosen beforehand. The combination of sub-grid and acceleration solvers was implemented throughout this research.

3.2.1. Raster datasets

The dataset containing the raster of surface elevation data for the area of model domain has been provided by the Dutch Ministry of Infrastructure and Water Management and the Landesamt für Natur, Umwelt und Verbraucherschutz (LANUV) of Northrhine-Westfalia (Figure 8a). The said Digital

Elevation Model was provided with 10x10m spatial resolution and also included the channel bathymetry data for the main channel and its tributaries. The surface elevation values given in this DEM refer to 2015 situation, which could imply additional uncertainty on the model outcome due to possible river bed evolution (both natural or anthropogenic) occurred within that time frame. Further elaboration on the influence of this uncertainty source could be found in Discussion section (Chapter 7).

LISFLOOD-FP model, according to its specifications, is designed to work best on 25 – 100 m grid resolutions of surface elevation data within the rural floodplain environment, although finer resolutions are preferable in urban areas (Bates et al., 2013). During both 1993 and 1995 flood events no significant urban inundation has been observed, therefore the model built to simulate those event should not suffer from the grid coarsening while the grid size remains no higher than 100 m.

Since it was established that adoption of 100x100m DEM resolution would not result in any sufficient negative effect on accuracy of the modelling outcome, this transition has been performed in order to reduce computation time of the model (Figure 8b). During the procedure new surface elevation values were determined using bilinear interpolation. Bilinear interpolation calculates the value of each pixel by averaging (weighted for distance) the values of the surrounding four pixels. This approach is suitable for continuous data and does not introduce any values outside of the given spectrum.

As one of the consequences of the DEM cell size increase, the information on the crest height of the first embankment line was corrupted leading to occasional situations when the dike height became too low to withhold observed water levels. This happened since average width of the dike crest is significantly lower than the new grid size. To overcome such problem, the embankments were reintroduced manually in the problematic locations. In the lower part of the studied reach of the Rhine river dike height data have suffered the most, showing average decrease in height around 2 m over several large areas along the river. For this part of the model domain (Wesel – Rees – Emmerich – Lobith) the new embankments were introduced over the old ones based on the crest height and crest slope before the transition (Figure 8c).

The embankments upstream of Wesel were affected to a lesser extent, however the inaccuracies created there after the transition have influenced the ability of the model to contain water within the first line of embankments at some locations. As a result, the dike overflow occurred during the simulation runs though it was not proposed by the observations. This source of uncertainty is addressed and studied closely in Discussions section (Chapter 7).

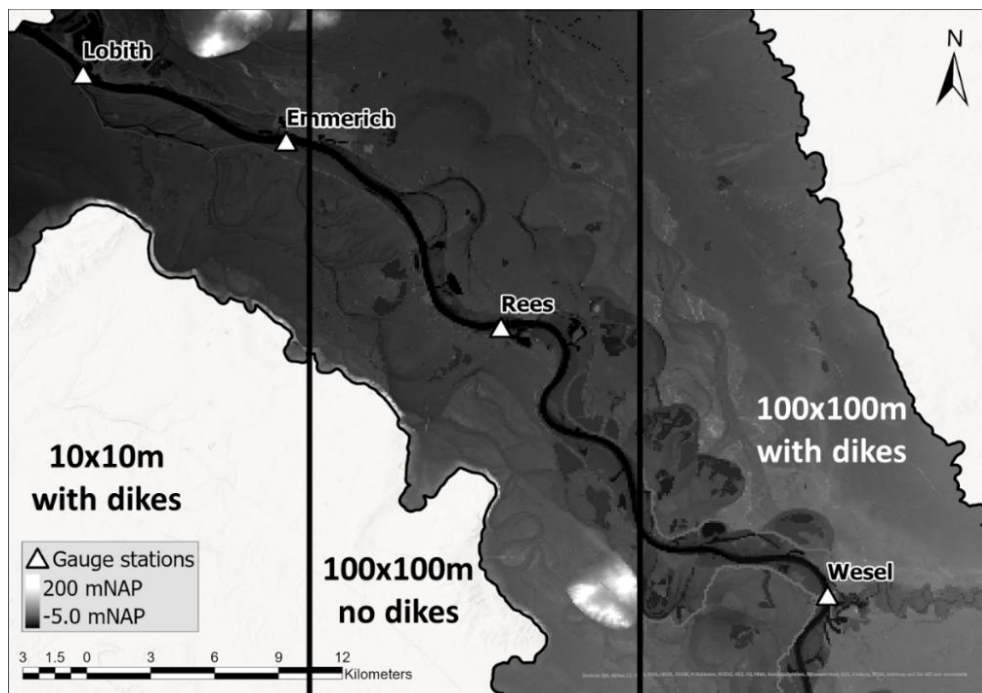


FIGURE 8 – DEM OF THE LOWER RHINE FOR: (A) $\Delta X = 10$ M; (B) $\Delta X = 100$ M WITH ABRUPT DIKES; (C) $\Delta X = 10$ M WITH MANUALLY RESTORED DIKES.

The map of floodplain roughness classes with associated Manning's friction coefficient values based on the land use data for the Lower Rhine basin has also been provided by the Dutch Ministry of Infrastructure and Water Management and LANUV for this research (Figure 9; Table 4). For this

research 6 general roughness classes were considered. These are: urban areas (1, 6, 7, 8, 10, 21), grasslands (9), brushwood (5), forests (12, 15, 16, 23; 13, 22; 18, 19, 20), marshes (11) and water bodies (2, 3, 4, 14, 24).

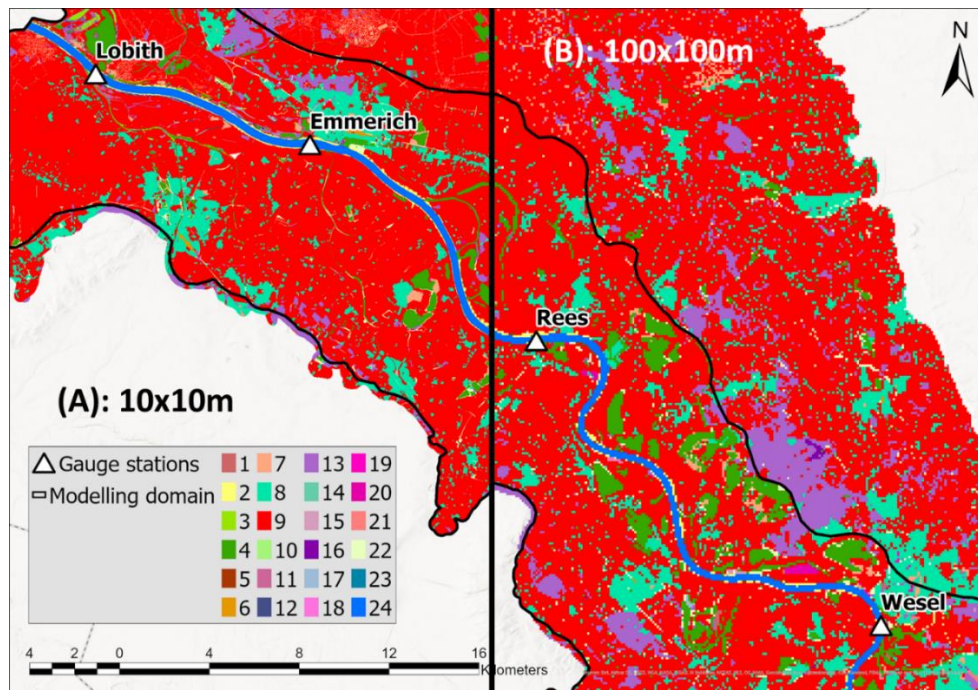


FIGURE 9 – ROUGHNESS CLASSES IN LOWER RHINE BASIN WITH (A): 10X10M OR (B): 100X100M RESOLUTION

Although, LISFLOOD-FP allows different spatial resolution for DEM and roughness definition files, the initial 10x10m raster was resampled to match the resolution of the surface elevation data. In that manner no significant changes to the modelling outcome should be implied. Thus, roughness raster has also been coarsened to 100x100m, however this time the value in each new cell was defined from the most frequent value of the initial grid cells falling into the area of a new one.

Each of the roughness classes given on the map has a specific Manning's friction coefficient value, n , written to it (Table 4). Typically, the coefficients inherent to the domain are chosen with reference to the published tables such as those given by Chow (1959). The Manning's friction coefficient in river channel (n_c) is generally found to be between 0.01 and 0.05 while its value on floodplains (n_{fp}) normally varies between 0.03 and 0.15. In this research the values for floodplain friction were found in accordance to their land use purpose, while the channel friction coefficient has been a subject to calibration.

TABLE 4. ROUGHNESS CLASSES

Class #	1	2	3	4	5	6	7	8
Description	urban	sand channel	clay channel	lakes	shrub	urban	urban	urban
Manning's n	0.030	0.029	0.029	0.024	0.029	0.032	0.036	0.039
Class #	9	10	11	12	13	14	15	16
Description	grass	urban	marsh	alluvial forest	forest	sand dunes	alluvial forest	alluvial forest
Manning's n	0.030	0.035	0.050	0.070	0.150	0.030	0.058	0.063
Class #	17	18	19	20	21	22	23	24
Description	pasture	park	park	park	urban	windbreak forest	alluvial forest	gravel channel
Manning's n	0.058	0.060	0.060	0.060	0.036	0.120	0.054	0.028

In order to implement different channel size assumption in the sub-grid solver of the LISFLOOD-FP model, the DEM for Lower Rhine basin had to be stripped off of the real channel bed elevations and substituted by the floodplain elevation values. In order to do so, the river channel location has been distinguished from the roughness classes inherent to the river channel (Class 24) using the roughness classes map (Figure 9). Then the representative floodplain elevation points were sampled manually all along the river channel for the full extent of the model domain. The obtained field of floodplain elevation points was interpolated on the cells where river channel could be found (again Class 24 of Roughness classes). In combination with the initial DEM values for river valley excluding the river channel, the new DEM has been established with the channel filled up to floodplain level (Figure 10).

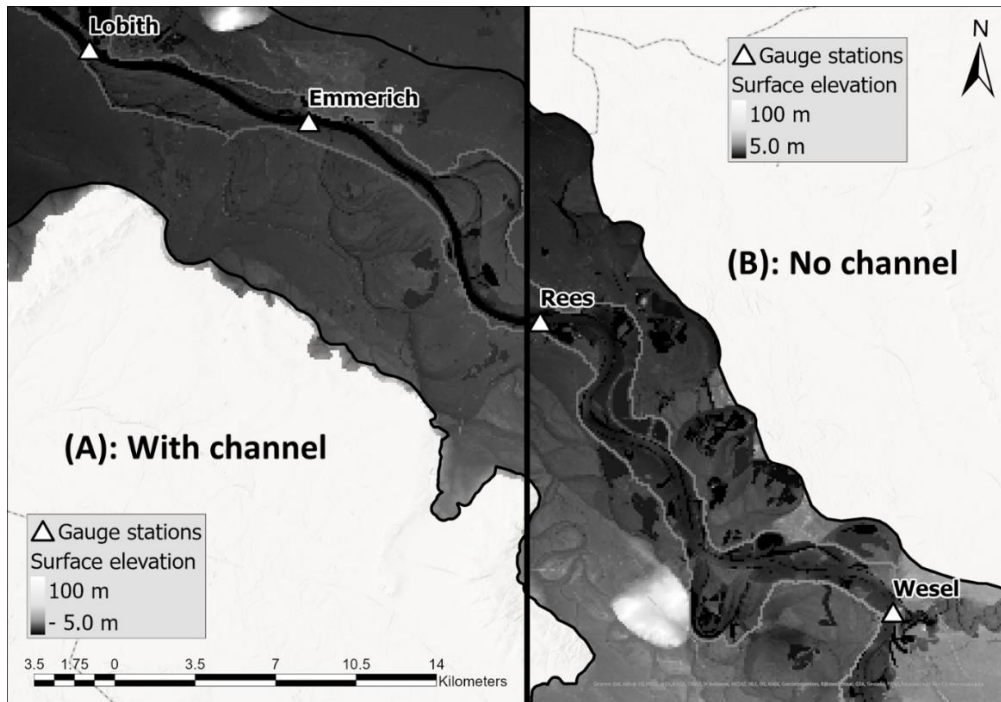


FIGURE 10 – DIGITAL ELEVATION MODEL OF LOWER RHINE BASIN WITH (A) AND WITHOUT (B) A RIVER CHANNEL

3.2.2. River network

The properties of the river channel including channel location, bed slope, width of the channel and its bankfull depth should be depicted from the DEM of the Lower Rhine basin for the reference case with elaborate bathymetry data. Introduction of the measured channel data to the research will allow the possibility of benchmark testing for the simulations which implement different channel size assumptions. The further channel size assumption runs require the same set of data except for the bankfull depth, which is represented through the equation parameters described in Chapter 4.

All of the river channel related model input in the sub-grid solver of LISFLOOD-FP requires to be imported in the form of several raster data containing certain channel characteristic values in the cells where the river flows through. To contain the stability of the model, as well as taking into account the simple morphology of the river channel in the Lower Rhine basin, those raster datasets have represented a situation of the single thread river channel.

Therefore, firstly all files containing river channel data were prepared in 1D format and only then transited into 2D raster datasets. 1D river channel datasets will be built based on initial resolution of the DEM (10x10m), however after the initial coupled 1D-2D model run, the output raster of river channel characteristic will adopt the grid size of the new DEM (100x100m).

The grid cells associated with the main river channel were identified using the map of roughness classes described above taking Class 24 as an ultimate river channel representative roughness class (Figure 9; Table 4). However, using this method to automatically detect the location of the river channel has excluded locations where water was contained between the protective groins near the banks of the river, which are presented throughout the Lower Rhine basin at quite large extent. While this of course has some effect on the modelling output, the flow there is limited during lower water periods due to the influence from the protective structures, and thus the negative effect of such assumption is restrained to some point.

Then, the centerline was created based on the obtained raster of river channel position, where the width of the river channel was found as twice the distance from the centerline to the closest river bank defined from DEM. It was found that over the study domain the width of the Rhine river changes from about 200 to approximately 400 m (Figure 11A). Additionally, the river tends to widen towards both upstream and downstream parts of the studied reach, thus having the largest width values closer to the boundaries of the domain.

In order to set the surface elevation and roughness data related to each cell containing river section, the information from 10x10m DEM was interpolated at river channel locations. It could be seen that the average depth of the channel stays at more or less the same level all over the model domain (Figure 11B). However, it could be noted that the section right downstream of Cologne can be characterised as the shallowest part of the studied reach, while the deepest part of the Lower Rhine is the Rees – Emmerich – Lobith section. The values for banks elevation, that were used to calculate the bankfull depth of the channel, have been estimated from the closest to the river floodplain elevation values as for the DEM with emitted channel (Figure 10B).

From the obtained channel bed elevation values the slope of the channel could be found both globally and locally for selected sections. The global channel bed slope was found equal to $I = 0.000182$.

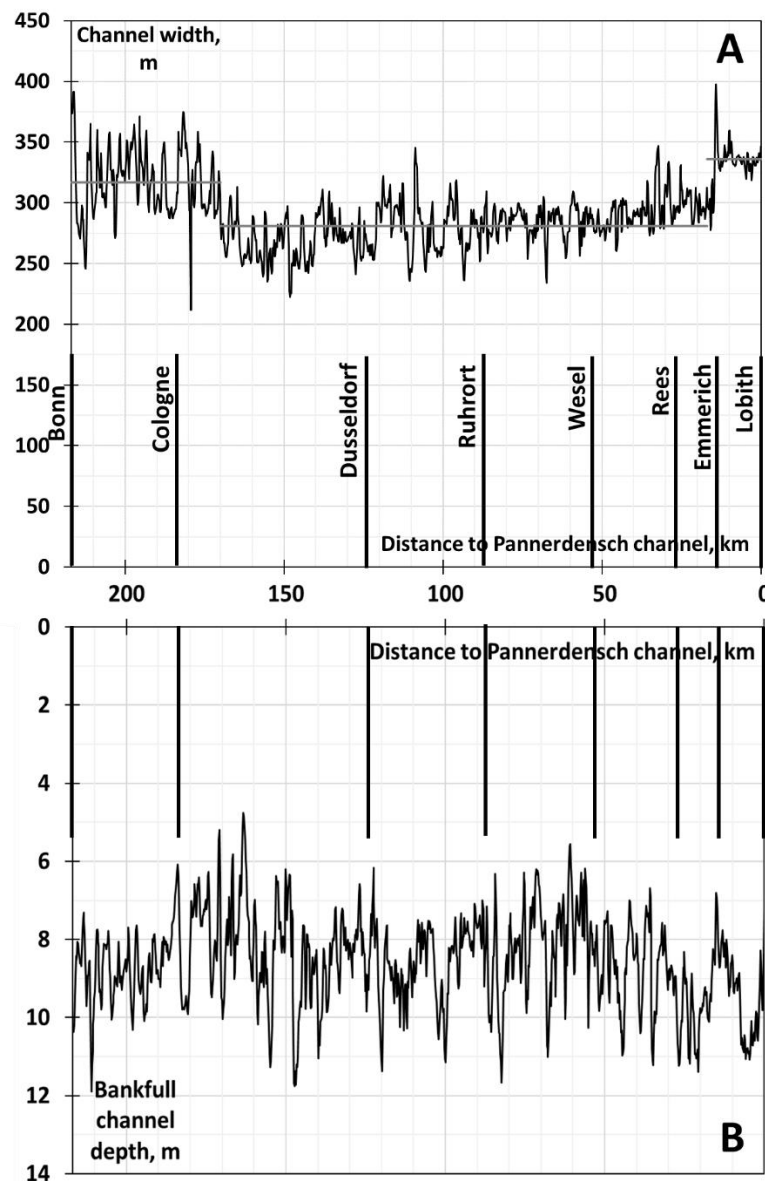


FIGURE 11 - VARIABILITY IN THE RIVER CHANNEL WIDTH (A) AND BANKFULL DEPTH (B) FOR THE LOWER RHINE BASIN

Apart from information on location, width, Manning's n friction coefficient and bed elevation of the channel, the complete river file should also include the reference to boundary condition along with potential tributary inflow. The tributaries could be represented as a part of river network or simply as a lateral at specified location. The latter approach has been chosen in this research. The further elaboration on the boundary condition model input could be found in Section 3.2.3.

3.2.3. Boundary conditions

The boundary conditions were specified at the upstream boundary of the modelling domain as a discharge measurement series at Bonn hydrological station during the studied flood events. It has been proved that LISFLOOD-FP model can be used to simulate hydrodynamics in river reaches even considering the non-steady situations like the flood events studied in this research (Bates et al., 2013). However, for dynamics state simulations there are strict conditions over the accuracy of the provided boundary conditions. It has been found that the inflow data precision should not exceed $\pm 10\%$ compared to the really observed data (Williams and Esteves, 2017). This condition was set as the aim while dealing with the discharge input data throughout this research.

A 15-minute discrete dataset of Rhine river discharge that were obtained from Global Runoff Data Centre (GRDC) operating under direction of the World Meteorological Organization (<https://www.bafg.de/GRDC/EN>) have been used as a boundary condition input in the model for both 1993 and 1995 floods. Additionally, the discharge series for the three Rhine tributaries has been obtained to account for lateral inflow within the domain. The description of the flood events used in this research could be found in Section 2.2.

As the modelling domain is limited to the Lower Rhine, the Bonn serves as the input location of the upstream boundary condition. However, since there were no discharge observations available for the studied events at Bonn hydrological station, the transition of the discharge measurements was required. The flow rate at the upstream boundary of the domain was, therefore, found as an average between values measured at Andernach and Cologne (deducting the Sieg inflow) gauges. During the calculations the lag between flood waves at all 3 stations was taken into account considering that runoff travel time between Andernach and Cologne equals 4.75 hours. This estimate was made based on the average time difference between discharge peaks at both stations. The time that flood wave had taken to travel from Andernach to Bonn was considered half of the Andernach – Cologne travel time. According to such estimates the Bonn discharge series was approximated for +2.375h temporal lag. Returning to the normal temporal reference, the overall discharge series at Bonn hydrological station which was used as the upstream boundary condition for the built model take the following form (Figure 12).

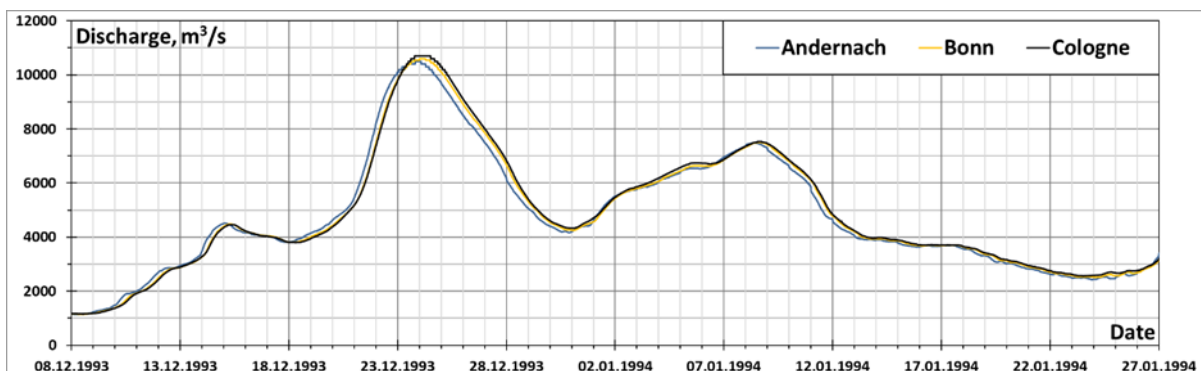


FIGURE 12 - DISCHARGE SERIES AT ANDERNACH, BONN AND COLOGNE HYDROLOGICAL STATIONS DURING 1993 FLOOD

Since the 15-minute discrete measurement data for Cologne station was not available for the 1995 flood event, and since average deviation of the calculated Bonn discharge from the measured Andernach discharge during 1993 flood was limited to 5% at maximum, the Andernach discharge series has been adopted as the upstream boundary condition in 1995 scenario (Figure 13).

The tributaries which are present within the studied area of the Rhine basin were represented as a lateral inflow points at their confluence locations. This approximation was done in order to reduce computational time and should not have any significant effect on the outcome of the model.

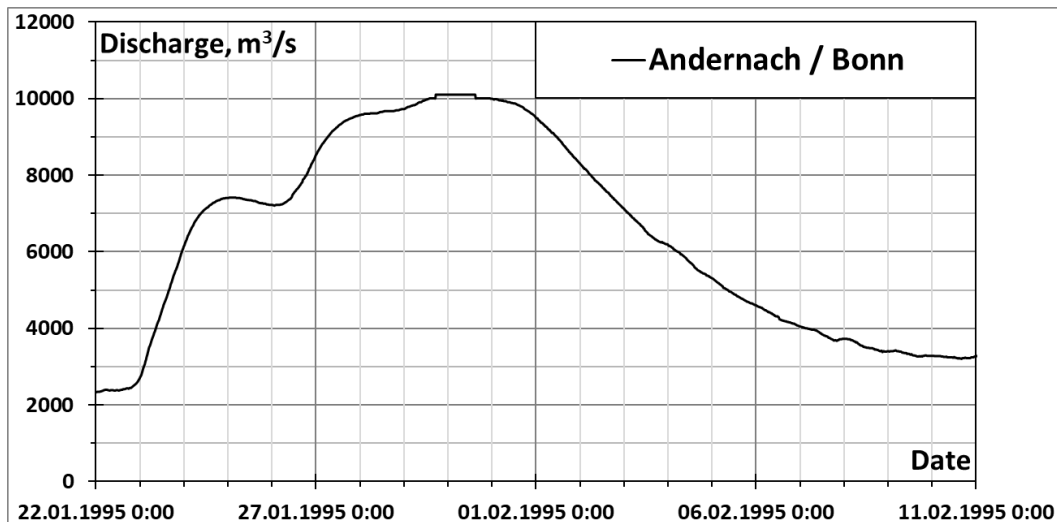


FIGURE 13 – DISCHARGE SERIES MEASURED AT ANDERNACH (APPLIED FOR BONN) DURING JANUARY, 1995 FLOOD EVENT

The lag was also implemented for the tributaries' discharge series to account for travelling time from the locations where the measurements were taken (Figure 7). The flood wave travel time was considered as 3 hours for the Sieg river, 12 hours for the Ruhr river and 2.5 hours for Lippe river. Additionally, the build-up coefficients of 1.07, 1.11 and 1.00, respectively, were used to account for the tributary inflow. The previous assumptions were made based on the work by Bomers et al. (2018).

The downstream boundary conditions were represented by the constant value of the water surface slope equal to the slope of the basin ($I = 0.000182$) as it has provided the most stable simulation results among other alternatives.

3.3. Calibration & Validation

The calibration of the model was performed based on the hydrological situation of January, 1995 flood event (Figure 5). The description of that event has been given in Section 2.2.2. Throughout the calibration procedure a spatially uniform value for Manning's friction coefficient in channel, n_{ch} , served as the calibration parameter. The aim of the calibration was to obtain the most suitable value of n_{ch} in order to accurately reproduce the hydrological situation on the Rhine river by means of the built model.

The 1995 flood event has been chosen for the calibration procedure as it represents much simpler hydrological situation with its single peak and shorter high water period. The simplicity of the flood wave will allow to better estimate the alignment of the simulated values with the measurement data both visually and using various statistical metrics. The shorter period of simulation, in its turn, will allow to perform many calibration simulations to faster determine the appropriate value for the calibration parameter, n_{ch} .

The procedure of the calibration included successive approximation approaches starting from the initial guess for the calibration parameter. Ultimately, the river channel Manning's friction coefficient value was approximated between 0.025 and 0.35 with 0.01 step. The applicability of each of the attempted Manning's coefficient values was studied using both visual analysis of the generated series of water level values at the gauge sites described previously (Section 3.1) and quantitative assessment of their compliance with the observed series. For the latter three different criteria were used, which are: Root Mean Square Error (RMSE), Nash-Sutcliffe Efficiency (NSE) and squared correlation coefficient. The description of the RMSE and Nash-Sutcliffe metrics could be found in Section 3.4. Additionally, the measure of statistical fit between the amount of simulated and observed flooded area has been calculated to show the spatial differences between the predicted inundation extents.

The validation of the model considered the December, 1993 flood event as the hydrological situation identification. This flood event, due to the complex nature of its genesis and related complex two-peak shape, serves as good measure of the model performance. Apart from the studied flooding event and the number of required simulation runs, the general approach to the validation procedure greatly coincides with the calibration process. The alignment between predicted and observed parameters of the flood event was tested using Root Mean Square Error (RMSE) and Nash-Sutcliffe Efficiency (NSE) metrics.

3.4. Statistical analysis

To quantitatively assess the alignment of the simulated parameters a goodness-of-fit (GOF) analysis was conducted. The GOF of the Q_{bf} predictors has been measured using several accuracy metrics describing relative error between observed and predicted values of water level.

The 1:1 line is considered as a perfect match between the model and measurements. The Theil (1958) measure of association, U , was used in this work in order to estimate the relative error with respect to this line. This metric examines a normalized distance between observed and simulated values, and unlike correlation coefficient, learns the proximity of the data pair to the 1:1 line. It was recommended for GOF analysis by Smith and Rose (1995). The Theil's measure of association, U , is defined by the following expression:

$$U = \frac{\sqrt{\frac{1}{n} \sum (y_i - \tilde{y}_i)^2}}{\sqrt{\frac{1}{n} \sum y_i^2 + \frac{1}{n} \sum \tilde{y}_i^2}}$$

With y_i – observed value, and \tilde{y}_i – predicted value. Smaller U values indicate better fit.

The Root Mean Square Error (RMSE) between measurement data and model will be used as recommended by Pineiro et al. (2008). It has the same units as the variables, and so it will allow to account for large differences between larger observations. The expression for RMSE is as follows:

$$RMSE = \sqrt{\frac{\sum (y_i - \tilde{y}_i)^2}{n}}$$

And the final metric used to account for accuracy of the model prediction will be Nash-Sutcliffe model efficiency coefficient (NSE). It was specially produced to assess the predictive skill of the hydrological model and is commonly used around the world. The NSE formula states the following:

$$NSE = 1 - \frac{\sum (y_i - \tilde{y}_i)^2}{\sum (y_i - \bar{y})^2}$$

Where \bar{y} is the mean of measured discharges. Although, NSE has been criticised recently for masking important model behaviours (Gupta and Kling, 2011), it will suffice for this model purposes.

4. Channel size estimates

In this work, three different types of bankfull discharge predictors were used: hydrology- and process-based, and one based on hydraulic geometry regional relationships. The hydrological predictors were calculated using the annual maximum flood series and annual mean flood series. All of the methods used consisted of estimating a particular bankfull discharge value.

The specified bankfull discharge values would then be transited into the bankfull channel depth estimate considering the remotely measured average width in the studied reach and rectangular river channel. The channel depth will be calculated using discharge general expression and Chezy formula for water velocity with Manning's formulation for Chezy parameter, C:

$$\begin{cases} Q = v \cdot W \\ v = C \cdot \sqrt{RI} \end{cases}$$

With W – river channel cross-sectional area, R – hydraulic radius. Assuming wide rectangular river channel, we get:

$$W = H \cdot B$$

$$R \approx H$$

The Manning's formula allows to use the friction coefficient value, n , instead of C , which enables the further calculation as it was estimated during the calibration procedure:

$$C = \frac{1}{n} \cdot H^{1/6}$$

Considering all of the above, the updated formulation for the Q value could be derived:

$$Q = \frac{1}{n} \cdot H^{1/6} \cdot H^{1/2} \cdot l^{1/2} \cdot H \cdot B = H^{5/3} \cdot \frac{B\sqrt{l}}{n}$$

From the obtained expression the value of H could be singled out, giving the following formula:

$$H = \left(\frac{Qn}{B\sqrt{l}} \right)^{3/5}$$

With $n \approx 0.028 \text{ s/m}^{1/3}$; $B \approx 292 \text{ m}$; $l \approx 0.000182$. This expression was also adapted to account for variability in river width over the model domain. The sub-grid model allows to specify channel depth as a function of river width, B , with a generalised function:

$$H = r \cdot B^p$$

With r and p being coefficients used to control the depth formulation. To enable width-dependent calculation of the bankfull depth the following assumptions could be made:

$$r = \left(\frac{Qn}{\sqrt{l}} \right)^{3/5} \approx 1.55 \cdot Q^{0.6} \quad \text{and} \quad p = -0.6$$

This approach has been implemented for bankfull depth calculation in all assumptions except for annual mean discharge estimate. Another method to account for the size of the channel with unknown bathymetry is used when the bankfull discharge is estimated through annual mean flow series, $Q_{k,\text{mean}}$ (where k stands for the return period of the chosen quantile). In that case, due to evident underestimation of the dominant discharge (since we assume $Q_{\text{bf}} \approx Q_{\text{dominant}} = Q_{k,\text{mean}}$), the quantile value will be assumed to be equal to the cross-sectional area of the channel. In other terms, the velocity in bankfull channel is set equal to $v = 1 \text{ m/s}$, so that the expression for water discharge will take the following form:

$$Q = v \cdot W = W = B \cdot H$$

Therefore, allowing to determine the bankfull depth using only quantile value and remotely measured channel width:

$$H = \frac{Q}{B}$$

4.1. Flood frequency assumptions

Hydrologic predictors of the dominant discharge are generally applicable for stable channels lacking major anthropogenic influence such as river engineering or bed modification from flow regulation or land use change in the watershed (Doyle et al. 2007). Although this is not the case for the studied part of the Rhine basin, it will be interesting to study the validity of such approach for channel representation under the heavy influence of anthropogenic factors.

Over a large span of studies conducted in coarse bed rivers a wide range of return intervals for Q_{bf} have been found (Wolman and Leopold, 1957; Andrews, 1980; Williams, 1978). The median value of the return interval of bankfull discharge from these studies, as was mentioned in Section 2.4, often falls between 1 and 2 years on the maximum annual flood series, whereas the mean value from these studies is often greater than 2 years (Sholtes, 2016). This indicates a positively skewed distribution and a larger range of values for the return interval of Q_{bf} , though Castro and Jackson (2001) found that the return interval of Q_{bf} for Pacific Northwest rivers has a mode of 1 year and is negatively skewed. The return interval of Q_{bf} for channels that have adjusted to disturbance by incising and/or widening will generally be greater than 2 years (Doyle et al. 2007).

The floods of a specific frequencies were calculated using log-Pearson Type 3 probability distribution and Weibull plotting position. Given probability density function then has the following formula (Millington et al., 2011):

$$\begin{aligned} & \text{for } \gamma \neq 0: \\ & \alpha = 4/\gamma^2 \quad \text{and} \quad \beta = \sigma\gamma/2 \quad \text{and} \quad \xi = \mu - 2\sigma/\gamma \\ & f(x) = \frac{(x - \xi)^{\alpha-1} \cdot e^{-\frac{(x-\xi)}{\beta}}}{\beta^\alpha \cdot \Gamma(\alpha)} \end{aligned}$$

Where μ is the location parameter, σ is the scale parameter, γ is the shape parameter, and $\Gamma(\alpha)$ is complete gamma function. For further details on log-Pearson Type 3 distribution refer to Hosking (1997). The parameters for this distribution are estimated according to Water Resources Council Method. It is also worth noticing that the quantiles for this method are calculated as follows:

$$X = 10^{(m+K \cdot s)}$$

Where s is standard deviation of the observed data. The K factor in the quantile expression, in its turn, depends on the skew coefficient (C_s) of the dataset. K could be interpolated from special K -table or calculated as follows (Ashkar & Ouarda, 1998):

$$K_T = \frac{2}{C_s} \left\{ \left[\frac{C_s}{6} \left(z - \frac{C_s}{6} \right) + 1 \right]^3 - 1 \right\}$$

The Weibull plotting position was determined as $T = (n+1)/m$, where T is return interval (years), m is the rank of the event (with 1 being the largest), and n is the number of events on the record.

The software used in this work, Flood Frequency Distribution (FFD 2.1), is a free MATLAB script created by Benkaci & Dechemi (2018) to analyse flood and estimate quantiles for different return periods and flood frequency relations. It consists of methods for 10 Probability Distributions which are based on either Method of Moments or L-Method.

The resulting quantiles are assessed with the lower and upper confidence intervals of 95% certainty. The efficiency of the obtained distribution is estimated through Correlation Coefficient R and Root Mean Square Error (RMSE) between quantile and observation data. Although the outcome of the script consists only of the flood with 2, 5, 10, 20, 50 100, 500, 1000 and 10000 years return period, the quantiles for remaining recurrence intervals could be determined from the Flood Frequency Distribution curves manually.

In this study the return periods of 1.5, 2 and 5 years will be considered closely for the annual maximum flow series of the Rhine river, and return periods of 2, 10 and 50 years – for the annual mean flow.

4.1.1. Annual maximum discharge

The log-Pearson 3 distribution for annual maximum discharge was calculated for 3 different locations with available discharge series data, these are Cologne, Dusseldorf and Lobith gauges (Figure 14). The discharge series for the chosen stations includes the period from 1900 to 1993 to account for the most possible range of extreme flood events and correctly represent the situation authentic to the 1993 flood.

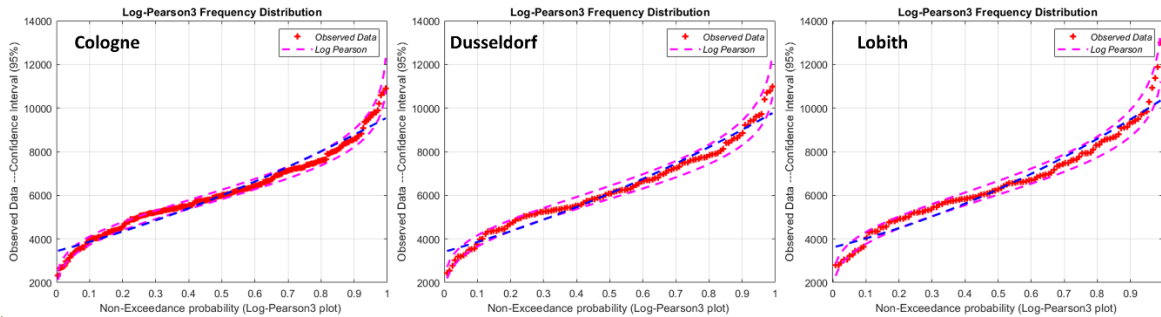


FIGURE 14 – FLOOD FREQUENCY DISTRIBUTION FOR ANNUAL MAXIMUM FLOW OF THE RHINE RIVER IN COLOGNE, DUSSELDORF AND LOBITH

The measurement-based series show a good fit with the obtained FFD plots regarding the area of interest which lies around non-exceedance probability value interval of 0.2 – 0.6 (Table 5). The extremes, however, are characterised with bigger confidence interval limits and less level of compliance with the calculated frequency distribution.

TABLE 5. FLOOD FREQUENCY DISTRIBUTION QUALITY ASSESMENT FOR ANNUAL MAXIMUM FLOW OF THE RHINE RIVER IN COLOGNE, DUSSELDORF AND LOBITH

	Cologne	Dusseldorf	Lobith
RMSE [m ³ /s]	103	125	167
R ²	0.996	0.996	0.994

Based on the derived equation the bankfull depth for each of the following scenarios was computed. The first set of scenarios includes the maximum annual flow quantiles that will be transited into the channel size estimate (Table 6). The required frequency to account for 1.5, 2 and 5 year maximum annual flow is 0.33, 0.5 and 0.8, respectively. The discharge values related to these frequencies are found according to the FFD plot (Figure 14).

TABLE 6. CALCULATION OF AVERAGE BANKFULL DEPTH FOR ANNUAL MAXIMUM DISCHARGE APPROXIMATIONS

T, years	1.5 years	2 years	5 years
Q _{Lobith} , m ³ /s	5606	6334	8176
Q _{Dusseldorf} , m ³ /s	5320	6126	7845
Q _{Cologne} , m ³ /s	5340	6033	7673
Q _{average} , m ³ /s	5422	6164	7898
H _{bf} , m	8.93	9.64	11.2

Thus, the average bankfull depth ranges around 9 – 11 m depending on the frequency of the chosen conveyance discharge. The bankfull depth variability within the study domain also occurs for each bankfull flow assumption: H_{bf} changes from 7.7 to 10 m with Q_{1.5,max}; from 8.3 to 11 m with Q_{2.0,max}; from 9.6 to 13 m with Q_{5.0,max}. The bankfull depth calculated from the difference between initial DEM and DEM with burnt out channel (Figure 11) changes along the domain from 6 to 12 m with an average of 8.6 m. This however, does not allow to draw a conclusion on the each of the assumptions compliance, since the differences in bankfull channel could have been compensated by uncertainty in channel width or floodplain surface elevation during the computation of such.

4.1.2. Annual mean discharge

The FFD has been calculated based on the mean annual discharge values within the period from 1900 to 1993 (Figure 15). The Correlation Coefficient for the provided Log-Pearson 3 distribution does not fall under the value of 0.99 while the Root Mean Square Deviation (RMSE) stays around 30 – 40 m³/s over the domain.

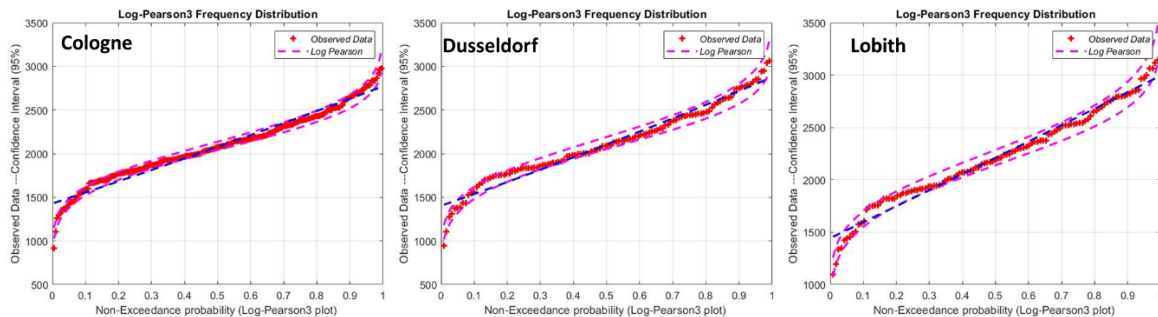


FIGURE 15 – FLOOD FREQUENCY DISTRIBUTION FOR ANNUAL MEAN FLOW OF THE RHINE RIVER IN COLOGNE, DUSSELDORF AND LOBITH

The compliance of the obtained FFD's was assessed using RMSE and R² metrics (Table 7).

TABLE 7. FLOOD FREQUENCY DISTRIBUTION QUALITY ASSESMENT FOR ANNUAL MEAN FLOW OF THE RHINE RIVER IN COLOGNE, DUSSELDORF AND LOBITH

	Cologne	Dusseldorf	Lobith
RMSE [m ³ /s]	26	39	38
R ²	0.996	0.992	0.994

Assuming the reach-averaged channel width equal to $B = 293$ m, the bankfull depth has been calculated for the flood frequencies of 2, 10 and 50 years (Table 8) which respond to 0.5, 0.9 and 0.98 probability, respectively. However, in the model the width-dependent formulation of H_{bf} was used. The equation for Q_{bf} to H_{bf} transition used in this channel size estimation method is presented in the introductory part of Chapter 4.

TABLE 8. CALCULATION OF AVERAGE BANKFULL DEPTH FOR ANNUAL MEAN DISCHARGE APPROXIMATIONS

T, years	2 years	10 years	50 years
$Q_{Cologne}$, m ³ /s	2089	2594	2873
$Q_{Dusseldorf}$, m ³ /s	2121	2676	2979
Q_{Lobith} , m ³ /s	2211	2806	3144
$Q_{average}$, m ³ /s	2140	2692	2999
H, m	7.31	9.19	10.2

Considering the average measured bankfull depth, the closest assumption is the $Q_{bf} = Q_{10,mean}$. Additionally, the bankfull cross-section area has been calculated from the DEM for the three discharge data locations (Table 9). Since the values given from DEM and ones obtained from FFD are of same order of magnitude, the assumption of the $Q_{k,mean}$ being equal to the cross-section area of the bankfull channel can be considered as valid estimation method which could give good results for the right circumstances.

TABLE 9. THE ASSESSMENT OF $W_{BF} = Q_{k,MEAN}$ ASSUMPTION

	W_{DEM} , m ²	2 years	10 years	50 years
Cologne	2288	+ 8.7%	- 13%	- 26%
Dusseldorf	2168	+ 3.0%	- 22%	- 36%
Lobith	3390	+ 35%	+ 17%	+ 7.3%
Average	2615	+ 15%	-7.0%	- 19%

4.2. Hydraulic geometry

Another method commonly used for estimation of the bankfull discharge in the specific reach of the studied river concerns indirect assessment based on a set of regional downstream hydraulic geometry relationships. Those could be obtained from some referential reaches or scaled from a reach serving as an analogue for this one.

The hydraulic geometry method is often opposed by the direct estimate of the Q_{bf} based on the field indicators of bankfull stage, as it uses the same set of river channel parameters. However, the main difference between those approaches lies in data availability for the specific location where the research interests are present.

This method also has its own limitation just like the others. Except for the common discussion points, like the feasibility of the bankfull discharge specification (Doyle et al., 2007) or the existence of well-defined floodplain, the main source of uncertainty while using hydraulic geometry relations is their extrapolation from a reference reach to the reach of interest (e.g. Rosgen, 1997, 2001). The significance of the similarity between the two location could sometimes be considered as not sufficient, thus making the usage of this method not appropriate in certain cases. It could happen when the studied channel section is unstable or has different forcing and boundary conditions compared to the original reach (Wilcock, 1997).

The estimate of bankfull discharge could be made using various sets of bankfull channel parameter. For instance, given all necessary data is available, Q_{bf} can be determined from the sudden leap in $Q - B/D$ relation. Moreover, plotting observed discharge values (Q) against the width (B) itself will also indicate an abrupt increase at approximated value of Q_{bf} . However, such elaborate data on the river valley morphological structure will be considered unavailable in this research in order to account for data scarce regions where the approaches for Q_{bf} assessment from this work could be used.

Therefore, the only hydraulic geometry relation which will be used to determine the bankfull discharge in the studied reach of the Rhine basin will be $Q - H$ curve. This relationship will allow to estimate Q_{bf} while only having at least daily river discharge and water level observation series minimum 10 years long. After the QH-curve is plotted, the bankfull discharge is determined as the location on a Q-axis where occurs change in slope of the relationship. This approach along with the other methods for bankfull discharge estimation has been tested for 95 sites in USA by Sholtes and Bledsoe (2016).

All calculations for Q_{bf} estimation were conducted using RWS open data obtained from Waterinfo service for the Lobith hydrological station capturing the period from 1980 to 2010. The period was cut shorter than was available from the RWS dataset on purpose to account for more up to date bathymetry and anthropogenic load conditions in the basin.

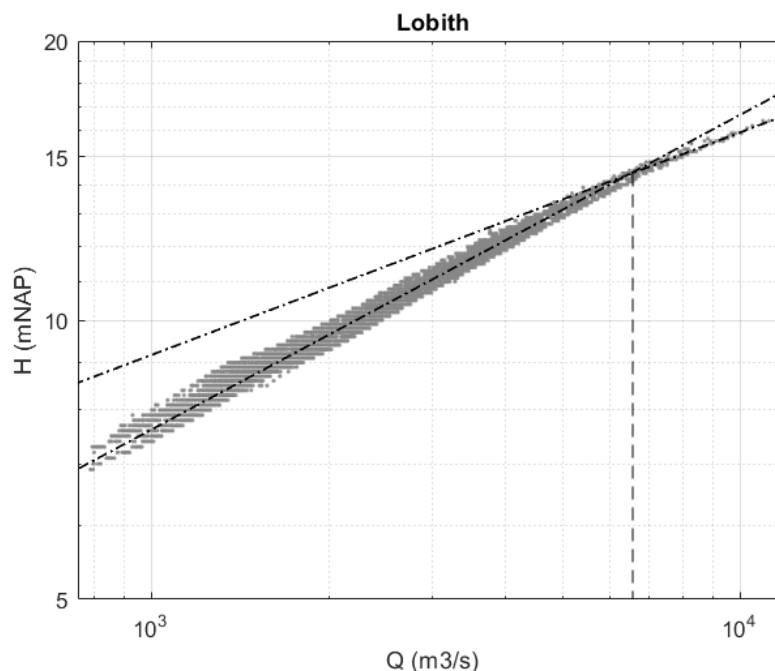


FIGURE 16 – QH-CURVE FOR LOBITH HYDROLOGICAL STATION WITH TREND LINES

On the QH-curve two separate parts could be distinguished (Figure 16). Although visually it is hard to distinct between those two, each of them is characterised by individual slope which is indicated by the dash-dotted lines. The point where two lines intersect is the location where the slope breaks. So, the Q value for that location could be considered as an estimate for Q_{bf} . The obtained bankfull discharge approximation equal to around $Q_{hg} = 6100 \text{ m}^3/\text{s}$.

As the method of hydraulic geometry allows to apply downstream situation further up the river, the value of Q_{hg} probably could be transited from Lobith to the whole domain with only minor uncertainty effect. However, the measurement made using DEM values (Table 9) show that the channel size is not constant over the studied domain, thus this assumption should be treated carefully. This subject will be faced in the discussion section of this report (Chapter 7).

4.3. Dominant discharge

The last approach to estimating the bankfull discharge considered in this research is concerning the values of channel forming discharge or dominant discharge. This method differs from the previous techniques since the value of the estimate is based on a physical processes happening in the channel. Such methods were explicitly studied over the past 20 years (Shields et al., 2003; Beechie et al., 2010). And while the previous (hydrological) predictors of bankfull discharge also represent an important channel forming process, namely the magnitude and frequency of flood flows since that is when the highest load on the channel bed is placed, the term “process-based” used to describe the predictors viewed in this section will refer to incorporation of both hydrologic and sediment transport processes to explicitly consider the effect of sediment yield in channel form.

In this work, two sediment yield metric will be used in Q_{bf} assessment, namely an effective discharge (Q_{eff}) which represents the discharge that transports the most sediment over time (Wolman and Miller, 1960), and half-yield discharge (Q_{hy}) which is a discharge associated with 50% of a cumulative sediment yield over a flow record (Emmett and Wolman, 2001; Vogel et al., 2003). This approach involves calculation of the discharge indices based on the sediment yield curve, and thus is more elaborate and data-demanding. Nonetheless, it can also provide more information to account for during the water resources management and design of anthropogenic intrusion (Soar and Thorne, 2001; Shields et al., 2003).

Generally, the performance of Q_{eff} as an bankfull discharge predictor is mixed depending on the type of sediment regime in the river. It seems that the assumption of $Q_{bf} = Q_{eff}$ often works sufficiently well for rivers with coarse bed, and thus with predominant bed load sediment transport (Emmett and Wolman, 2001; Hassan et al., 2014), while drastically underestimating bankfull discharge in suspended load- dominated rivers with fine bed (Soar and Thorne, 2001; Hassan et al., 2014).

The half-yield discharge tends to be larger than Q_{eff} , especially in fine bed rivers (Vogel et al. 2003; Sholtes, 2015). Therefore, it could serve as a better predictor for bankfull discharge in some situations. However, the ability of Q_{hy} to correctly predict Q_{bf} has not been studied closely across the wide range of river types and flow regimes (Sholtes and Bledsoe, 2016).

It has also been found that the discharge associated with 75% of cumulative sediment yield, Q_{75y} , can serve as a predictor for bankfull discharge in fine bed rivers (Copeland et al., 2005). This however compromises the physical basis of this approach to some extent, as usually not all sediment considered in the 75% of cumulative yield participate in channel forming.

To account for data-scarce situation the sediment transport data used in this analysis were taken from regional rating curve created for Rees hydrological station by Asselman (2000). The general expression for the sediment rating curve takes the following form:

$$C = p + a \cdot Q^b$$

With C – sediment concentration, mg/l; $p = 29.3$, $a = 1.96 \cdot 10^{-6}$, $b = 1.93$ – rating curve coefficients. R^2 for the Rees station sediment rating curve reached the value of 0.44 (Asselman, 2000). Due to such low R^2 value a substantial measure of uncertainty has been introduced into the sediment yield calculation. It should be taken into account while studying the results of the given analysis and drawing conclusion based on any findings. This subject will be faced in the Discussions section of this report (Chapter 7).

For the calculation of Q_{eff} and Q_{hy} , the methodology derived by Biedenharn et al. (2000) was used. The computational procedure consisted of 3 recommended steps. In Step 1, the flow-frequency distribution is derived from available flow-duration data. In Step 2, sediment data is used to construct a

bed-material load rating curve. In Step 3, the flow-frequency distribution and bed-material load rating curve are combined to produce a sediment-load histogram, which displays sediment load as a function of discharge for the period of record. The histogram peak indicates the effective discharge.

Further all 3 steps will be described briefly in a number sub-steps some of which are dependent on the available data and some are strictly necessary to reach the goal of the analysis.

Firstly, the record from a single gauging station (Lobith) was used to develop the flow-frequency distribution. As the gauge is located within the project reach, it can be assumed representative for the whole domain. It is also important that watershed conditions have remained unchanged during the selected flow period. The period of record on the Lobith station spans well over 30 years before the studied flood event and does not contain any data gaps, thus it can be assumed representative of the natural flow sequence over the chosen period. However, since only daily mean data has been available for the required period, some of the short term discharge variability (extreme values) could have been lost. Thus, the results of the analysis should be viewed with a portion of caution.

The discharge range was calculated by subtracting the minimum discharge in the flow record from the maximum discharge to establish the discharge classes for the analysis. 25 discharge classes were created according to the recommendation in the guideline (Biedenharn et al., 2000) with the class interval equal to $445 \text{ m}^3/\text{s}$.

The frequency of occurrence for each discharge class has been determined from the record of observed flows (Figure 17). For convenience the actual frequency was converted to percentage frequency. The percentage frequency represents the proportion of the flow record falling within the upper and lower limits of each discharge class. As, all discharge classes display flow frequencies greater than zero and there are no isolated peaks in individual classes at the high end of the range of observed discharges, it means that no outliers are disturbing the data and the discharge classes were established correctly.

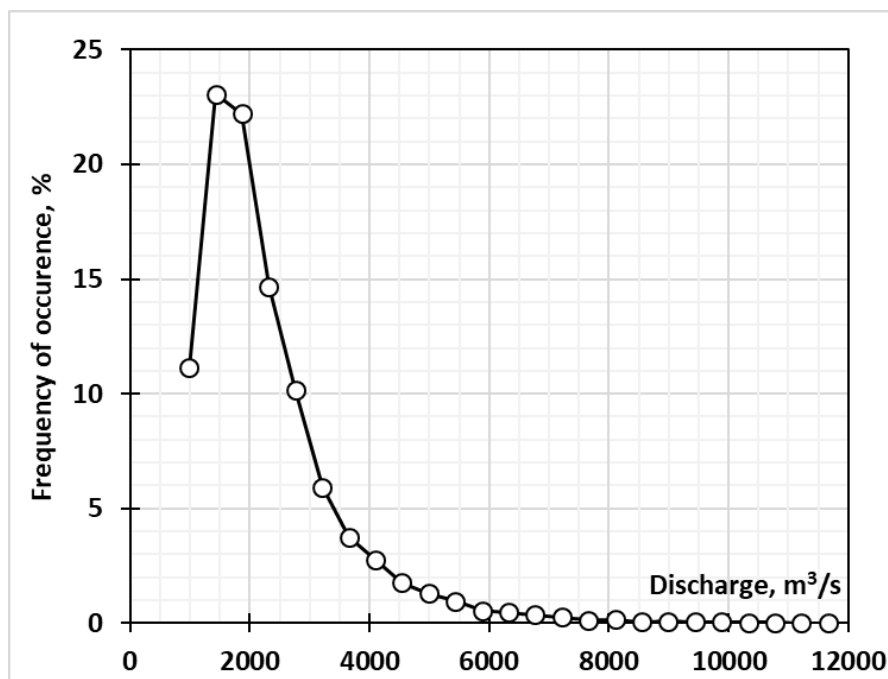


FIGURE 17 – FREQUENCY OF DISCHARGE VALUES OCCURRENCE FOR LOBITH HYDROLOGICAL STATION

Consequently, the sediment data is required to generate the bed-material load rating curve. This data may be obtained from measurements at a gauging station if the gauge is in close proximity to the project reach. Due to assumption of data-scarce region, the sediment rating curve for Rees gauge station was used instead of the sediment transport series as was stated previously (Figure 18).

In streams dominated by suspended load, a best-fit regression curve, fitted to the data, may be adequate to produce a bed-material load function. Frequently this takes the form of a power function:

$$Q_s = aQ^b$$

where Q_s is the bed-material load discharge, Q is the water discharge, a is a regression coefficient, and b is a regression exponent. However, the rating curve determined by Asselman (2000) adopt a slightly different type of equation, which was shown previously.

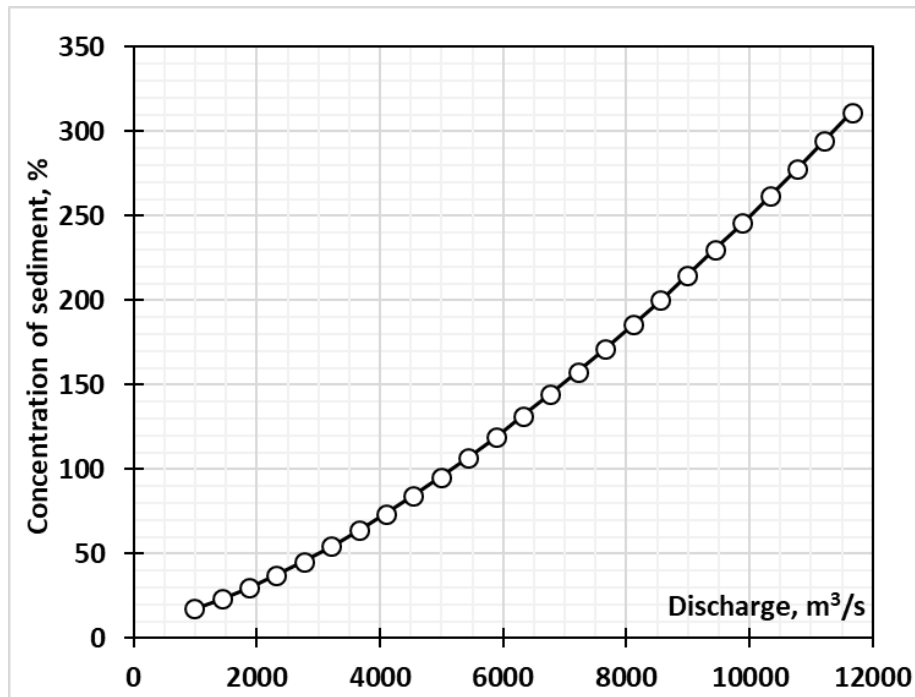


FIGURE 18 – SEDIMENT RATING CURVE FOR REES HYDROLOGICAL STATION

The discharges used to generate the bed-material load histogram are the mean discharges in each class in the flow frequency distribution. The histogram is generated by using those representative discharges and the bed-material load rating curve to find the bed-material load for each discharge class and multiplying this load by the frequency of occurrence of that discharge class. The results are plotted as a graph representing the total amount of bed-material load transported by each discharge class during the period of record (Figure 19).

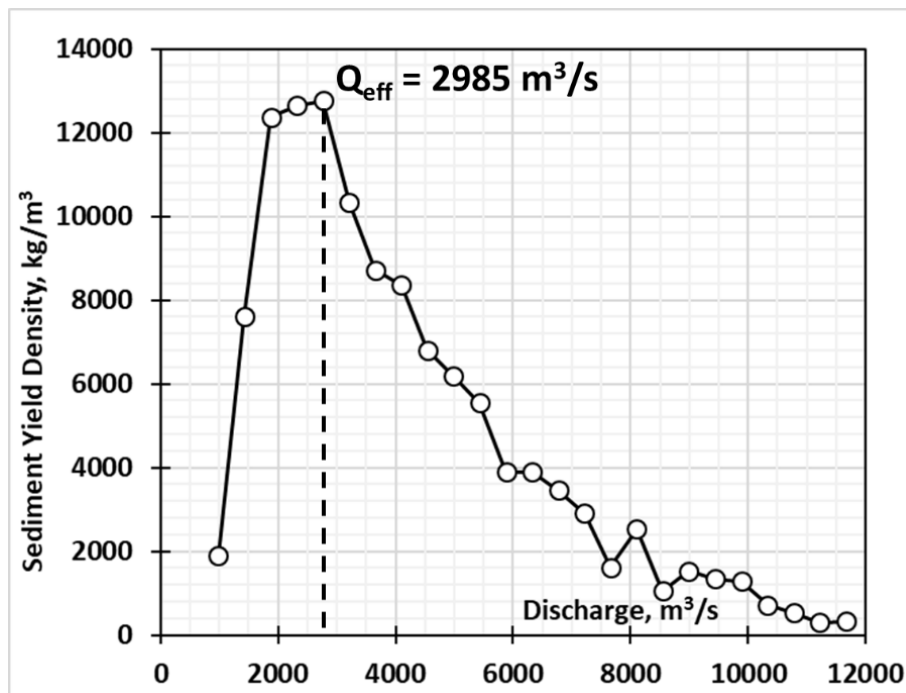


FIGURE 19 – SEDIMENT YIELD DENSITY INTERPOLATED TO LOBITH HYDROLOGICAL STATION

The bed-material load graph displays a continuous distribution with a single mode (peak). For such situation, the effective discharge corresponds to that peak. In this case the effective discharge has been found equal to $Q_{\text{eff}} = 2985 \text{ m}^3/\text{s}$.

The return period for the effective discharge is expected to vary between sites depending on the flow and sediment-transport regime of the individual river or reach. Experience indicates that it lies within the range 1.01 and 3 years with a preponderance between 1.01 and 1.2 years, irrespective of the type of river (Hey, 1997). The annual maximum discharges of 1.01 and 1.2 years return period at Lobith station vary from 3000 to 5000 m^3/s , thus meaning that either the estimation of the Q_{eff} is too low or the effect of anthropogenic activity on a watershed and in the channel has influenced the sediment transport in the studied part of the Rhine basin in recent years before 1993 flood. Either way, no known sources of uncertainty were present in effective discharge calculation procedure. So, the determined value of Q_{eff} should be taken as it was found by this method.

Additionally, the graph of cumulative sediment yield has been drawn to determine the value of Q_{hy} (Figure 20). According to it, the half-yield discharge equals $Q_{\text{hy}} = 3400 \text{ m}^3/\text{s}$, while $Q_{75\text{y}} \approx 5000 \text{ m}^3/\text{s}$.

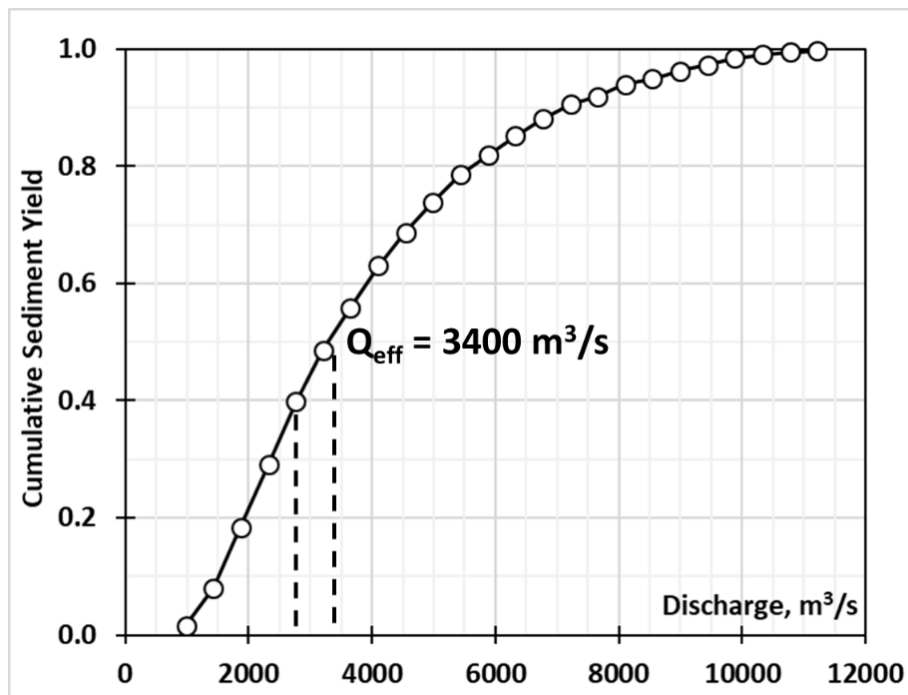


FIGURE 20 – CUMULATIVE SEDIMENT YIELD CURVE FOR LOBITH HYDROLOGICAL STATION

5. Results of reference case scenario

5.1. Calibration

5.1.1. Flood extent

In the absence of the flood extent maps for the studied events it is hard to judge on the precision of the outcome other than from qualitative perspective. It is known that during the 1995 flood no embankments were overflowed in this part of the Rhine's basin, thus the results of the model will be considered based on that knowledge. The inundation spatial pattern in this analysis is related to the peak water level condition and is assigned to January 31st, 1995.

It could be seen that this condition is completely fulfilled in the model outcome for $n = 0.028$ adopted as the roughness coefficient value (Figure 21). However, the simulated pattern of the flood extent in the lower part of the basin proves to have sufficiently higher accuracy compared to its upper reaches as we would see further.

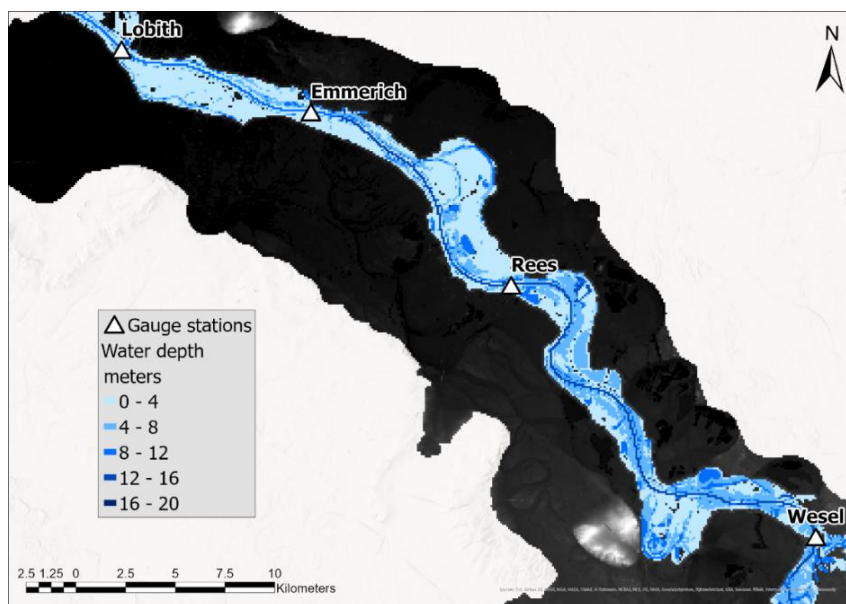


FIGURE 21 – SIMULATED FLOOD EXTENT ON JANUARY 31ST, 1995 IN THE DOWNSTREAM PART OF THE LOWER RHINE BASIN

It is important to understand that the overflowed water which was “wasted” on overflows happened due to model uncertainty are influencing the water level prediction accuracy up to some extent. Also the water is shown to fill the empty capacities such as dock reservoirs, but they do not overflow in this locations.

The water level simulation in the middle reach of the selected part of the basin shows some extent of minor discrepancies from the actual flood extent spatial pattern (Figure 22). The dike overflow occurs on several occasions (A, B, C, D) along the river channel. While the overflows A, B and D are evidently happened due to the inaccuracies created during the grid size transition (marked by too few overflow pixels on the dikes crest), the overflow C most likely was indeed caused by the water level increase at the location. Whether it was observed during the 1995 flood event or not is unknown, however the water level between Cologne and Ruhrort gauges is slightly underestimated during the flood's peak. Thus making it more likely that such simulated inundation represents the real situation.

The upper reach of the studied part of the Rhine basin also has one dike overflow location close to Cologne (Figure 23). Similar to the overflows A, B and D from the Figure 22, those overflows (E, F, G) are most likely to be an error of calculation due to incorrectly transited crest heights of the embankments. This is also shown by the manner in which overflow has happened. In that case dike are only overflowed in a few separate locations along the prolonged embankments section.

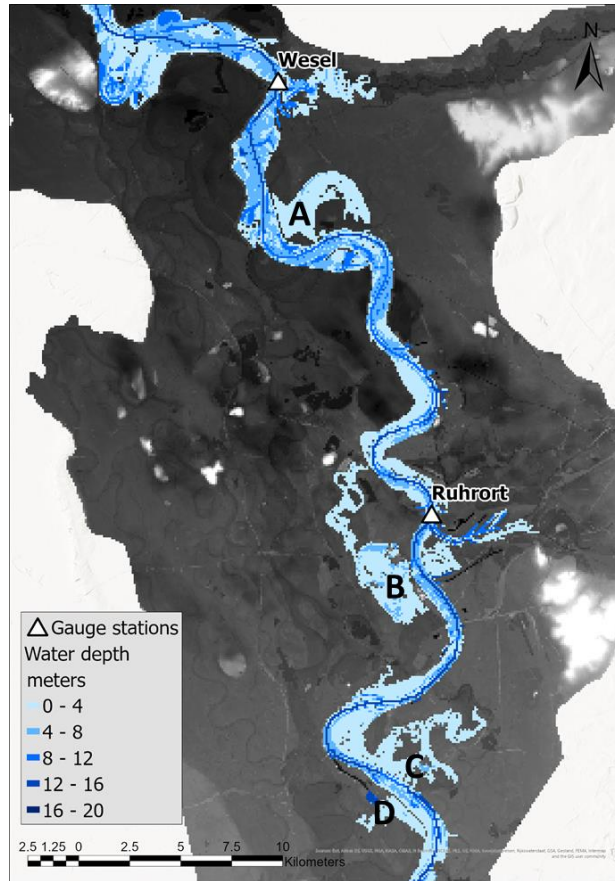


FIGURE 22 – SIMULATED FLOOD EXTENT ON JANUARY 31ST, 1995 IN THE MIDDLE PART OF THE LOWER RHINE BASIN

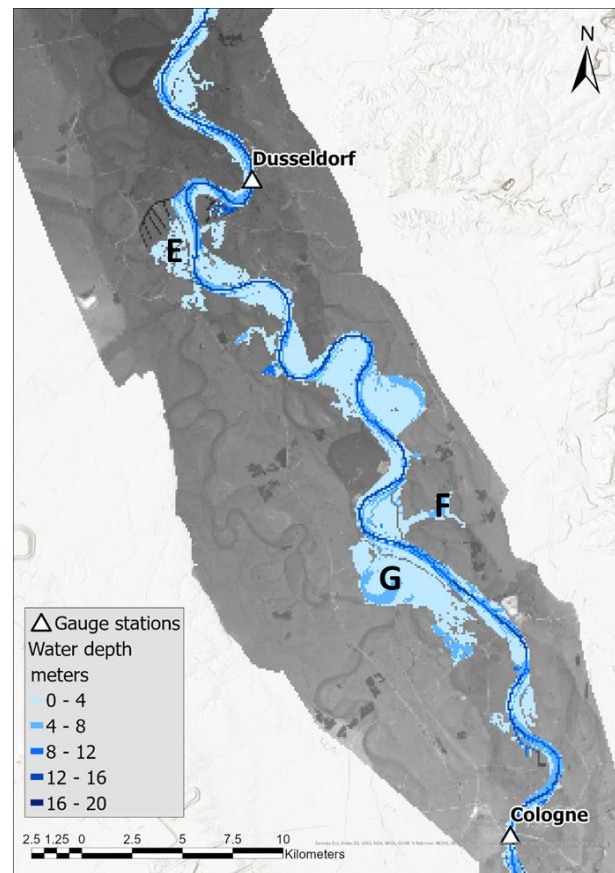


FIGURE 23 – SIMULATED FLOOD EXTENT ON JANUARY 31ST, 1995 IN THE UPSTREAM PART OF THE LOWER RHINE BASIN

As was mentioned earlier, all the abovementioned overflows which were caused by the mistakes made during the coarsening of the grid have also impacted the water level simulation outcome to some unknown extent. Considering the areas of the territory flooded solely due to overflows A – G (except for C due to probably natural causes) and average depth there, the total volume of the water which was taken from the river reaches 84.9 million m³ (Table 10).

TABLE 10. VOLUME OF THE DIKE OVERFLOW HAPPENED DUE TO UNCERTAINTIES IN THE MODEL INPUT FILES IN SIMULATION OF JANUARY, 1995 FLOOD

	A	B	D	E	F	G	Total
Area, km ²	7.8	10.5	2.4	2.6	2.0	13.6	38.9
Depth, m	1.5	2.0	4.0	1.0	3.0	2.5	–
Volume, m ³	11.7 · 10 ⁶	21.0 · 10 ⁶	9.6 · 10 ⁶	2.6 · 10 ⁶	6.0 · 10 ⁶	34.0 · 10 ⁶	84.9 · 10 ⁶

Such amount represents around 4% of the overall volume of water within the studied reach at the moment when the water level peak values were observed. In other terms, the absence of the grid coarsening effect on the crest height of embankments has resulted in underestimation of the water level downstream of the overflows by up to 35 cm during the flood's peak. This could explain the peak underestimation occurring on Ruhrort, Wesel and Rees stations, however the underestimation observed at Emmerich and Lobith gauges is too large to be justified solely by this reason. The further elaboration on this uncertainty source could be found in Chapter 7.

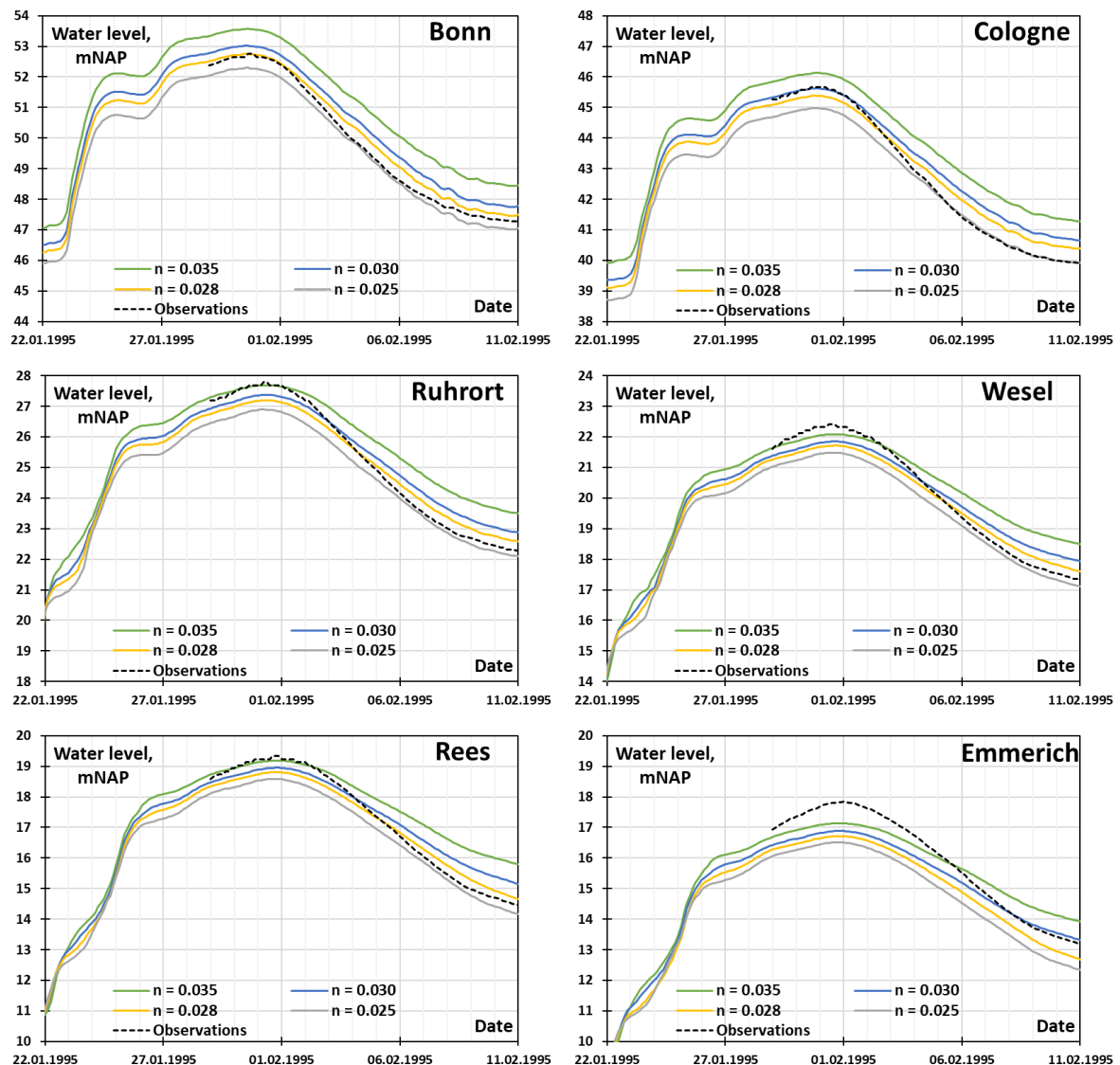


FIGURE 24 – MODEL CALIBRATION BY COMPARING PREDICTED AND MEASURED WATER LEVEL SERIES IN LOWER RHINE DURING THE JANUARY, 1995 FLOOD

5.1.2. Water level at gauge location

The calibration simulations performed on the 1995 flood event hydrological data based on the spatially uniform Manning's n friction coefficient value show controversial results regarding water level prediction along the Lower Rhine basin (Figure 24). As could be seen from the comparison graph below, the rate at which the simulated water level series aligns with measurements changes spatially from the upstream part to the downstream part of the model domain. In order to determine the source of such instability in model efficiency, the separate analysis for different river sections represented by 6 monitoring locations has been done.

Within the studied reach of the Rhine river 3 different segments could be distinguished regarding the quality of the calibration based on the visual comparison of water level series measured and simulated by the model. These are:

1. Bonn – Cologne – Dusseldorf;
2. Ruhrort/Duisburg – Wesel – Rees;
3. Emmerich – Lobith.

Segment 1 is characterised by the best simulated water level compliance with the observed values at the peak of the flood wave by friction coefficient values $n = 0.028$ (Figure 24). However, the water level values during the recession of the flood wave are consistently overestimated by the model with such value of calibration parameter both in Bonn and Cologne. The modelling outcome of the run which used $n = 0.025$ as the calibration parameter value, on the other hand, shows better alignment during lower water level. The best prediction of the peak water level was done in runs with $n = 0.028$ and 0.030 in Bonn and Cologne, respectively. The quantitative analysis of the given series shows $n = 0.028$ and $n = 0.025$ to be the best suited parameter values among the studied in this research for both Bonn (Table 11a) and Cologne stations (Table 11b).

TABLE 11. ASSESSMENT OF CALIBRATION PARAMETERS EFFICIENCY FOR LOWER RHINE

a. Bonn	$n = 0.035$	$n = 0.030$	$n = 0.028$	$n = 0.025$
RMSE [m]	1.41	0.29	0.07	0.07
NSE	0.67	0.93	0.98	0.98
b. Cologne	$Q_{1.5,max}$	$Q_{2.0,max}$	$Q_{5.0,max}$	$Q_{2,mean}$
RMSE	1.43	0.29	0.18	0.11
NSE	0.71	0.91	0.96	0.98
c. Ruhrort	$Q_{1.5,max}$	$Q_{2.0,max}$	$Q_{5.0,max}$	$Q_{2,mean}$
RMSE	0.95	0.25	0.13	0.22
NSE	0.79	0.94	0.97	0.95
d. Wesel	$Q_{1.5,max}$	$Q_{2.0,max}$	$Q_{5.0,max}$	$Q_{2,mean}$
RMSE	0.72	0.24	0.15	0.26
NSE	0.82	0.94	0.96	0.94
e. Rees	$Q_{1.5,max}$	$Q_{2.0,max}$	$Q_{5.0,max}$	$Q_{2,mean}$
RMSE	0.91	0.27	0.09	0.19
NSE	0.76	0.93	0.98	0.95
f. Emmerich	$Q_{1.5,max}$	$Q_{2.0,max}$	$Q_{5.0,max}$	$Q_{2,mean}$
RMSE	0.34	0.26	0.51	0.97
NSE	0.90	0.92	0.85	0.72

* values indicating good match between measurements and the model are in bold

Table 11a also shows that the values of RMSE and NSE for the Bonn station are the best for the $n = 0.028$ and $n = 0.025$ values, however the same metrics for Cologne station (Table 11b) indicate $n = 0.025$ as the most appropriate calibration parameter. The latter happens since water level values simulated with $n = 0.025$ match the observed situation on a longer period of time during the recession of the flood wave. Though considering the topic of the study, which is to assess different assumptions for the flood inundation modelling, the preference should be given to the $n = 0.028$ which was found to better estimate the hydrograph peak in both occasions.

The model runs in Segment 2 built with various n values fail to predict the values during both peak and recession of the flood wave (Figure 24). It should be noticed those of the calibration runs which were able to catch either the peak value or recession curve ($n = 0.035$ and $n = 0.030$) do not fully represent the situation seen in measurement data either drastically overestimating lowest values or underestimating the peaks.

The set of selected calibration parameters has also shown reduced sensitivity of the model results to the Manning's coefficient variability as the range of predicted values decreased compared to Segment 1 from almost 2 to around 1 m. This makes it harder to implement single best solution for the calibration parameter value.

All 3 gauges within Segment 2 were shown to be most appropriate represented by the model whilst using Manning's coefficient $n = 0.028$ (Table 11c-e). Therefore, despite the lack of the match in peak values with the measurement dataset, $n = 0.028$ could be viewed as sufficient for the modelling purposes. The maximum deviation of water level value within Segment 2 compared to the results of $n = 0.028$ run is limited to 0.7m (5.7% of maximum depth) at Wesel gauge during the high water stage. Such range could be caused by the accuracy loss during the grid cell size transition, thus being viewed as rather insignificant.

Segment 3 is represented by major discrepancies between the simulated and observed situations (Figure 24). The maximum difference between measured and modelled values equals to more than 1.5 m at location of Emmerich hydrological station for any n value which has not been observed at any other location with the model domain. This occurs to be almost 10% of the maximum depth observed during the 1995 flood event. However, the further adjustment of the Manning's friction coefficient values gives unnatural modelling results upstream of the Segment 3, which implies restrictions on the use of roughness coefficient values higher than $n = 0.035$.

Predictably, the quantitative assessment for Segment 3 stations shows the similar picture presenting $n = 0.030$ as the most suitable Manning's friction coefficient value among studied (Table 11f). It seems that the further increase of the n values only leads the rise of the error between simulated and observed water levels due to the heterogeneous rate of increase in lower and higher water parts of the hydrograph.

Additionally, all stations' water level series simulated by the model were joined into a single datasets for each of the calibrated Manning's coefficient value in consideration. To do so, they were detrended by deducting the location-specific average observed water levels. These sets were then plotted against the measurement data to determine the coherence between those on a whole basin level (Figure 25).

All of the reviewed models with various friction coefficients were found to generally underestimate the highest while overestimating the lowest water level values to a different extent. Furthermore, from the correlation graph it could be seen that lower roughness values result in better representation of the water level in general. It could be seen, however, that though both models with $n = 0.028$ and $n = 0.025$ friction estimates show better results all along the range of water level variance, the best statistical coincidence of the simulated and observed values regardless of the spatial reference were found for the value of $n = 0.028$.

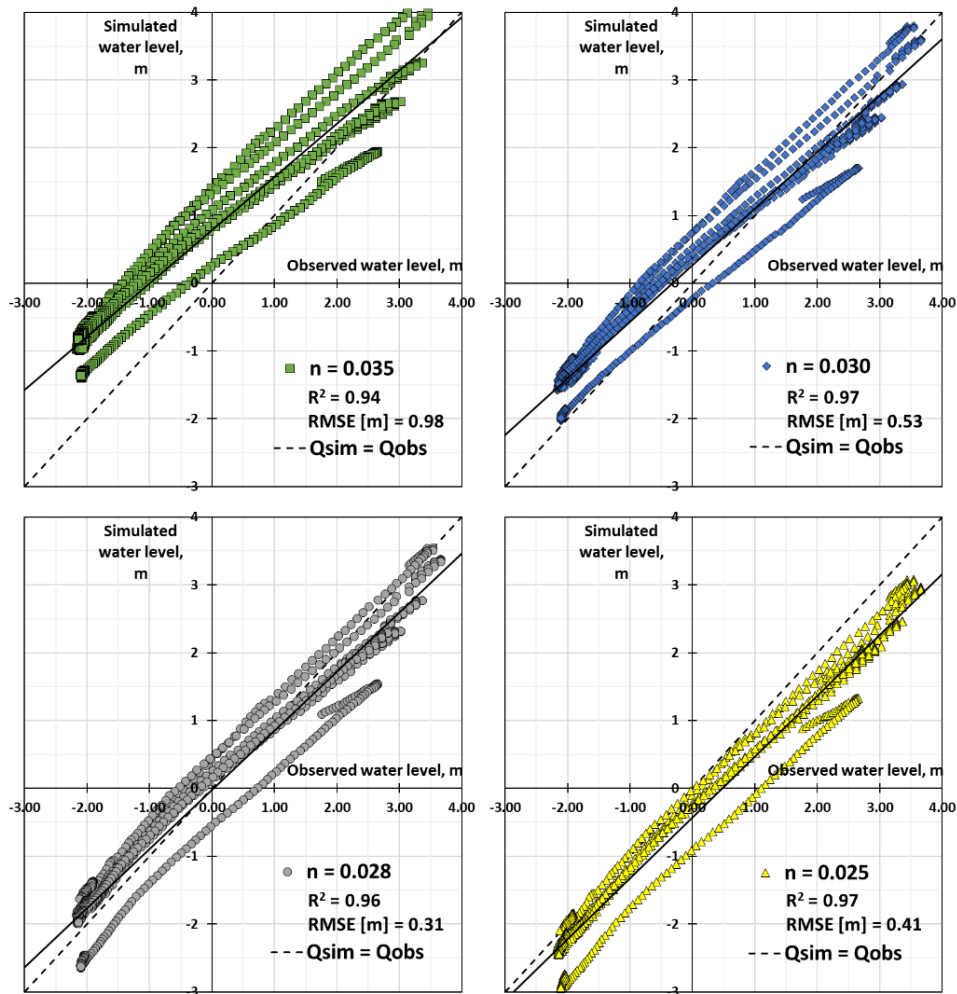


FIGURE 25 – CALIBRATION BETWEEN DETRENDED WATER LEVEL PREDICTIONS AND MEASUREMENT REGARDLESS OF THEIR LOCATION

Therefore, the calibration regarding water level at stations data comparison suggests the Manning's coefficient value of $n = 0.028$ to be used during the research. This values will be furtherly validated on the 1993 flood event dataset. The full set of the criteria for $n = 0.028$ simulation of 1995 flood could be found in Table 12. The least accurate predictions using $n = 0.028$ as a Manning's friction coefficient estimate is found in the downstream part of the Lower Rhine basin. An average deviation of the simulated water levels is equal to 0.51 m while the average value gives an underestimation of 0.7 m. However, such situation is observed regardless of the calibration parameter used, and thus, should be caused by other source of uncertainty. The most probable version is that some kind of unstable zone is created near the downstream boundary of the model, introducing high deviations from the measurement data.

TABLE 12 – INTEGRATED OVERVIEW OF CALIBRATION RUN PERFORMANCE WITH MANNING'S $N = 0.028 \text{ S/M}^{1/3}$ FOR JANUARY, 1995 FLOOD

	Bonn	Cologne	Ruhrort	Wesel	Rees	Emmerich
O_{average}	49.2	42.0	24.4	19.4	16.5	15.2
M_{average}	49.4	42.3	24.5	19.4	16.5	14.5
RMSE [m]	0.07	0.18	0.13	0.15	0.09	0.51
NSE	0.98	0.96	0.97	0.96	0.98	0.85

5.2. Validation

5.2.1. Water level at gauge location

With the calibration procedure passed giving the channel friction coefficient estimate of $n = 0.028$, it had to be validated on the independent dataset. For this purposes, the 1993 flood event was used as described in Section 2.2.1.

The results of the validation run of the model have shown that the pattern of the simulated and observed water level values alignment hold compared to the findings of calibration run. Over the studied part of the Rhine basin the peak water levels tend to be slightly underestimated by the model while lower values could be overestimated to some extent (Figure 26). Also the same situation is observed at Emmerich gauge when all values are calculated lower than according to the measurement series, though to a lesser extent. Nevertheless, the differences in peak values of simulated and observed water level at Emmerich station are only somewhat less than in 1995 case scenario. Based on the 1993 dataset they reach up to 1 m at the flood's peak.

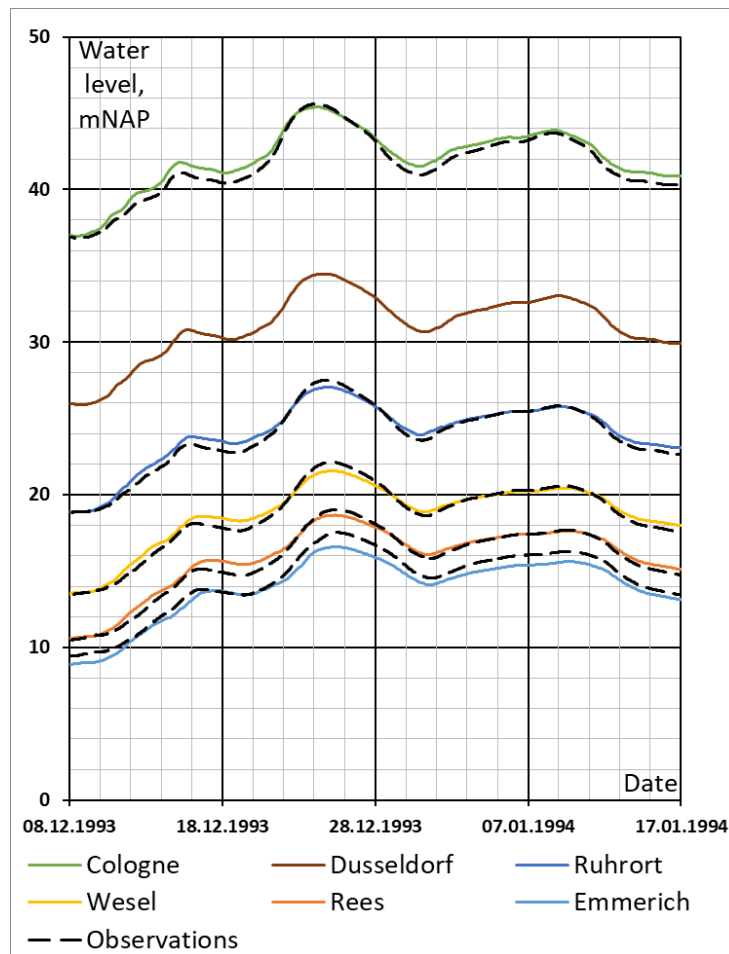


FIGURE 26 – COMPARISON OF PREDICTED AND OBSERVED WATER LEVEL SERIES OF DECEMBER, 1993 FLOOD IN LOWER RHINE

The quantitative analysis of the simulated and measured data series similarity also shows better results compared to calibration outcome (Table 13). The major part of the basin characterised by Ruhrort, Wesel and Rees station indicate a sufficiently high compatibility according to RMSE and NSE values. The most problematic section of the study area, namely the reach downstream of Emmerich gauge, also substantial compliance with the measurement data displaying and incredible improvement from $NSE = 0.85$ to $NSE = 0.95$. All this joined with the calibration results allow us to consider $n = 0.028$ as an adequate estimate for Manning's friction coefficient in order to perform the further analysis and answer the determined research questions.

TABLE 13. INTEGRATED OVERVIEW OF VALIDATION RUN PERFORMANCE FOR DECEMBER, 1993 FLOOD

	Cologne	Dusseldorf	Ruhrort	Wesel	Rees	Emmerich
O_{average}	40.7	-	23.0	17.8	14.8	13.5
M_{average}	41.1	30.2	23.1	17.9	15.0	13.0
RMSE [m]	0.21	-	0.10	0.10	0.08	0.28
NSE	0.96	-	0.98	0.98	0.99	0.95

5.2.2. Flood extent

Considering the model outcome for flood extent, it shows the picture comparable to the 1995 situation (Figure 27; Figure 28; Figure 29). While the observations say that the first line of embankments have succeeded in retaining the flood water in 1993, the model mainly suggests the same scenario for the most part of the study domain. However, similarly to the previous scenario several overflows could be observed at the same locations along the studied river reach. The flood extent was studied at its maximum on December 25th, 1993.

The flood extent map shows no signs of any overflows in the downstream part of the basin (Wesel – Rees – Emmerich – Lobith) for the peak water level situation (Figure 27). Most of the floodplain except for the dead channels and other water reservoirs is covered with a layer of water approximately 2 m deep while the maximum depth is reached at channel location and equals up to 18.3 m over the domain. The simulated water level coincidence with the measurement data (Figure 26) hints at the good quality of the flood extent predictions made by the model.

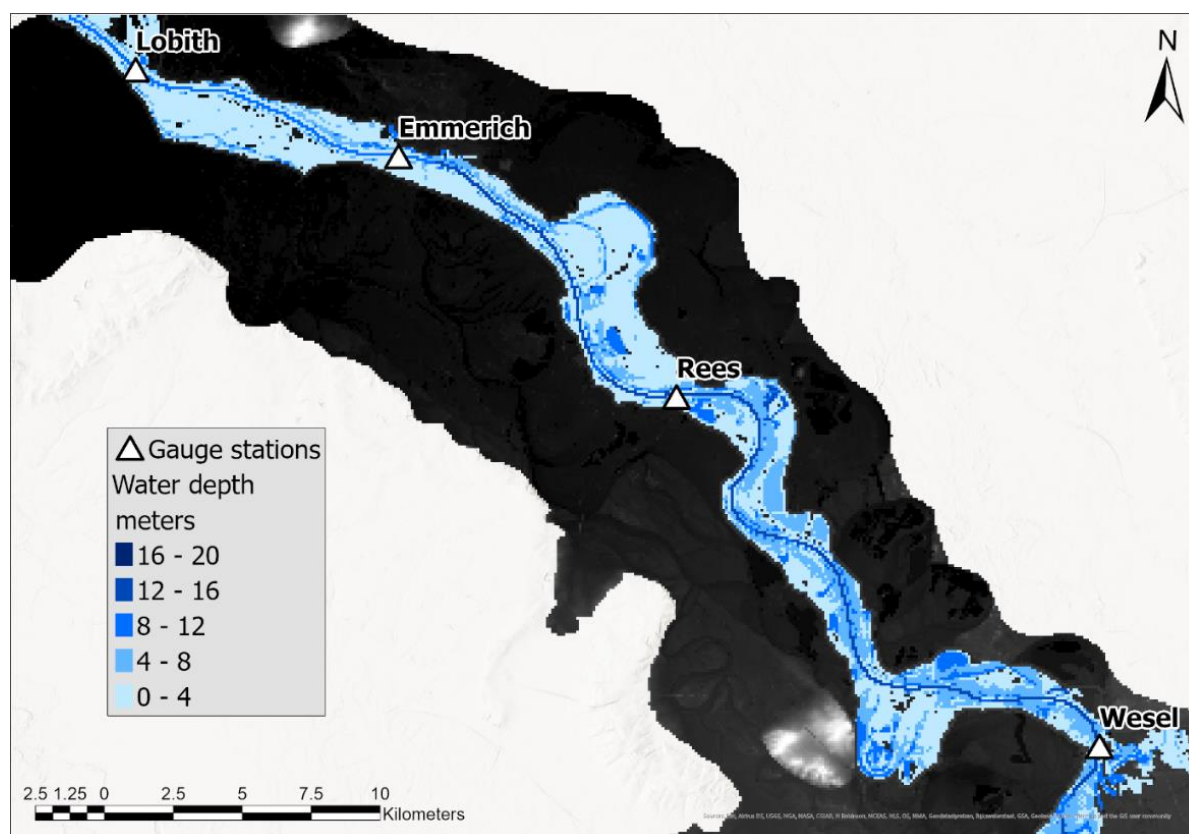


FIGURE 27 – SIMULATED FLOOD EXTENT ON DECEMBER 25TH, 1993 IN THE DOWNSTREAM PART OF THE LOWER RHINE BASIN

Several overflows have been simulated by the model in the middle part of the domain and, while all of them are similar to the ones described during the calibration scenario, the overall inundated area is smaller in 1993 (Figure 28). This happened due to differences in maximum water level between the two studied floods. The peak values in 1993 are on average at least 0.5 m lower than that in 1995. This in its turn leads to reduced flood extent in B and C location compared to the calibration scenario.

It is important to note that, based on the flood inundation map, the section between Rees and Ruhrort gauges is characterised by increased water depth at the floodplain compared to rest of the domain (Figure 27; Figure 28). This is most likely due to morphological features of the floodplain, which is characterised by lower surface elevation. Additionally, the floodplain become wider in that section of the domain as the area is less urbanised compared to other parts of the Lower Rhine basin. The water depth at this section varies around 4.5 m at whole width of the embanked area while water depth near the dikes' toes does not exceed 3.0 m most of the times over the rest part of the studied reach.

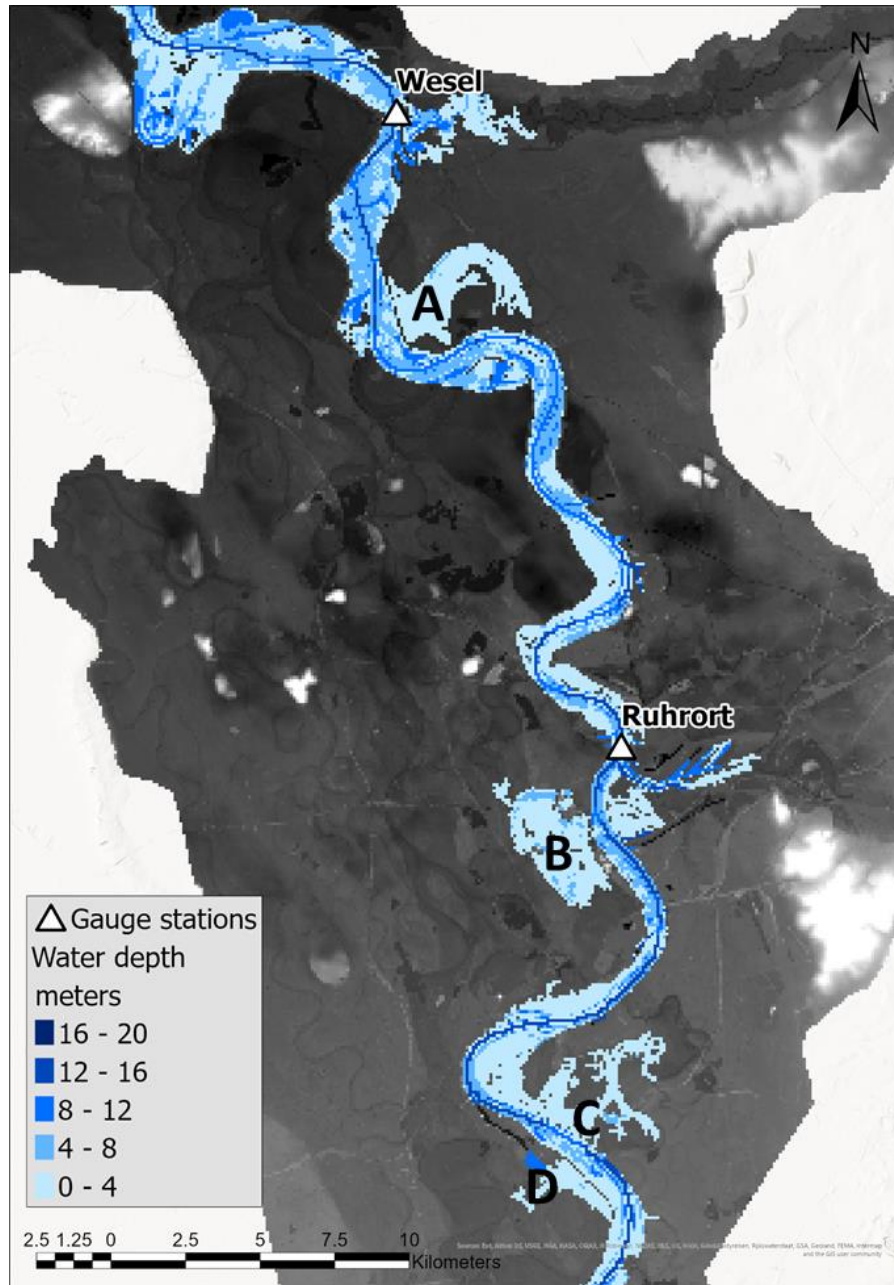


FIGURE 28 – SIMULATED FLOOD EXTENT ON DECEMBER 25TH, 1993 IN THE MIDDLE PART OF THE LOWER RHINE BASIN

The upper reach of the studied part of the Rhine basin is again characterised by several minor overflows (E, F) and one single major overflow (G). While the area inundated due to the overflows at specified locations do not differ significantly from 1995 to 1993 flood, the depth pattern slightly changes to account for less water extent coming from the river over the embankments (Figure 29).

However, the historic overflow to the Cologne old city that was described in Section 2.2.1, has not been predicted by the model. This was probably due to updated by 2015 situation DEM, which also included new dikes in some location such as in Cologne.

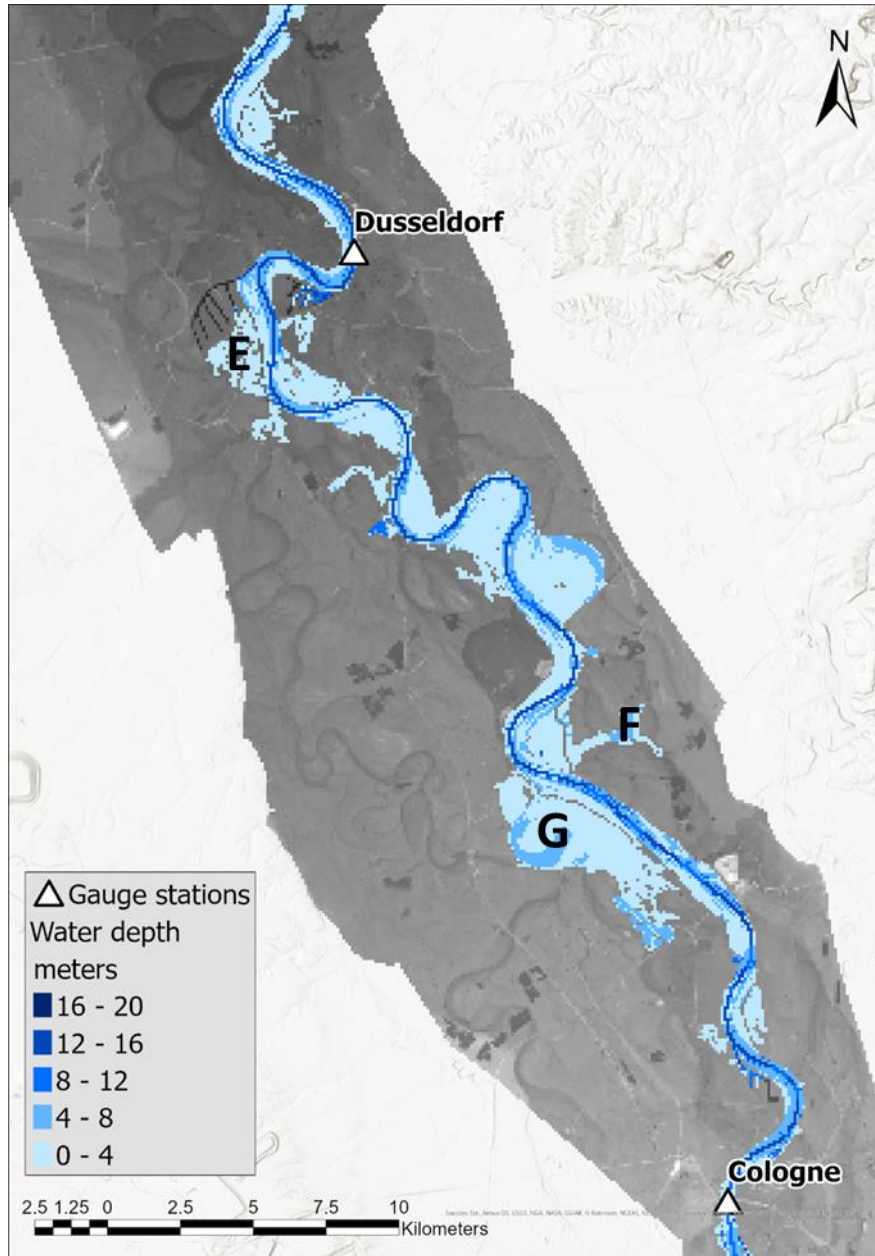


FIGURE 29 – SIMULATED FLOOD EXTENT ON DECEMBER 25TH, 1993 IN THE UPSTREAM PART OF THE LOWER RHINE BASIN

All of this leads to decrease in the effect which inaccuracies in DEM coarsening implies on the modelling results. This could be one of the reasons why the simulated water level values in 1993 scenario are better aligned to the measurement data compared to 1995 flood. The overall area inundated outside of the embankments according to the model has been reduced up to 32.9 km² for 1993 flood simulation (compared to ≈ 45 km² in 1995). Thus, the volume of the river water “lost” due to unaccuracies also becomes smaller compared to 1995 event and equals to 74.3 million m³ (Table 14). Such amount of water could be accounted for up to 30 cm rise downstream of the observed dike overflows at the peak of the flood. This is almost the exact amount by which water level peak is underestimated at Lobith gauge according to the model output (Figure 26).

TABLE 14. VOLUME OF THE DIKE OVERFLOW HAPPENED DUE TO UNCERTAINTIES IN THE MODEL INPUT FILES IN SIMULATION OF DECEMBER, 1993 FLOOD

	A	B	D	E	F	G	Total
Area, km ²	6.4	7.3	2.1	2.5	2.0	12.6	32.9
Depth, m	1.0	2.5	3.5	1.5	3.5	2.5	–
Volume, m ³	$6.4 \cdot 10^6$	$18.3 \cdot 10^6$	$7.3 \cdot 10^6$	$3.8 \cdot 10^6$	$7.0 \cdot 10^6$	$31.5 \cdot 10^6$	$74.3 \cdot 10^6$

6. Channel size estimates assessment

6.1. Annual maximum discharge

The first bankfull discharge estimate to be addressed will be the 1-in-2 years annual maximum flow ($Q_{2.0,max}$) as it is known as the most commonly applied assumption for the Q_{bf} . It can be seen from the simulated hydrographs for the studied part of the Rhine basin that the $Q_{2.0,max}$ channel size assumption gives visually sufficient approximation of the hydrodynamic processes in the river (Figure 30). Moreover, there is a fictional improvement to be seen compared to the flow prediction made based on a real bathymetry reference case. However, this is caused by the uncertainties drawn into the model formulation and is purely a coincidence.

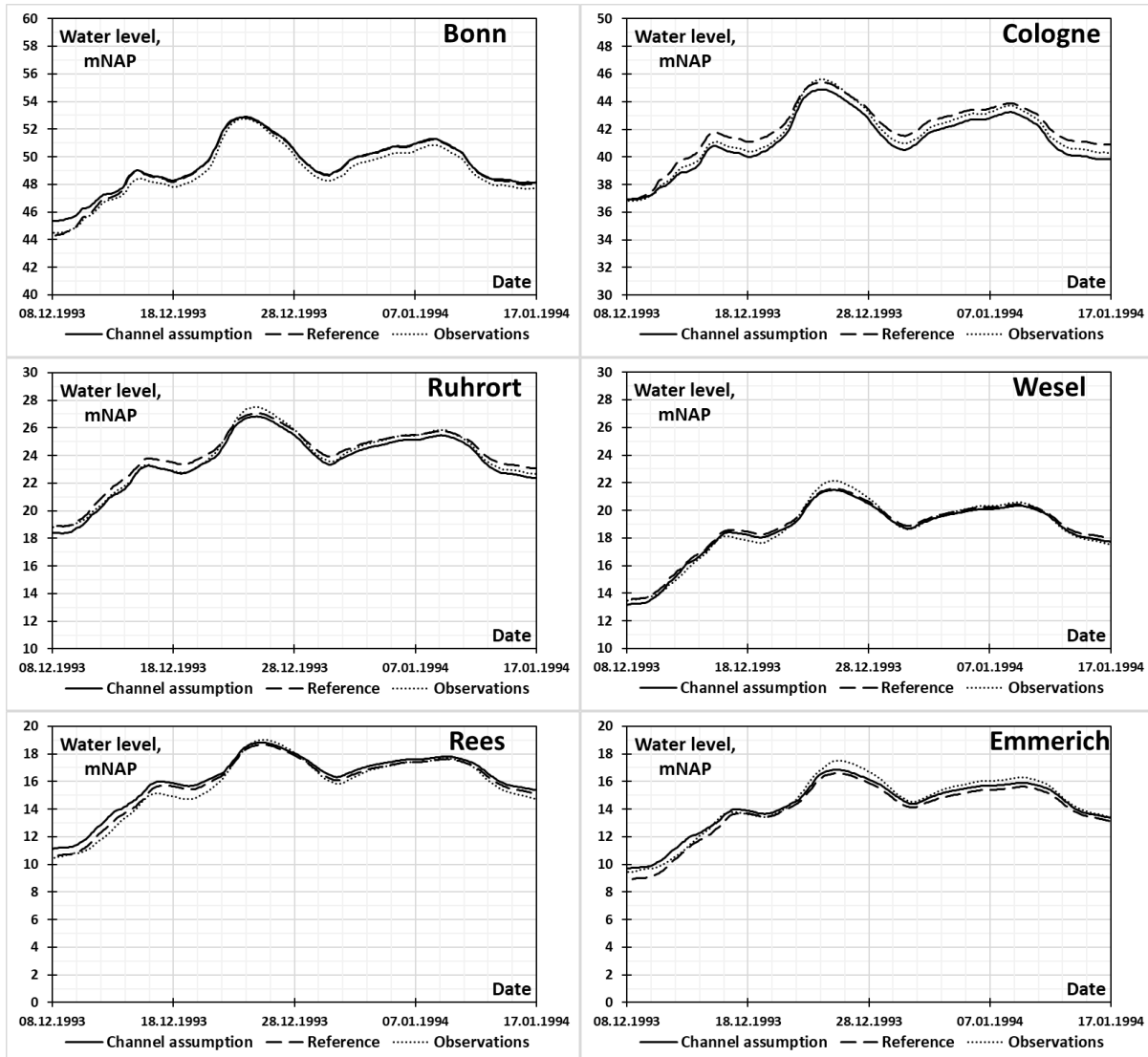


FIGURE 30 – COMPARISON BETWEEN MEASUREMENT DATA, REFERENCE SCENARIO AND PREDICTION FOR WATER LEVEL IN LOWER RHINE USING ANNUAL MAXIMUM DISCHARGE WITH 2 YEARS RETURN PERIOD AS BANKFULL FLOW APPROXIMATION

To supplement to the second research question answer, the annual maximum discharges of different probability (1-in-1.5 years; 1-in-5 years) have been also studied to find the best possible alignment with the measurement data (Figure 31).

From the series of simulated water level values for Q_{bf} equal to $Q_{1.5,max}$, $Q_{2.0,max}$ and $Q_{5.0,max}$ it seems that discharge of 1.5 year return period as an estimate of channel conveyance shows better results on few stations over the domain. Namely, those are located in a Cologne – Ruhrort section of the Rhine. However, the water level series at the most of the gauge locations still show better conformity for bankfull discharge equal to 1-in-2 years annual maximum flow.

Predictably, $Q_{bf} = Q_{5.0,max}$ shows substantial underestimation of the water levels during the simulated flood event due to larger river channel capacity. Though, the extent of undervaluation decreases in the downstream part of the studied reach (Rees – Emmerich – Lobith) probably due to the gradual increase in bankfull discharge coming from the inflowing tributaries' flow and consequent increase in bankfull channel size.

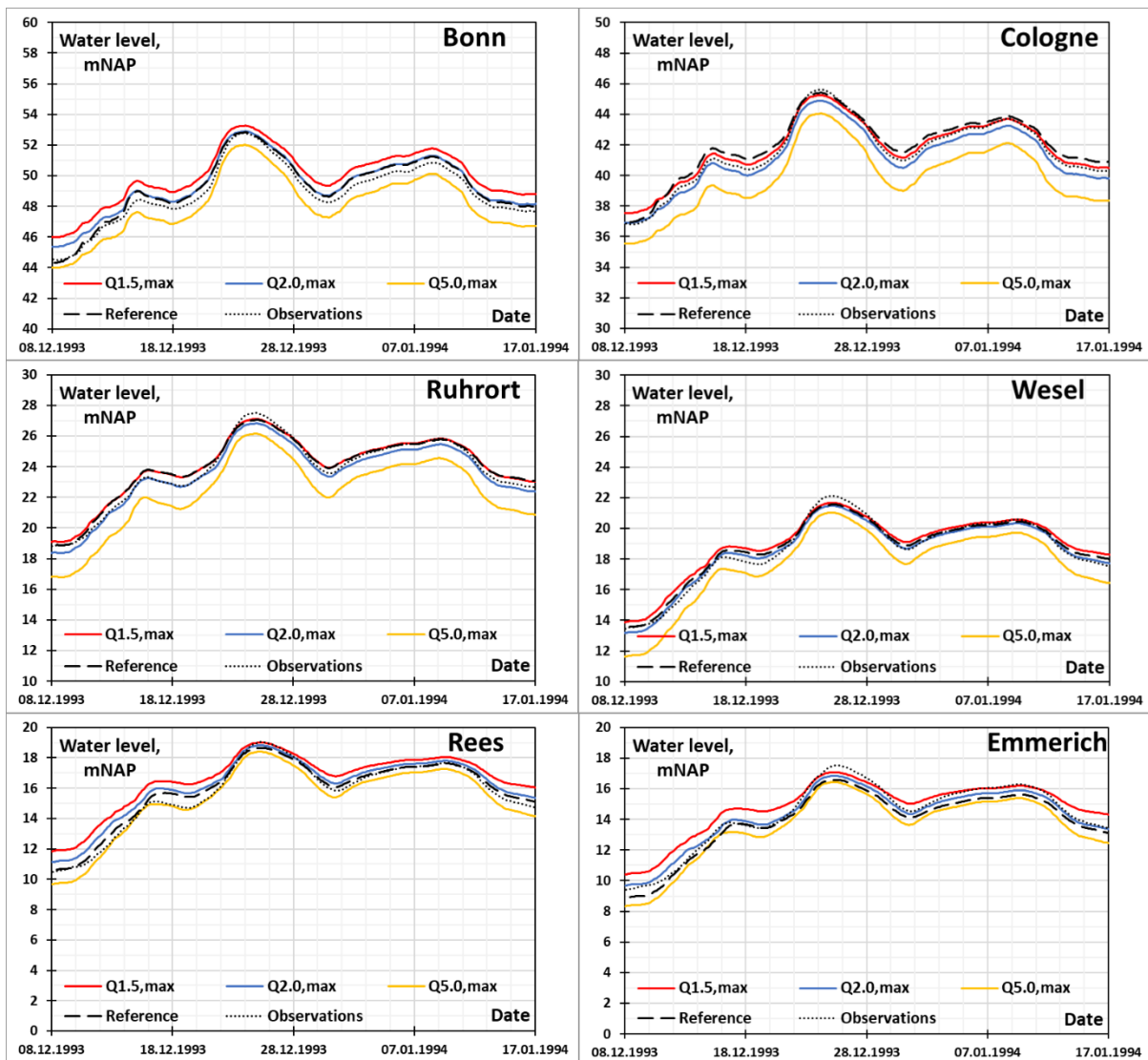


FIGURE 31 – COMPARISON BETWEEN MEASUREMENT DATA, REFERENCE SCENARIO AND PREDICTION FOR WATER LEVEL IN LOWER RHINE USING ANNUAL MAXIMUM DISCHARGE WITH 1.5, 2.0 AND 5.0 YEARS RETURN PERIOD AS BANKFULL FLOW APPROXIMATION

The correlation plot of the predicted and observed detrended (with average measured value) water level values has been designed to study how good does model represent the water level series in each location (Figure 32). It has shown how model accounts for highest and lowest values of water level and homogeneity of the data set.

From the correlation plots it becomes evident that $Q_{5.0,max}$ assumption tend to underestimate the water level values at all studied locations. The $Q_{bf} = Q_{1.5,max}$ estimate in its turn overestimates lower water level values constantly with up to 1.5 m in the downstream part of the basin, while it almost perfectly simulates peak water surface elevation. From the set of correlation plots for $Q_{2.0,max}$ assumption only 2 of them show any significant deviations from the measurement data. Those “bad” stations are Bonn and Rees, where the low flow is poorly predicted by the model. This however, compensates by almost constant under estimation of the flood peaks, which is also depicted in the correlation plots.

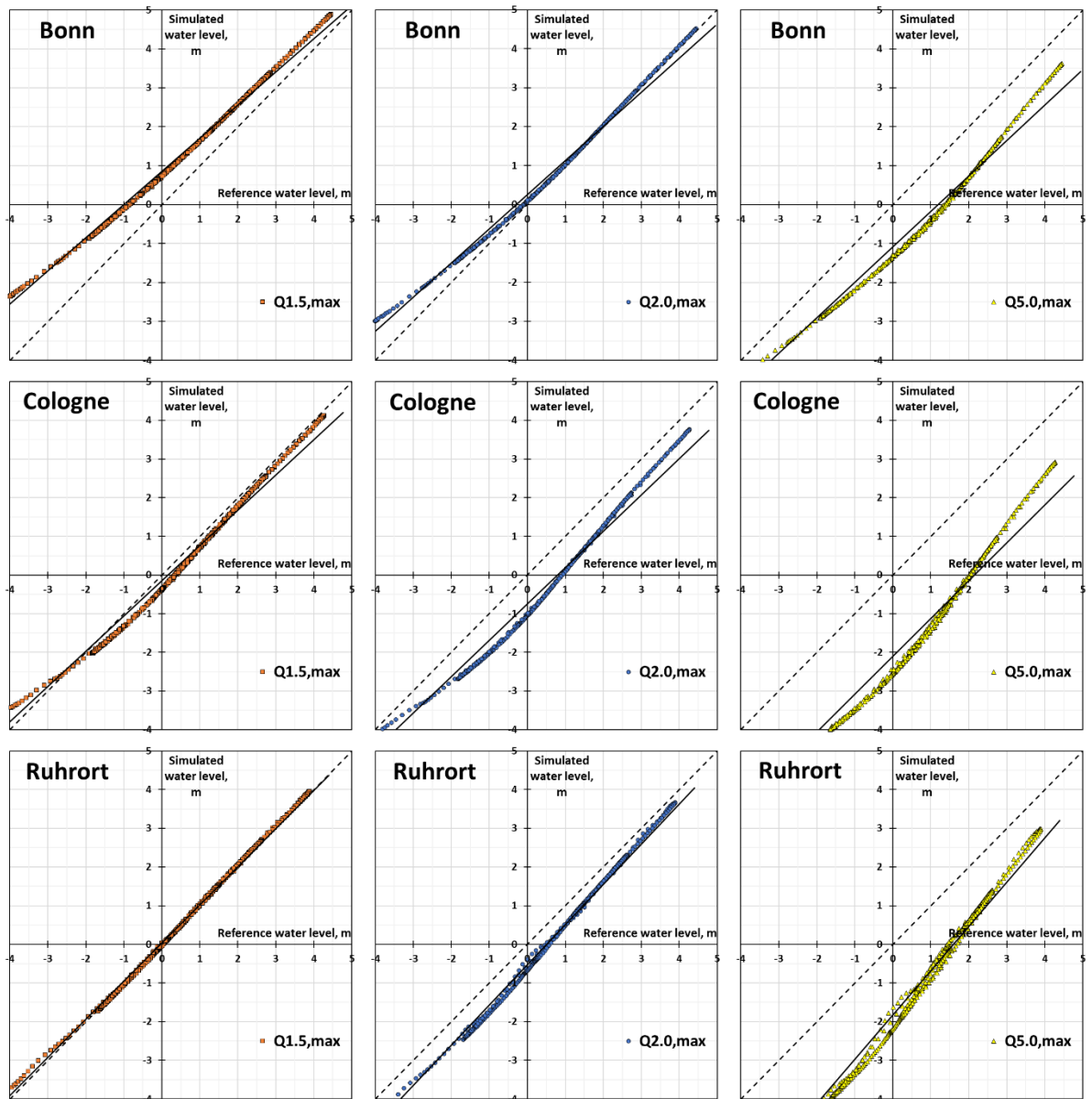


FIGURE 32 – CORRELATION PLOT FOR PREDICTED AND REFERENCE WATER LEVELS IN LOWER RHINE USING ANNUAL MAXIMUM DISCHARGE WITH 1.5, 2.0 AND 5.0 YEARS RETURN PERIOD AS BANKFULL FLOW APPROXIMATION (PART 1)

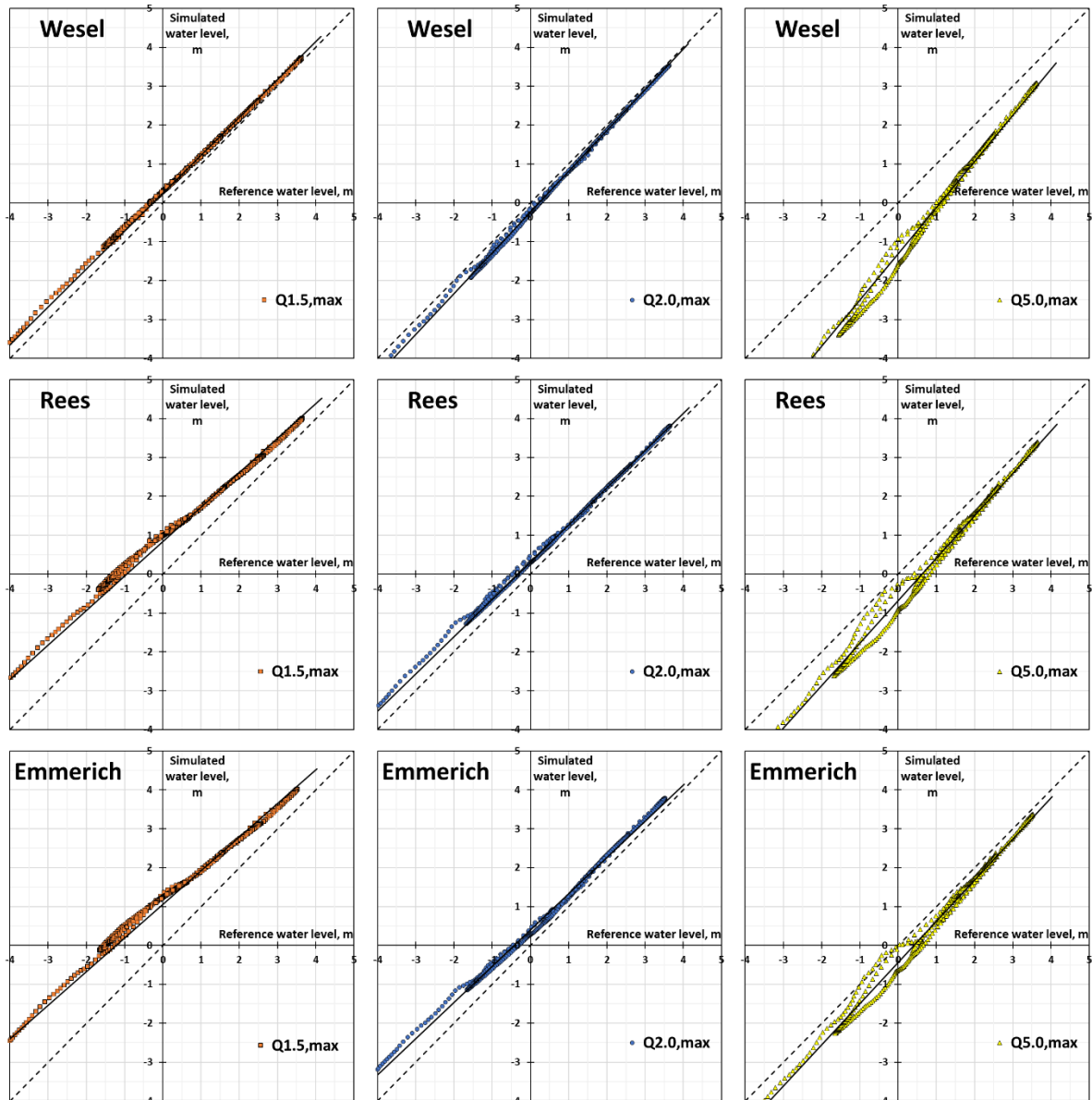


FIGURE 33 – CORRELATION PLOT FOR PREDICTED AND REFERENCE WATER LEVELS IN LOWER RHINE USING ANNUAL MAXIMUM DISCHARGE WITH 1.5, 2.0 AND 5.0 YEARS RETURN PERIOD AS BANKFULL FLOW APPROXIMATION (PART 2)

6.2. Annual mean discharge

The $Q_{2,\text{mean}}$ assumption implies a large overestimation of the water levels during the 1993 flood event (Figure 34). The most significant differences occur during lower water stages as well as on rising and falling limb of a flood wave. On the other hand, the flood wave peaks are simulated with significantly better accuracy in the downstream part of the studied reach (Ruhrort – Wesel – Rees – Emmerich – Lobith). This, however, does not apply to Bonn and Cologne stations most probably due to the spatial variability in bankfull discharge which tends to grow gradually downstream.

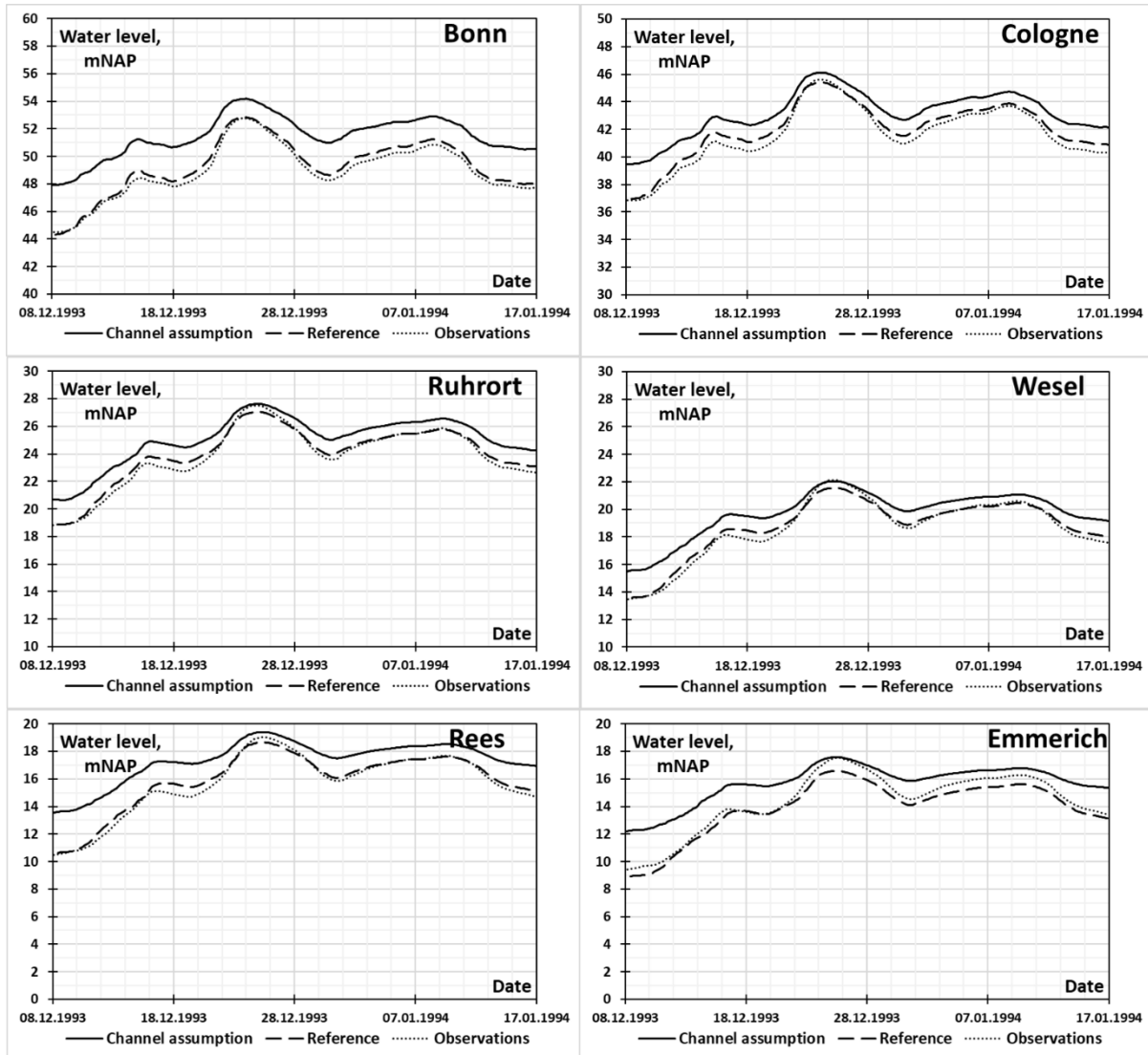


FIGURE 34 – COMPARISON BETWEEN MEASUREMENT DATA, REFERENCE SCENARIO AND PREDICTION FOR WATER LEVEL IN LOWER RHINE USING ANNUAL MEAN DISCHARGE WITH 2 YEARS RETURN PERIOD AS BANKFULL FLOW APPROXIMATION

The series of simulated water levels related to $Q_{\text{bf}} = Q_{10,\text{mean}}$ situation show sufficient rate of alignment with the reference case scenario in the river section between Cologne and Wesel stations (Figure 35). The water level values calculated for Bonn, Rees and Emmerich gauges overestimate the measurement data on average by 0.5 – 1.0 m. Due to the underestimation of the simulated peak in Emmerich inherent to all model versions, it is visually good estimated by the model in case of $Q_{10,\text{mean}}$. However, this most probably falls into the uncertainty range which is heavily present at the two downstream stations of the domain.

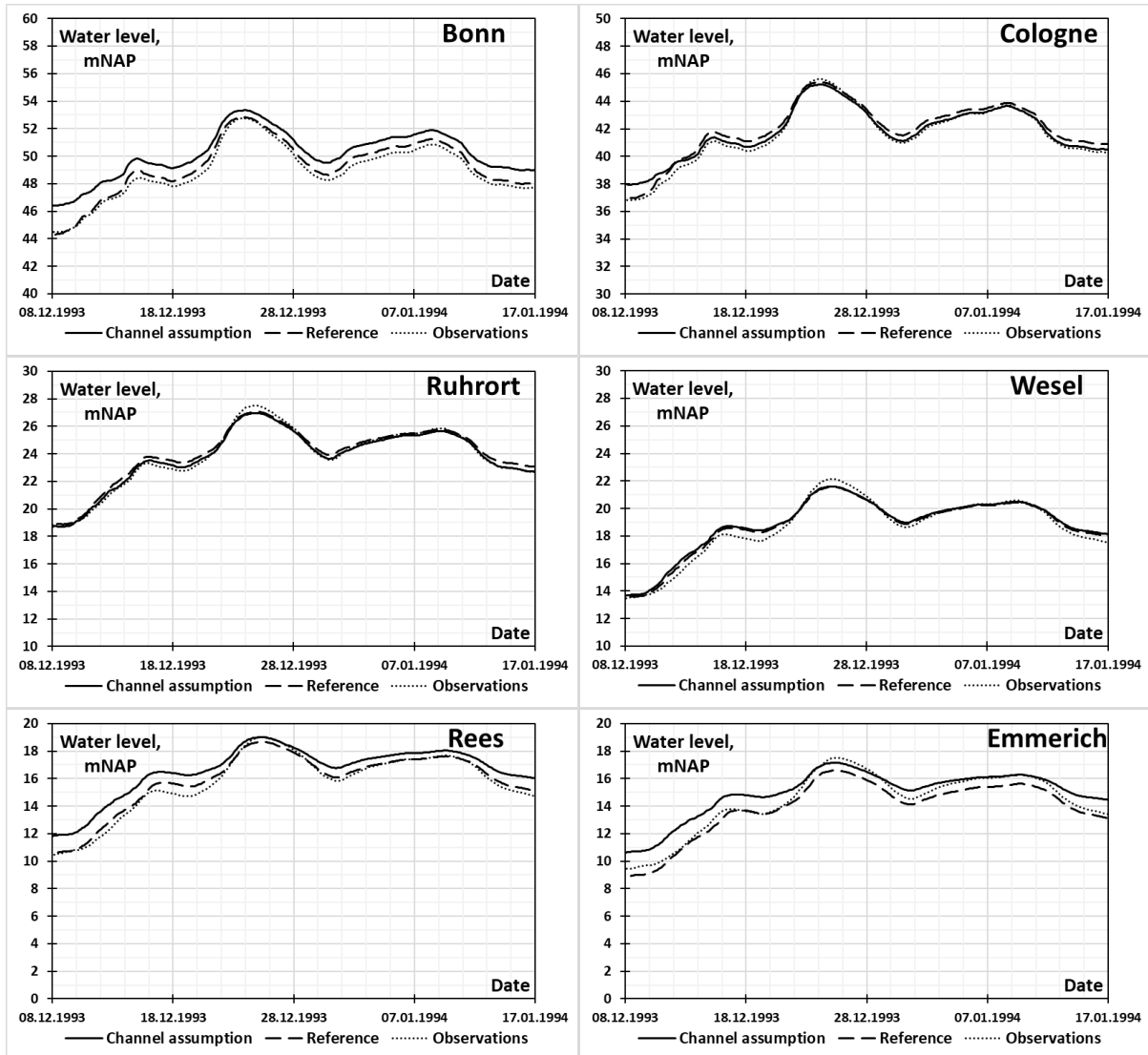


FIGURE 35 – COMPARISON BETWEEN MEASUREMENT DATA, REFERENCE SCENARIO AND PREDICTION FOR WATER LEVEL IN LOWER RHINE USING ANNUAL MEAN DISCHARGE WITH 10 YEARS RETURN PERIOD AS BANKFULL FLOW APPROXIMATION

The spatial pattern of alignment between modelled water levels and measurement datasets in case of $Q_{bf} = Q_{50,mean}$ is the opposite of the previous conditions (Figure 35). The most accurate estimation of the water level at gauge location happens in Bonn, Rees and Emmerich (Figure 36). Meanwhile, the simulated values tend to underestimate the real situation in the Cologne – Ruhrort – Wesel section.

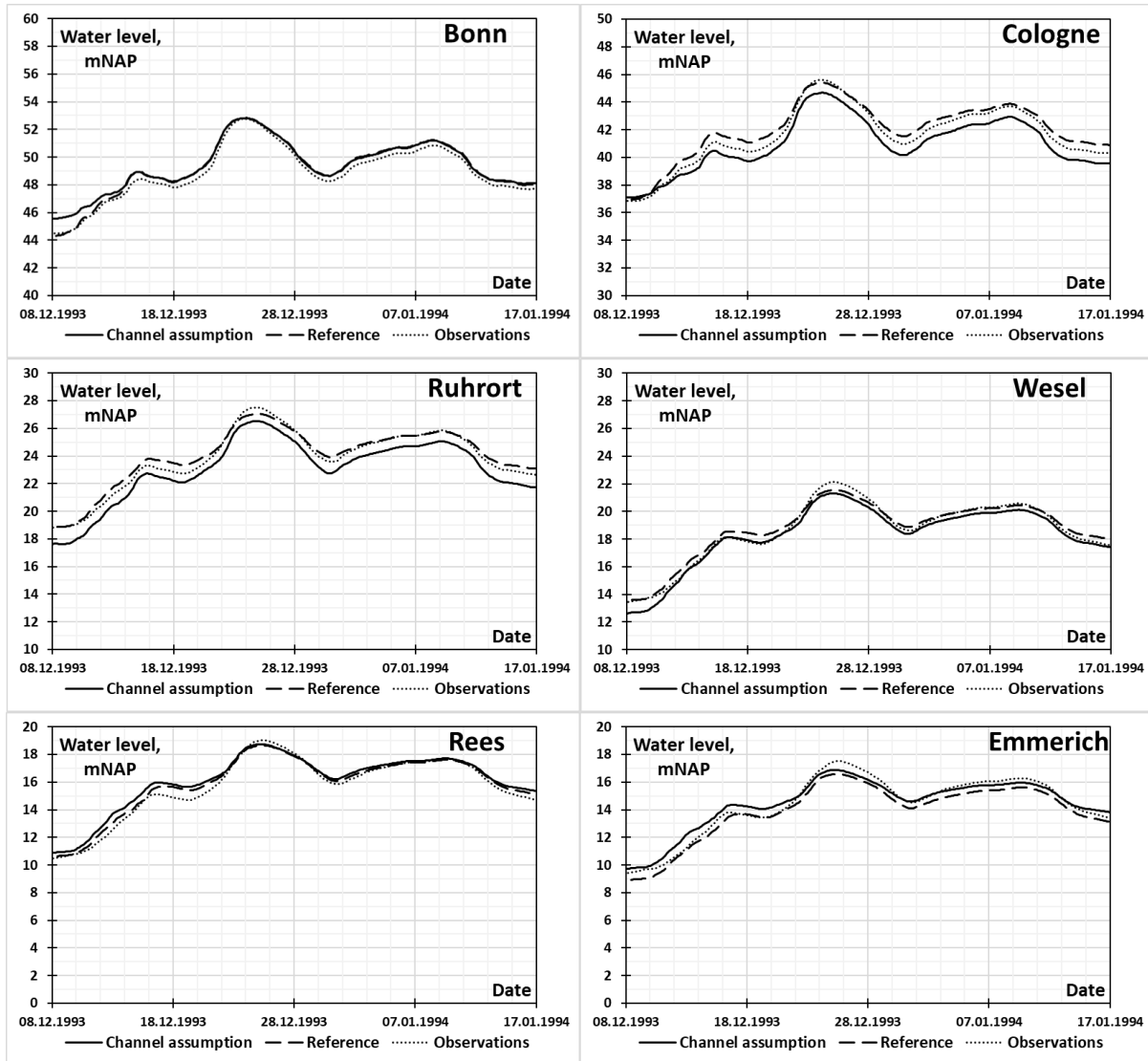


FIGURE 36 – COMPARISON BETWEEN MEASUREMENT DATA, REFERENCE SCENARIO AND PREDICTION FOR WATER LEVEL IN LOWER RHINE USING ANNUAL MEAN DISCHARGE WITH 50 YEARS RETURN PERIOD AS BANKFULL FLOW APPROXIMATION

From the analysis of the annual mean discharge approximation for channel size, it seems that the assumption of uniform bankfull discharge along the studied reach of the Rhine river does not hold. The main source of such controversy is the assumption of cross-sectional area uniformity all along the domain. From the formulation of H_{bf} for this problem, it seems that the overall significance of the channel width grows compared to the annual maximum assumption.

$$\text{Annual mean discharge: } H \sim B^{-1.0}$$

$$\text{Annual maximum discharge: } H \sim B^{-0.6}$$

Therefore, it is extremely important to account for the differences in channel width even within single river reach while using 1-in-k years annual mean discharge approximation method for channel size estimation. All of the sections that were distinguished as a results of annual mean bankfull discharge simulations correspond to specific sections with different average channel width (Figure 11). According to the spatial channel width distribution, the areas with wider stream tend to better align with higher bankfull discharge estimations.

Apparently, it is not the immediate channel width which implies the larger influence on the modelling outcome but it is a slightly downstream section of the river. This could be seen from the example of Cologne and Emmerich simulated water series. Both of the mentioned stations are located near the pronounced spike in channel width. Furthermore, those spikes represent different nature of their origin: while the sudden decrease in width of the channel downstream of Cologne is caused by the

artificial structure interference (the narrowing under the bridge), the widening downstream of Emmerich station is stable over some distance and is related to the widening of the floodplain there.

Considering all of the methods described so far (which could be generalised as methods based on hydrologic metrics frequency analysis) the maximum match of flood extent to the reference situation was observed during $Q_{bf} = Q_{10,mean}$ simulation (Figure 37). According to the visual comparison, the best representation of flood inundation area is achieved while using 1-in-1.5 years annual maximum discharge as predictor of river conveyance or with 1-in-10 years annual mean discharge as an estimation of bankfull cross-section.

However, bearing in mind the fact that the flood extent obtained from the reference scenario has been found overestimated during high water periods (Sections 5.1.1 and 5.2.2), it becomes hard to draw any definite judgement on the goodness of the simulated inundation area values. Thus, the overall area of inundation caused by the dike overflow due to the inaccuracy of the DEM has reduced for the $Q_{2.0,max}$ predictor from referential value of 39 km² to 25 km² at the peak point of the flood. Therefore, the difference in flood inundation in case of 1-in-2 years annual maximum flow estimate compared to the Verification run was also partially reduced by almost 15 km² at expense of inaccurately simulated areas in Reference scenario.

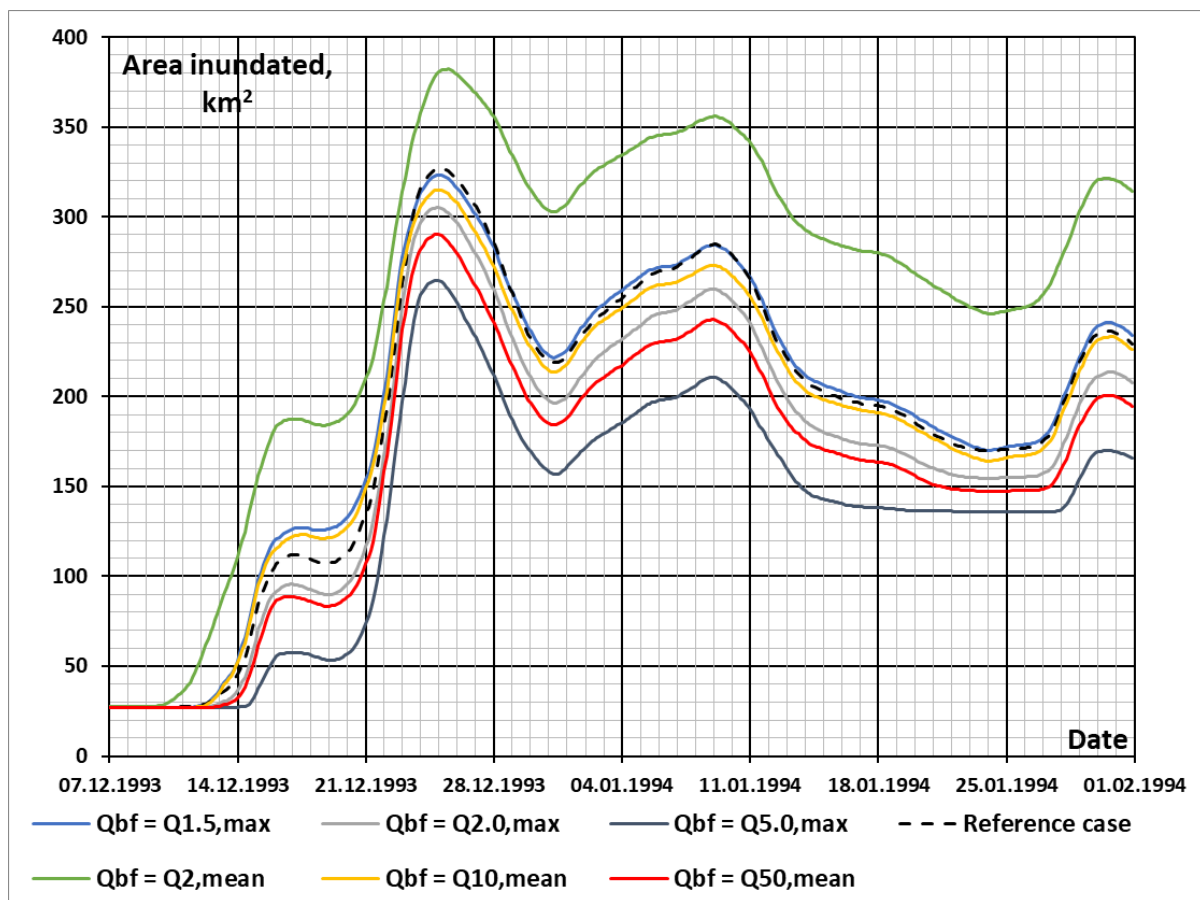


FIGURE 37 – COMPARISON BETWEEN MEASURED AND PREDICTED INUNDATED AREA IN LOWER RHINE USING ANNUAL MEAN AND MAXIMUM DISCHARGES APPROXIMATION

The same applies for all scenarios which give lower water level values at specific locations of the domain. The differences in flood extent could be seen on Figure 38 and Figure 39. All of the major overflows, which were distinguished previously (Sections 5.1.1 and 5.2.2), have been reduced in their maximum sizes over the middle and upper part of the studied basin considering $Q_{bf} = Q_{2.0,max}$ assumption. Additionally, as the water from the overflows was reintroduced to the area within the embankments, the maximum water depth have risen slightly compared to the Reference solution.

Except for the abovementioned deviations from the initial flood inundation pattern, the general flooded area has remained. The Rhine is still predicted to hold its waters within the first line of embankments, without major overflows except for the ones related to imperfection of the model.

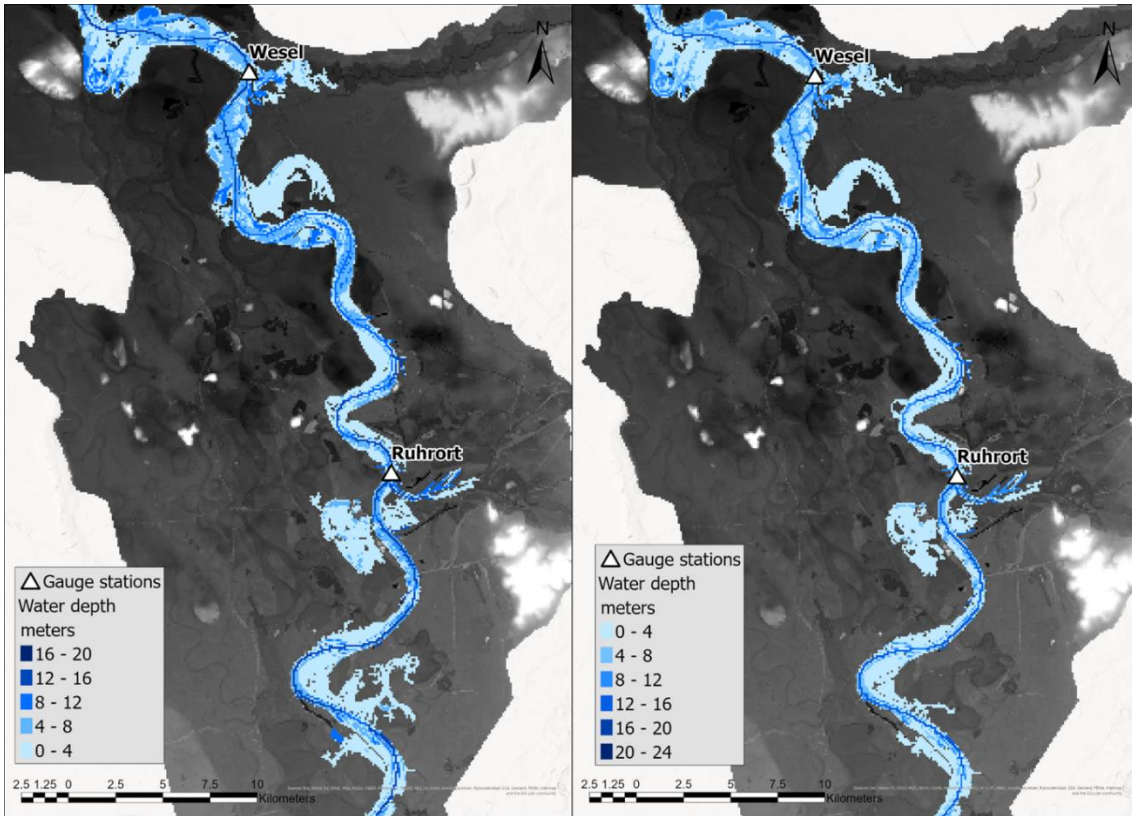


FIGURE 38 – COMPARISON BETWEEN MODELLED FLOOD EXTENTS IN MIDDLE PART OF THE LOWER RHINE FOR REFERENCE SCENARIO (LEFT) AND 1-IN-2 YEARS ANNUAL MAXIMUM DISCHARGE ASSUMPTION

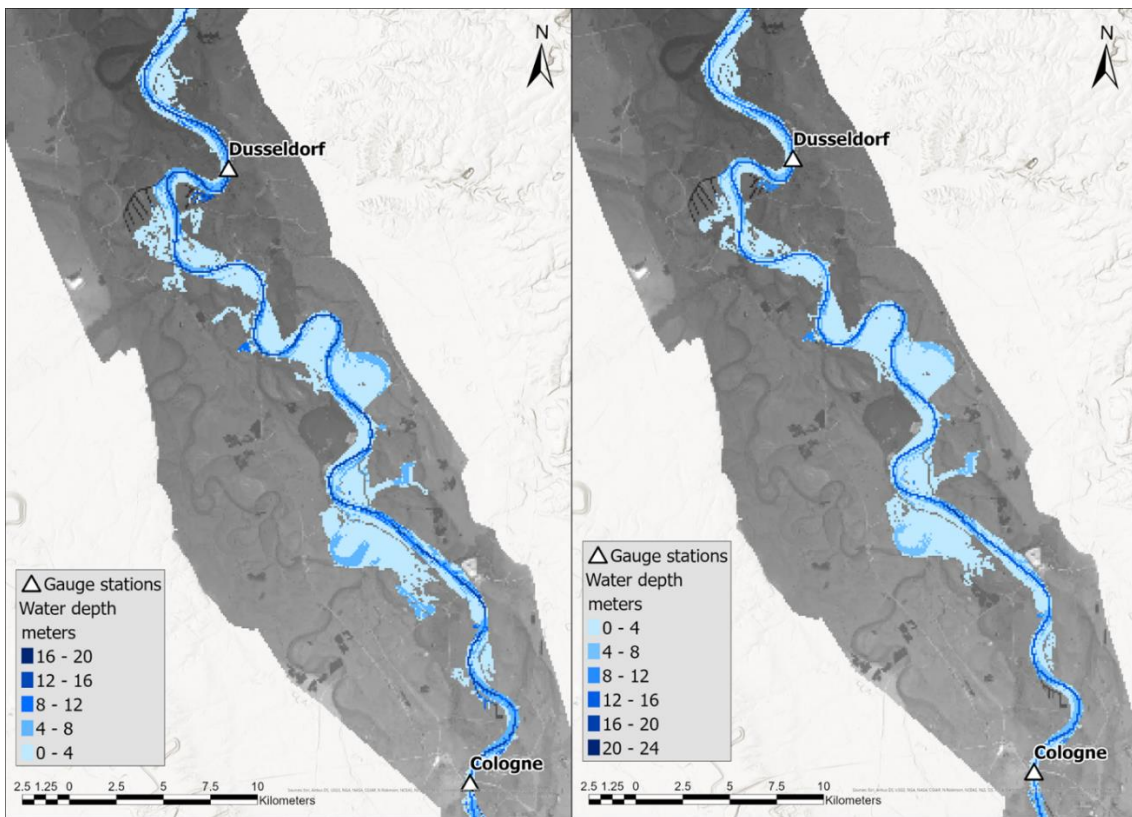


FIGURE 39 – COMPARISON BETWEEN MODELLED FLOOD EXTENTS IN UPPER PART OF THE LOWER RHINE FOR REFERENCE SCENARIO (LEFT) AND 1-IN-2 YEARS ANNUAL MAXIMUM DISCHARGE ASSUMPTION

6.3. Hydraulic geometry

Due to the similarity of the bankfull discharge estimations with the 1-in-2 years annual maximum flow predictor, the outcoming water level series over the domain also share the same properties in both cases (Figure 30; Figure 40). Therefore, in order to read more thorough description of the model output for this case you could look at Section 6.1.

For $Q_{bf} = Q_{hg}$, the flow is most accurately simulated in the middle and upstream part of the studied reach (Bonn – Cologne – Ruhrort – Wesel). Though the flood peaks there are slightly underestimated at Ruhrort and Wesel stations, the overall alignment of this simulation water level series with the outcome of the Reference scenario is sufficiently good.

The downstream part of the studied reach, on the other hand, is characterised by some substantial discrepancies during flood wave rise and recession. While this is the problem to bear in mind while making the decisions based on the model output, the model still shows sufficiently good results considering peak and inundation extent prediction. So, the fit, F , between hydraulic geometry assumption and Reference case inundation has reached over 93%. The F metrics shows the rate of inundated cells correctly predicted by the target model run to the total amount of cells being inundated by both datasets at specified point in time.

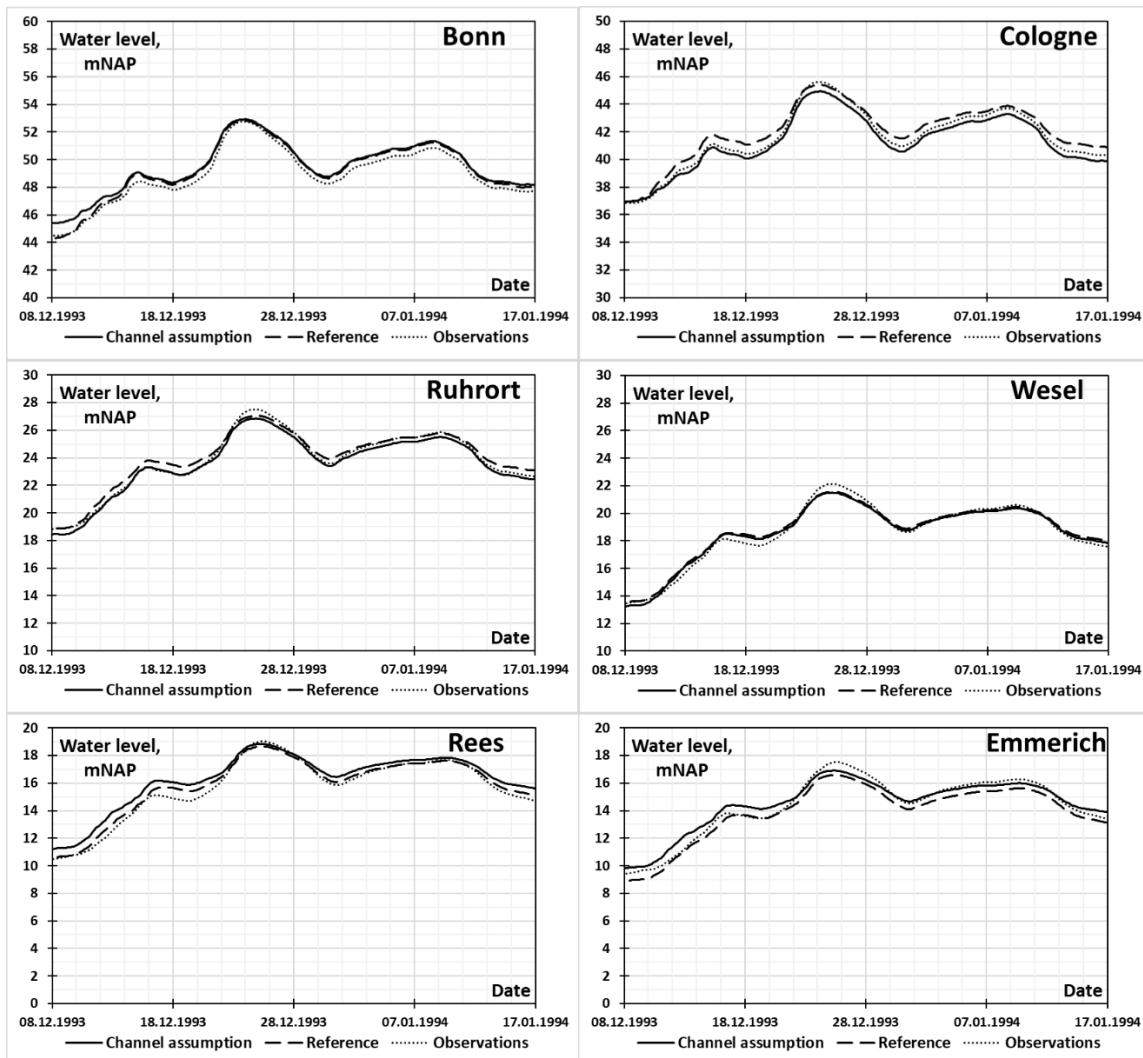


FIGURE 40 – COMPARISON BETWEEN MEASUREMENT DATA, REFERENCE SCENARIO AND PREDICTION FOR WATER LEVEL IN LOWER RHINE USING HYDRAULIC GEOMETRY RELATIONSHIPS TO DETERMINE BANKFULL FLOW APPROXIMATION

The obtained results show that derivation of bankfull channel characteristics from hydraulic geometry relations could serve as a useful tool in case of absence of elaborate bathymetry data. However, from the conducted analysis it should not be concluded that the given method applies for all possible river reaches, and thus, it should be used with caution and preferably in association of other approaches and calibration procedure.

It is also worth noticing that the studied reach of the Rhine river is the subject to huge anthropogenic load. Thus, an important conclusion could be drawn from the fact that the hydraulic geometry assumption has shown a sufficiently good simulation results even under such circumstances. This means that regionalised dependencies such as QH-curve used in this work could still be used to study hydrological situation of largely urbanised river basins given that those dependencies account for such forcing.

6.4. Dominant discharge

The outcome of the simulation based on the $Q_{bf} = Q_{eff}$ assumption have shown drastic overestimation of the water level along the studied reach (Figure 41). The largest discrepancies could be observed in the upstream part of the basin at Bonn and Cologne stations, where the decrease in the depth of the channel (Figure 11) probably leads to creation of the backwater curve.

Downstream of this section the overestimation still occurs but to a lesser extent and is mostly limited to the periods of flood wave rise and recession. Moreover, the simulated water level series for Q_{eff} assumption manages to capture the peak levels with an accuracy comparable to the Reference scenario at all gauges downstream of Cologne.

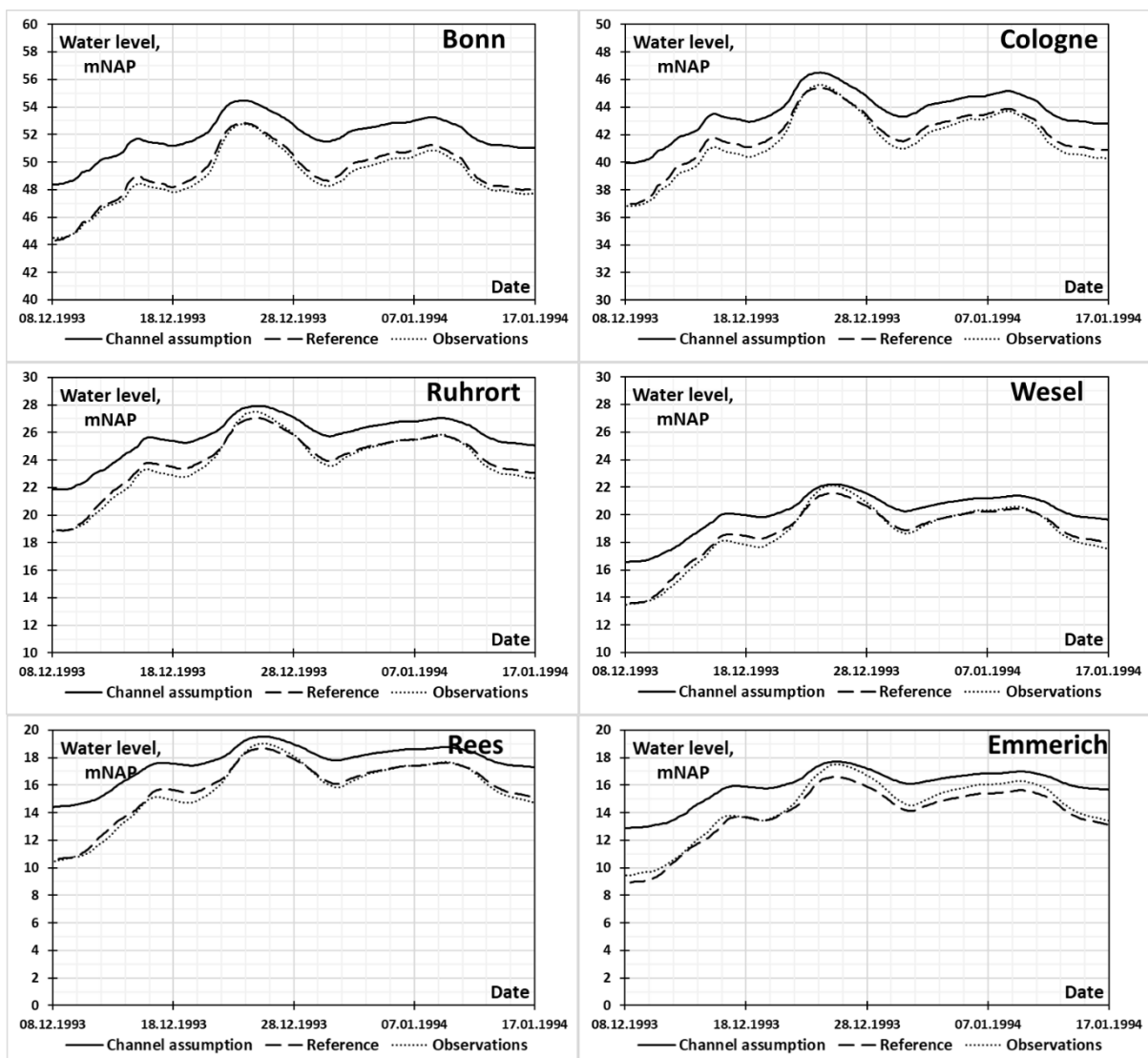


FIGURE 41 – COMPARISON BETWEEN MEASUREMENT DATA, REFERENCE SCENARIO AND PREDICTION FOR WATER LEVEL IN LOWER RHINE USING EFFECTIVE DISCHARGE AS BANKFULL FLOW APPROXIMATION

It is worth noticing that the increased water levels lead to more overflows happening over the domain. However, all of the overflows occur in the middle and upper part of the studied Rhine reach (**Error! Reference source not found.**). The overall area of inundated territory reaches almost 450 km² at its maximum, which is about 1.5 times higher than in Reference case. And while this could explain

the reduced overestimation of the simulated water levels downstream, it will be shown further that the overflow could not be responsible for such change in accuracy of the peak prediction (Chapter 7).

Such huge overestimation of the water level value was caused by extremely low value of Q_{eff} , thus allowing to draw a conclusion about the fit of this bankfull discharge estimation. Considering the obtained effective discharge value, it could in no way be used as a predictor for the value conveyance at the studied reach of the Rhine river.

However, other studies show that many river channels all over the world could be and are being sufficiently good represented by $Q_{bf} = Q_{eff}$ assumption. This does not happen for the domain in question and there are few possible explanations for that. Firstly, the Rhine basin is highly urbanised and many anthropogenic activities happen in the Rhine channel itself which could include also manipulations with the bed and its material. The possible river bed strengthening or sand dredging or damping could heavily influence the effect of proposed discharge-sediment relationships. Secondly, the quality and applicability of the sediment rating curve used during calculation of the effective discharge is a subject to discussion. There is no clear picture for the dataset it was built on as well as quite low value of $R^2 = 0.44$ hints at some troubles with using it for further research. Finally, it has been found that the climate change affects the sediment transport dependencies in the Rhine basin to some extent (Asselman, 1995), which could also reduce the accuracy of such analysis to some extent.

Additionally, although the value of Q_{hy} does not come far from the effective discharge value, a separate simulation had been run for the assumption of $Q_{bf} = Q_{hy}$ (Figure 42).

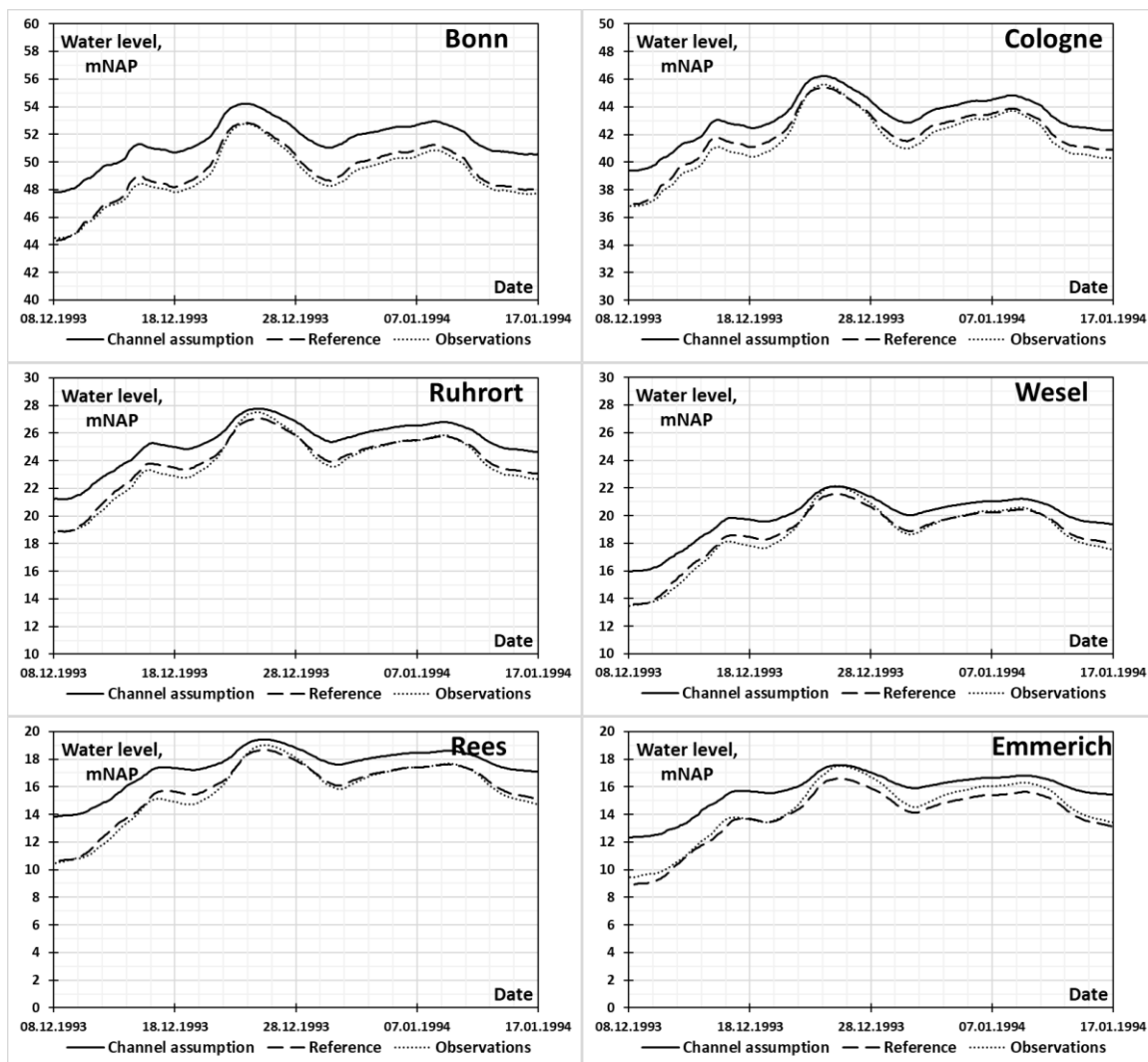


FIGURE 42 – COMPARISON BETWEEN MEASUREMENT DATA, REFERENCE SCENARIO AND PREDICTION FOR WATER LEVEL IN LOWER RHINE USING HALF-YIELD DISCHARGE AS BANKFULL FLOW APPROXIMATION

All the same characteristics observed for $Q_{bf} = Q_{eff}$ assumption's water level series are also inherent to the half-yield scenario however with slightly less difference compared to the referential case.

Therefore, $Q_{bf} = Q_{hy}$ assumption as well as an estimate of $Q_{bf} = Q_{eff}$ should not be applied for the heavily urbanised areas based on the results of this analysis.

6.5. Goodness-of-fit analysis

This study contains the analysis of application of 4 methods for estimating the value of bankfull discharge for the section of Rhine river between Bonn and Lobith. All of the featured methods are indirect and use a single discharge value predictor to assess Q_{bf} . These are the named predictors which could be used to estimate channel size through the bankfull discharge value:

1. Annual maximum discharge with various return periods (1.5, 2.0 and 5.0 years);
2. Annual mean discharge with various return periods (2, 10 and 50 years);
3. Discharge of the break in slope on QH rating curve;
4. Channel forming discharge based on various sediment metrics ($Q_{effective}$, $Q_{half-yield}$).

To quantitatively assess the alignment of the simulated parameters a goodness-of-fit (GOF) analysis was conducted. The GOF of the Q_{bf} predictors has been measured using several accuracy metrics describing relative error between reference and predicted values of water level.

The GOF analysis in this research have been consisted of 3 main statistical metrics. The first is the Theil (1958) measure of association, U. It estimates the relative error with respect to perfect match 1:1 line. This metric examines a normalized distance between observed and simulated values, and unlike correlation coefficient, learns the proximity of the data pair to the 1:1 line. Additionally, the Root Mean Square Error (RMSE) between measurement data and model will be used as recommended by Pineiro et al. (2008). It has the same units as the variables, and so it will allow to account for large differences between larger observations. And the final metric used to account for accuracy of the model prediction will be Nash-Sutcliffe model efficiency coefficient (NSE). It was specially produced to assess the predictive skill of the hydrological model and is commonly used around the world. Although, NSE has been criticised recently for masking important model behaviours (Gupta and Kling, 2011), it will suffice for this model purposes.

TABLE 15. INTEGRATED GOODNESS-OF-FIT METRICS (PART 1)

Bonn	$Q_{1.5,max}$	$Q_{2.0,max}$	$Q_{5.0,max}$	$Q_{2,mean}$	$Q_{10,mean}$	$Q_{50,mean}$	Q_{hg}	Q_{eff}	Q_{hy}
RMSE [m]	1.30	0.31	0.71	7.55	1.88	0.34	0.36	10.21	7.56
NSE	0.72	0.93	0.85	-0.61	0.60	0.93	0.92	-1.17	-0.61
U	0.023	0.006	0.017	0.028	0.014	0.006	0.006	0.032	0.028
Cologne	$Q_{1.5,max}$	$Q_{2.0,max}$	$Q_{5.0,max}$	$Q_{2,mean}$	$Q_{10,mean}$	$Q_{50,mean}$	Q_{hg}	Q_{eff}	Q_{hy}
RMSE	0.13	0.17	2.99	3.36	0.26	0.44	0.14	5.57	3.65
NSE	0.98	0.97	0.46	0.39	0.95	0.92	0.97	-0.02	0.33
U	0.009	0.005	0.042	0.022	0.006	0.008	0.005	0.028	0.023
Ruhrort	$Q_{1.5,max}$	$Q_{2.0,max}$	$Q_{5.0,max}$	$Q_{2,mean}$	$Q_{10,mean}$	$Q_{50,mean}$	Q_{hg}	Q_{eff}	Q_{hy}
RMSE	0.10	0.15	2.80	2.02	0.05	0.90	0.12	4.92	3.23
NSE	0.98	0.97	0.52	0.66	0.99	0.85	0.98	0.16	0.45
U	0.014	0.009	0.071	0.030	0.005	0.021	0.008	0.046	0.038
Wesel	$Q_{1.5,max}$	$Q_{2.0,max}$	$Q_{5.0,max}$	$Q_{2,mean}$	$Q_{10,mean}$	$Q_{50,mean}$	Q_{hg}	Q_{eff}	Q_{hy}
RMSE	0.29	0.10	1.54	2.06	0.19	0.30	0.10	3.96	2.80
NSE	0.95	0.98	0.75	0.66	0.97	0.95	0.98	0.35	0.54
U	0.029	0.009	0.067	0.039	0.012	0.015	0.009	0.053	0.045

TABLE 16. INTEGRATED GOODNESS-OF-FIT METRICS (PART 2)

Rees	$Q_{1.5,max}$	$Q_{2.0,max}$	$Q_{5.0,max}$	$Q_{2,mean}$	$Q_{10,mean}$	$Q_{50,mean}$	Q_{hg}	Q_{eff}	Q_{hy}
RMSE	1.22	0.32	0.38	4.32	1.22	0.27	0.50	6.32	4.95
NSE	0.80	0.95	0.94	0.30	0.80	0.96	0.92	-0.03	0.19
U	0.071	0.019	0.040	0.065	0.036	0.017	0.023	0.078	0.070
Emmerich	$Q_{1.5,max}$	$Q_{2.0,max}$	$Q_{5.0,max}$	$Q_{2,mean}$	$Q_{10,mean}$	$Q_{50,mean}$	Q_{hg}	Q_{eff}	Q_{hy}
RMSE	0.55	0.09	0.93	3.19	0.79	0.16	0.17	4.62	3.44
NSE	0.90	0.98	0.83	0.43	0.86	0.97	0.97	0.17	0.38
U	0.052	0.011	0.068	0.062	0.032	0.014	0.015	0.073	0.064

* values indicating good match between measurements and the model are in bold

From the accuracy metrics values presented in Table 15 some new insights could be pointed out. First of all, it becomes evident that the best accuracy in prediction of the observed flood was achieved while implementing the assumption of Q_{bf} equal to 1-in-2 years annual maximum flow, $Q_{2.0,max}$. Such conclusion could be drawn based on the since it has reach the most number of the best-fitted metrics values (lowest RMSE; highest NSE; lowest U) among all the gauge stations. There are only two occasion where $Q_{2.0,max}$ was not considered the best matched parameter: both are RMSE values at Ruhrort and Rees, respectively. Those values, though still are close to become the best fitted. While using this method to account for channel size of the river, average deviation of the predicted water level values does not exceed 20 cm which is quite reasonable margin of error for a hydrodynamic model built without explicit knowledge on channel bathymetry.

Additionally, another approach shows good prospects. It is the assumption of $Q_{bf} = Q_{hg}$, where Q_{hg} was found from the QH rating curve of one of the stations in the basin. The main advantage of this method before any assumption based on flood frequency analysis is its regional applicability. Since the rating curves tend to comply with ruling regional dependencies, findings made on gauged location could be transited to those without available measurements.

Finally, another possible solution comes to mind while looking at the GOF metrics table. From the values of accuracy criteria for assumptions $Q_{bf} = Q_{10,mean}$ and $Q_{bf} = Q_{50,mean}$ it becomes clear that both of them give accurate predictions of the water level but only at selected location along the studied reach. However, what makes it more interesting is that the sections of good accuracy metrics alternate for the two approaches. For instance, $Q_{50,mean}$ assumption gives quite good water level predictions at Bonn, (Wesel), Rees and Emmerich, while $Q_{bf} = Q_{10,mean}$ approach gives better results for Cologne, Ruhrort and Wesel. Furthermore, one could add to that knowledge the fact that those alternating sections coincide with the areas of larger (Bonn, Cologne, Rees, Emmerich) and smaller (Dusseldorf, Ruhrort, Wesel) river channel width (Figure 11). Taking into account that knowledge, the possible explanation comes to mind that the changes of the river conveyance caused by the topographical features of different segments of the Lower Rhine (through changing channel width) could lead to variability in the accuracy of the channel size estimates even on such scale.

Such distinction justifies the scenario in which the studied part of the Rhine basin could be divided into 2 sections corresponding to various channel width condition. Then those sections could inherit most appropriate channel size assumption to enhance the modelling outcome as they would be viewed as different regions with their own morphological dependencies. However, it will require the additional research to understand how exactly different annual mean discharge assumptions are behaving on more study cases, as it has not been in the focus of the broad study recently.

7. Discussion

Before going into drawing the conclusions to the conducted research, it is important to discuss controversial aspects of it and determine the uncertainty sources which could affect the outcome of some analyses or even whole research questions.

The first point for discussion comes from the usage of 2015 Digital elevation model to account for 1993 – 1995 situation when the studied flood events have occurred. Over the period of 20 years passed from the latest flood, both channel and floodplains surface elevation values could have changed at significant extent over the modelling domain. However, while some local changes may have been occurred in floodplains (like the embankment restoration in Cologne old city after 1995 flooding event), the vast regional alterations are highly unlikely to happen since almost the entire Lower Rhine basin represents well-established urban areas with little space to organise new land use. Additionally, no major differences in channel bed are awaited since the Lower Rhine channel is artificially stabilised for navigational purposes as it is an important navigation route for trades and other vehicles. However, the simulation results are proved to sufficiently well predict the water level using 2015 DEM with channel bed surface elevation values. Thus, the effect of possible changes in the bathymetry of the channel could be considered negligible and not important to the outcome of the model runs.

Another major topic for discussion concerns the applicability of the results obtained throughout the whole research, as single case study is used to answer the risen research question. Indeed, by the means of this thesis research no global conclusions could be made, however the obtained results will show typical picture for most of the Western and Central European large river at some extent. This is due to the fact that the dependencies which determine the applicability of one or another channel size assumption have tendency to work regionally based on the meteorological and hydrological conditions which are more or less the same for the defined region. Additionally, besides hydrometeorological conditions the local characteristics of the river basin play their role. This is why the obtained results could only be transited to the relatively flat urbanised basins of large rivers in Europe. However, based on the established framework, modelling cases could be replicated further all over the world continuing to enhance the knowledge on regional features regarding channel size estimates performance even for areas with scarce data availability. In this case, though, it would be better to establish the set of regionally appropriate channel estimates based on a single or several case studies.

Among minor discussion topic there are few regarding the assumptions which were made to obtain several bankfull flow estimates. Namely, this is the adoption of sediment rating curve for Rees station (Section 4.3). Due to a low R^2 value a substantial measure of uncertainty has been introduced into the sediment yield calculation. As it is has become known after the simulation has been run, the sediment transport-based estimates do not work properly for the given scenario. There are two possible reasons on why this happened. Firstly, the Rhine basin is highly urbanised and many anthropogenic activities happen in the Rhine channel itself including those involved with the sediments or the river bed material. Therefore, the drawn regional dependencies could be interfered by the discrepancies coming from this source. Additionally, sediment transport was found to be affected significantly by the ongoing climate change which could also affect the applicability of the used sediment rating curves. Secondly, the quality and applicability of the sediment rating curve used during calculation of the effective discharge is a subject to discussion. There is no clear picture for the dataset it was built on as well as quite low value of $R^2 = 0.44$ hints at some troubles with using it for further research. Most probably the both factors have influenced to some extent, and so the sediment transport-based assumption for bankfull flow estimate did not work for this specific scenario.

Finally, the transition of the Digital Elevation Model from 10x10 m resolution to the 100x100 m grid has caused few uncertainty sources, such as overflow through the first embankment line in specific locations over the Middle and upper part of the studied domain. This became a reason of substantial volume of water flown away from the active part of the river valley, thus decreasing the water level predicted by all the simulation runs conducted during the research. This probably was the main reason why many of the simulations ended up in underestimating the peak water level values. The calculation has shown that it has decreased the water level in the area enclosed by the first embankment line of the river valley by up to 20 – 30 cm in the downstream part of the domain.

Moreover, to study the effect of the incorrectly predicted overflow on the model outcome, additional simulation has been done for the situation of infinitely high dikes. Such scenario represents a situation where no overflow is possible throughout the whole modelling domain. According to that simulation, the effect of dike overflow due imperfectly described embankments height is limited by 30

cm at its maximum (Figure 43; Table 17), as was proposed by the calculations in Sections 5.1.1 and 5.2.2.

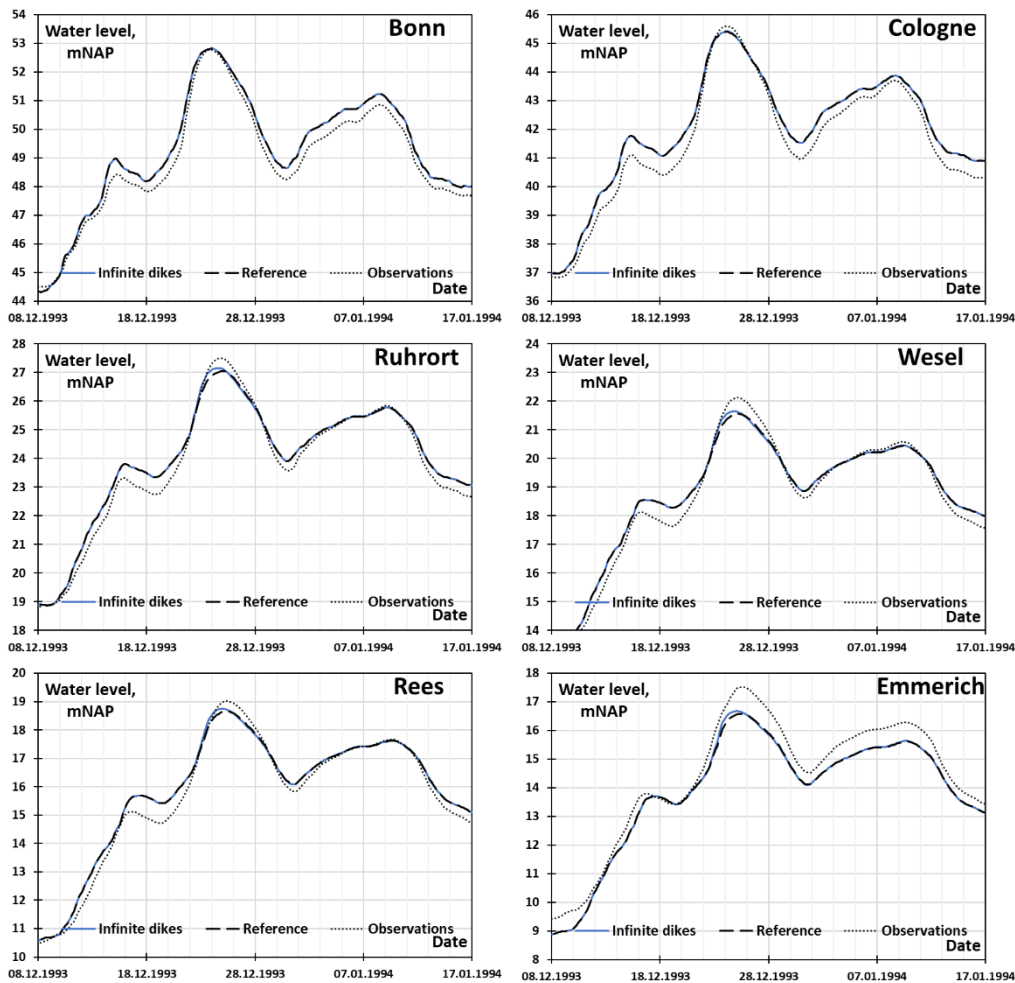


FIGURE 43 – COMPARISON BETWEEN MEASUREMENT DATA, REFERENCE SCENARIO AND PREDICTION FOR WATER LEVEL IN LOWER RHINE USING INFINITE DIKES ASSUMPTION

The largest deviation from the reference case is observed, unexpectedly, at Ruhrort station decreasing further downstream and upstream from 30 cm to 10cm at Lobith and 20 cm at Dusseldorf stations (Table 17). Such situation was probably caused by the tributaries influence on the downstream part of the basin where they could alleviate some of the excessive overflow negative effects on the water level simulation accuracy.

TABLE 17. MAXIMUM OBSERVED DEVIATION OF THE WATER LEVEL PREDICTION FROM THE REFERENCE CASE SCENARIO FOR INFINITE DIKE ASSUMPTION

	Bonn	Cologne	Dusseldorf	Ruhrort	Wesel	Rees	Emmerich	Lobith
Maximum deviation, m	0.0	0.0	0.2	0.3	0.2	0.2	0.2	0.1

Nevertheless, looking at the outcome of the infinite dike scenario simulation, it could be concluded that no major impact on the accuracy of the modelling in this research has been implied by the imperfect dike representation.

8. Conclusions & Recommendations

8.1. Conclusions

The objective of this master thesis study was to obtain better understanding of different channel size estimated influence on the performance of the flood inundation model in conditions of absence of elaborate bathymetry data and overall data scarcity. It was important to answer the research questions which were determined in Section 1.2, to reach this objective.

Research question 1:

How does 1-in-2 years bankfull discharge assumption influence the outcome of flood inundation modelling?

It was found, from the simulation run with 1-in-2 years annual maximum flow assumption for bankfull discharge, that the performance of the model built for the Lower Rhine basin does not differ significantly from the lack of elaborate channel bed elevation data based on the calculated statistical metrics. It was determined that only at 2 stations along the modelling domain the water level series related to assumption of bankfull discharge equal to maximum flow with 2 years return period do not comply with the series of reference case scenario (with measured bathymetry data included). These were Cologne and Ruhrort, however the average deviation of the water level there was limited by approximately 5% and 4% of maximum observed water depth on average, respectively. The established standard of the water level simulation is 10% of the measured water depth (Williams and Esteves, 2017), therefore this could be viewed as appropriate deviation given the fact of good fit at other station.

The two prediction datasets were even found to share its properties regarding the comparison to the measured water level (underestimation of peaks, overestimation in lower water periods). Although, the 1-in-2 years annual maximum flow assumption was found to underestimate the inundated area value by relatively sufficient amount ($\approx 20 \text{ km}^2$), this value proved to be compensated by lower amount of water that have overflowed the first embankment line in several locations due to DEM inaccuracy. The flood extent predicted by both reference model and model of 1-in-2 years annual maximum flow assumption has remained the same considering that the wrongly predicted overflows would be excluded. Therefore, 1-in-2 years bankfull discharge assumption could be used for hydrodynamic modelling in locations with conditions similar to the Lower Rhine basin situation.

Research question 2:

How do flood inundation models perform considering other methods to estimate the river channel size are applied compared to 1-in-2 years bankfull discharge assumption?

In order to answer the second research question, the goodness-of-fit analysis was conducted as well as a set of visual conclusion were made from the comparison plots. The bankfull flow assumptions apart from 1-in-2 years annual maximum flow assumption were concerning different flood frequency characteristics, regional hydraulic geometry relationships and sediment transport-based approach.

Firstly, annual maximum discharges of other frequency of occurrence were assessed. Based on the correlation plots. it was found that 1-in-1.5 years annual maximum flow assumption gives significantly better peak water level predictions compared to any other method used in this thesis research. However, the level of low flow over estimation was considered too high for the flood inundation modelling. 1-in-5 years annual maximum flow assumption was considered as ill-fitting as it gave constant underestimation of water level values by 0.5 – 1.7 m over the study area.

Then there were annual mean discharge values assumptions for different recurrence periods. Those assumptions have been found much more dependent on the width value of the river channel for non-uniform bankfull depth estimation (dependency by power -1, compared to the power -0.6 for annual maximum discharges). Therefore, the domain was divided into 2 section where the specific value for frequency of annual mean flow was producing the best fit for the model run. The distinguished regions involved the section of the river between Cologne – Dusseldorf – Ruhrort with the best fit given by $Q_{10, \text{mean}}$ assumption, and two other sections upstream from Cologne and downstream from Wesel with better representation by $Q_{50, \text{mean}}$ assumption.

The hydraulic geometry assumption has shown an estimate for bankfull discharge extremely close to 1-in-2 years annual maximum flow assumption, therefore the results obtained for this scenario are almost fully identical to the previous case. The difference is that this method could be used in case if no discharge data is available for the studied basin, as the regional QH rating curve will allow to estimate it based only on water level data. For hydraulic geometry assumption, the flow is most accurately simulated in the middle and upstream part of the studied reach (Bonn – Cologne – Ruhrort – Wesel). Though the flood peaks there are slightly underestimated at Ruhrort and Wesel stations, the overall alignment of this simulation water level series with the outcome of the Reference scenario is sufficiently good. The downstream part of the studied reach, on the other hand, is characterised by some substantial discrepancies during flood wave rise and recession. While this is the problem to bear in mind while making the decisions based on the model output, the model still shows sufficiently good results considering peak and inundation extent prediction. It is also worth noticing that the studied reach of the Rhine river is the subject to huge anthropogenic load. Thus, an important conclusion could be drawn from the fact that the hydraulic geometry assumption has shown a sufficiently good simulation results even under such circumstances. This means that regionalised dependencies such as QH-curve used in this work could still be used to study hydrological situation of largely urbanised river basins given that those dependencies account for such forcing.

The outcome of the simulation based on both sediment transport based estimates (effective and half-yield discharge assumptions) have shown drastic overestimation of the water level along the studied reach. Such huge overestimation of the water level value was caused by extremely low value of effective and half-yield discharge. Under the given circumstances these parameters could in no way be used as a channel size estimates for the Lower Rhine basin. However, other studies show that many river channels all over the world could be and are being sufficiently good represented by effective discharge assumption. This does not happen for the domain in question and there are few possible explanations for that which are presented in Discussion section.

8.2. Recommendations

As a result of this master thesis project several recommendations regarding the topic of this research could be done.

Firstly, it could be suggested that the methods to account for the channel size in rivers without elaborate bathymetry that have shown good results in this research, namely 1-in-2 years annual maximum flow assumption and hydraulic geometry method, could be used for the modelling purposes in rivers with conditions similar to the Lower Rhine. The set of river basin conditions for which those estimates were tested to work finely: the large watershed area, relatively flat and densely populated; the hydrometeorological conditions similar to the Western and Central European with single not too well pronounced (thus prolonged) high water period preferably during the winter month.

Moreover, the values of effective and half-yield discharge – show really poor performance values for the studied reach of the Rhine river. However, after some consideration, it is easy to guess the reason which have implied such situation. As one of the main navigation arteries of Western and Central Europe, Rhine river basin is characterised by the large amount of various activities including sediments ditching, damping, strengthening of the river banks and channel bed, etc. All those activities aided by the climate change impact could cause the sediment-related regional dependencies to change over time rapidly. This implies caution while using such type of channel size estimations in hydrodynamic modelling.

It was also found that the annual mean discharge assumption performance is highly dependent on the average channel width and its variability along the specified river reach. Therefore, highly urbanised areas could pose great difficulties on the flood inundation modelling in case of sudden width changes which happens a lot within the populated areas where there are many possible structures that could impose narrowing effect on the river channel. Thus, it could be concluded that $Q_{k,mean}$ assumptions are too unstable to be used on large urbanised areas without any supporting parameters. The solution would be representing the large basin as a set of the smaller catchments with distinctive channel approximation techniques.

Furthermore, it will require the additional research to understand how exactly different annual mean discharge assumptions are behaving with other study cases, as it has not been in the focus of the broad study recently.

The other regions of the world could also be studied using the framework established in this research. Modelling cases could be replicated further all over the world continuing to enhance the knowledge on regional features regarding channel size estimates performance.

References

1. Abebe, Yared & Seyoum, Solomon & Vojinovic, Zoran & Price, Roland. (2016). Effects of Reducing Convective Acceleration Terms in Modelling Supercritical and Transcritical Flow Conditions. *Water*, 8.
2. Andreadis, K. A., Schumann, G. J.-P., and Pavelsky, T. (2013), A simple global river bankfull width and depth database, *Water Resour. Res.*, 49, 7164– 7168, doi:10.1002/wrcr.20440.
3. Andrews, E. D. (1980). "Effective and bankfull discharges of streams in the Yampa River basin, Colorado and Wyoming." *J. Hydrol.*, 46(3–4), 311–330.
4. Ashkar, Fahim & Ouarda, Taha. (1998). Approximate Confidence Intervals for Quantiles of Gamma and Generalized Gamma Distributions. *Journal of Hydrologic Engineering*. 3. 43-51. 10.1061/(ASCE)1084-0699(1998)3:1(43).
5. Asselman, N.E.M. (1995). The impact of climate change on suspended sediment transport in the river Rhine, *Studies in Environmental Science*, Vol. 65, pp. 937-942
6. Asselman N.E.M. (2000) "Fitting and interpretation of sediment rating curves", *Journal of hydrology*, 234 (3-4), 228-248
7. Bates, P.D., Trigg, M., Neal, J. and A. Dabrowa (2013) LISFLOOD-FP. User manual, School of Geographical Sciences, University of Bristol, University Road, Bristol, BS8 1SS, UK.
8. Beechie, T. J., et al. (2010). "Process-based principles for restoring river ecosystems." *BioScience*, 60(3), 209–222.
9. Benkaci T. & Dechemi N. (2021). Flood Frequency Distribution (FFD 2.1), GitHub https://github.com/TBenkHyd2/Flood_Freq_Matlab. Retrieved July 22, 2021.
10. Biedenharn, David & Copeland, Ronald & Thorne, Colin & Soar, Philip & Hey, Richard. (2000). Effective Discharge Calculation: A Practical Guide. 60.
11. Bomers, A., Schielen, R.M.J. & Hulscher, S.J.M.H. Consequences of dike breaches and dike overflow in a bifurcating river system. *Nat Hazards* 97, 309–334 (2019).
12. Bjerklie D.M. (2007). Estimating the bankfull velocity and discharge for rivers using remotely sensed river morphology information, *Journal of Hydrology*, Vol. 341 (3–4), p. 144-155
13. Bradbrook, K.F., S.N. Lane, S.G. Waller and P.D. Bates (2004) Two dimensional diffusion wave modelling of flood inundation using a simplified channel representation, *Int. J. of River Basin Management*, 2:3, 211-223, doi:10.1080/15715124.2004.9635233
14. Castro, J.M. and P.L. Jackson (2001). Bankfull Discharge Recurrence Intervals and Regional Hydraulic Geometry Relationships: Patterns in the Pacific Northwest, USA. *J. of Am. Wat. Res. As.* 37. 1249-1262.
15. Chow, V. T. (1959). *Open-channel hydraulics*, McGraw-Hill, New York.
16. Copeland, R. R., Soar, P. J., and Thorne, C. R. (2005). "Channel-forming discharge and hydraulic geometry width predictors in meandering sand-bed rivers." *Impacts of Global Climate Change*, ASCE, Reston, VA, 1–12.
17. De Almeida, A.M. and P.D. Bates (2013) Applicability of the local inertial approximation of the shallow water equations to flood modelling. *Water Resources Research*, 49, 4833-4844
18. Doocy, S., Daniels, A.M., Mclvor Murrey, S. and T.D. Kirsch (2013) The Human Impact of Floods: A Historical Review of Events 1980-2009 and Systematic Literature Review, *PLoS Curr.*
19. Doyle, M. W., Shields, D., Boyd, K. F., Skidmore, P. B., and Dominick, D. (2007). "Channel-forming discharge selection in river restoration design." *J. Hydraul. Eng.*, 10.1061/(ASCE)0733-9429(2007)133:7(831), 831–837.
20. Emmett, W. W., and Wolman, M. G. (2001). "Effective discharge and gravel-bed rivers." *Earth Surf. Processes Landforms*, 26(13), 1369–1380.
21. Endreny, T.A. (2007) Estimation of channel bankfull occurrence from instantaneous discharge data, *J. Hydr. Eng.*, 12, 5, pp 524 – 531, DOI: 10.1061/(ASCE)1084-0699(2007)12:5(524)
22. Engel, H. (1993) Derzeit erkennbare Abflupentwicklungen im Rhein und seinen Nebenflüssen und Änderung des Niederschlagsverhaltens in den zugehörigen Einzugsgebieten. DVWK meeting "Der Rhein im Wandel" (Ludwigshafen)
23. Engel, H. (1997). The flood events of 1993/1994 and 1995 in the Rhine River basin. IAHS-AISH publication, 21-32.
24. Engel, H. and M. Disse (2001). Flood Events in the Rhine Basin: Genesis, Influences and Mitigation. *Natural Hazards*. 23. 271-290. 10.1023/A:1011142402374.

25. Fewtrell, T.J., Duncan, A., Sampson, C.C., Neal, J.C. and P.D. Bates (2011) Benchmarking urban flood models of varying complexity and scale using high resolution terrestrial LiDAR data. *Physics and Chemistry of the Earth*, 36, 281-291.
26. Gomez, B., Coleman, S.E., Sy, V.W.K., Peacock, D.H. and Kent, M. (2007), Channel change, bankfull and effective discharges on a vertically accreting, meandering, gravel-bed river. *Earth Surf. Process. Landforms*, 32: 770-785. <https://doi.org/10.1002/esp.1424>
27. Hey, R.D. (1997) Stable river morphology, *Applied Fluvial Geomorphology for River Engineering and Management*, pp. 223-236, John Wiley, Chichester, U.K.
28. Johnson, P.A. and Heil, T.M. (1996), UNCERTAINTY IN ESTIMATING BANKFULL CONDITIONS¹. *JAWRA Journal of the American Water Resources Association*, 32: 1283-1291. <https://doi.org/10.1111/j.1752-1688.1996.tb03497.x>
29. Harman C., M. Stewardson, R. De Rose (2008) Variability and uncertainty in reach bankfull hydraulic geometry, *J. Hydr.*, 351(1–2), 13-25, <https://doi.org/10.1016/j.jhydrol.2007.11.015>.
30. Hassan, M. A., Brayshaw, D., Alila, Y., and Andrews, E. (2014). "Effective discharge in small formerly glaciated mountain streams of British Columbia: Limitations and implications." *Water Resour. Res.*, 50(5), 4440–4458.
31. Lee, W.H., Choi, H.S. (2018). Characteristics of Bankfull Discharge and its Estimation using Hydraulic Geometry in the Han River Basin. *KSCE J Civ Eng* 22, 2290–2299
32. Leopold, L. B. 1994. *A View of the River*. Cambridge, Mass: Harvard University Press.
33. Mersel, M. K., Smith, L. C., Andreadis, K. M., and Durand, M. T. (2013), Estimation of river depth from remotely sensed hydraulic relationships, *Water Resour. Res.*, 49, 3165– 3179, doi:10.1002/wrcr.20176.
34. Millington, Nick; Das, Samiran; and Simonovic, Slobodan P., (2011) "The Comparison of GEV, Log-Pearson Type 3 and Gumbel Distributions in the Upper Thames River Watershed under Global Climate Models". *Water Resources Research Report*. 40. <https://ir.lib.uwo.ca/wrrr/40>
35. Neal, J.C., G. Schumann, and P.D. Bates (2012), A subgrid channel model for simulating river hydraulics and floodplain inundation over large and data sparse areas, *Water Resour. Res.*, 48
36. Neal, J.C., L. Hawker, J. Savage, M. Durand, P.D. Bates and C.C. Sampson (2020), Representation of river channels in large scale flood inundation models, *ESSOAr*, doi:10.1002/essoar.10504180.1
37. Parker, G., Wilcock, P. R., Paola, C., Dietrich, W. E., and Pitlick, J. (2007), Physical basis for quasi-universal relations describing bankfull hydraulic geometry of single-thread gravel bed rivers, *J. Geophys. Res.*, 112, F04005, doi:10.1029/2006JF000549
38. Peterson, W.; Birdsall, T.; Fox, W. (September 1954). "The theory of signal detectability". *Transactions of the IRE Professional Group on Information Theory*. 4 (4): 171–212.
39. Rentschler, J. and M. Salhab (2020) *People in Harm's Way: Flood Exposure and Poverty in 189 Countries*. Policy Research Working Paper. No. 9447. Wash. DC: The World Bank
40. Riha, J. and P. Golik (2005), Probability Estimation of River Channel Capacity, *Int. Symp. On Water Man. And Hydr. Eng.*, V.07,
41. Rosgen, D. L. (1997). "A geomorphological approach to restoration of incised rivers." *Proc., Conf. Management of Landscapes Disturbed by Channel Incision*, S. S. Y.Wang, E. J. Langendoen, and F. D. J. Shields, eds., Univ. of Mississippi, Oxford, MS, 1–11.
42. Rosgen, D. L. (2001). "A hierarchical river stability/watershed-based sediment assessment methodology." *Proc., 7th Federal Interagency Sedimentation Conf., Federal Interagency Sedimentation Project*, Vicksburg, MS, II–91–II–106.
43. Sampson, C. C., A. M. Smith, P. D. Bates, J. C. Neal, L. Alfieri, and J. E. Freer (2015), A high-resolution global flood hazard model, *Water Resour. Res.*, 51, 7358–7381, doi:10.1002/2015WR016954.
44. Shields, F. D., Jr., Copeland, R. R., Klingeman, P. C., Doyle, M. W., and Simon, A. (2003). "Design for stream restoration." *J. Hydraul. Eng.*, 10.1061/(ASCE)0733-9429(2003)129:8(575), 575–584.
45. Sholtes Joel S. & Bledsoe Brian P. (2016) Half-Yield Discharge: Process-Based Predictor of Bankfull Discharge. *Journal of Hydraulic Engineering*, 142(8), American Society of Civil Engineers, doi: 10.1061/(ASCE)HY.1943-7900.0001137
46. Smith, E. P., and Rose, K. A. (1995). "Model goodness-of-fit analysis using regression and related techniques." *Ecol. Modell.*, 77(1), 49–64.

47. Smith, L. C., and Pavelsky, T. M. (2008), Estimation of river discharge, propagation speed, and hydraulic geometry from space: Lena River, Siberia, *Water Resour. Res.*, 44, W03427
48. Soar, P. J., and Thorne, C. R. (2001). "Channel design for meandering rivers." U.S. Army Corps of Engineers, Engineering Research and Development Center, Coastal Hydraulic Lab., Vicksburg, MS
49. State Office for Information and Technology in North Rhine-Westphalia, Population of the municipalities of North Rhine-Westphalia on December 31, 2020 (in German). Retrieved June 21st, 2021.
50. Theil, H. (1958). *Economic forecasts and policy*, North Holland, Amsterdam, Netherlands.
51. Teng J., A.J. Jakeman, J. Vaze, B.F.W. Croke, D. Dutta, S. Kim (2017). Flood inundation modelling: A review of methods, recent advances and uncertainty analysis, *Environmental Modelling & Software*, Vol. 90, p. 201-216, <https://doi.org/10.1016/j.envsoft.2017.01.006>
52. Vogel, R. M., Stedinger, J. R., and Hooper, R. P. (2003). "Discharge indices for water quality loads." *Water Resour. Res.*, 39(10), 1273.
53. Wilkerson, G.V. (2008), Improved Bankfull Discharge Prediction Using 2-Year Recurrence-Period Discharge¹. *JAWRA Journal of the American Water Resources Association*, 44: 243-257. <https://doi.org/10.1111/j.1752-1688.2007.00151.x>
54. Wilcock, P. (1997). "Friction between science and practice: The case of river restoration." *Eos, Trans. Am. Geophys. Union*, 78(41), 454–454.
55. Williams, G. P. (1978), Bank-full discharge of rivers, *Water Resour. Res.*, 14(6), 1141– 1154, doi:10.1029/WR014i006p01141.
56. Williams, J. & Esteves, L.. (2017). Guidance on Setup, Calibration, and Validation of Hydrodynamic, Wave, and Sediment Models for Shelf Seas and Estuaries. *Advances in Civil Engineering*. 2017. 1-25. 10.1155/2017/5251902.
57. Winsemius, H. C., L. P. H. Van Beek, B. Jongman, P. J. Ward, and A. Bouwman (2013), A framework for global river flood risk assessments, *Hydrol. Earth Syst. Sci.*, 17, 1871–1892
58. Woodyer K.D. (1968) Bankfull frequency in rivers, *Journal of Hydrology*, Volume 6, Issue 2, Pages 114-142, ISSN 0022-1694, [https://doi.org/10.1016/0022-1694\(68\)90155-8](https://doi.org/10.1016/0022-1694(68)90155-8)
59. Wolman, M. G., and Leopold, L. B. (1957). "River flood plains; some observations on their formation." U.S. Geological Survey, Washington, DC
60. Wolman, M.G. and J.P. Miller (1960), Magnitude and Frequency of Forces in Geomorphic Processes, *Journal of Geology*, 68, 54–74.
61. Yamazaki, D., S. Kanae, H. Kim, and T. Oki (2011), A physically based description of floodplain inundation dynamics in a global river routing model, *Water Resour. Res.*, 47, W04501